SURFACE ENGINEERED QUANTUM DOTS IN PHOTOELECTROCHEMISTRY AND SUPRAMOLECULAR ASSEMBLY

This research has been supported by the Strategic Research Orientation "Nanofabrication" of the MESA$^+$ Institute for Nanotechnology and NanoNed, a National Nanotechnology Program coordinated by the Dutch Ministry of Economics Affairs.

Title: Surface Engineered Quantum Dots in Photoelectrochemistry and Supramolecular Assembly

D.V. Dorokhin
Ph.D Thesis
University of Twente, MESA$^+$ Institute for Nanotechnology,
Enschede, The Netherlands

ISBN 978-90-365-2977-8

Printed by: Ipskamp Drukkers B.V., Josing Maatweg 43, 7545 PS Enschede,
The Netherlands

SURFACE ENGINEERED QUANTUM DOTS IN PHOTOELECTROCHEMISTRY AND SUPRAMOLECULAR ASSEMBLY

PROEFSCHRIFT

ter verkrijging van
de graad van doctor aan de Universiteit Twente,
op gezag van de rector magnificus,
prof. dr. H. Brinksma,
volgens besluit van het College voor Promoties
in het openbaar te verdedigen
op vrijdag 05 februari 2010 om 16.45 uur

door

Denis Viktorovich Dorokhin

geboren op 21 november 1980
te Moskou, Rusland

Dit proefschrift is goedgekeurd door:

Promotoren:	Prof. Dr. G.J. Vancso
	Prof. Dr. Ir. D.N. Reinhoudt
Assistent Promotoren:	Dr. N. Tomczak
	Dr. A.H. Velders

This thesis is dedicated to my parents

Contents

Chapter 1

General Introduction

1.1 Introduction

Surface chemistry and engineering are essential in the development of functional nanoscale materials. In particular, novel luminescent materials are a target of intensive research. Molecular hybrids displaying not only a physical function, like luminescence, but also a desired chemical functionality are being developed for applications in optoelectronics, sensing, and biology. Luminescent probes are designed for labeling and targeting tissues and cell compartments, for their ability to be activated by an external stimulus, or for their ability to act simultaneously as homing devices and nanoreporters. In this context, semiconductor nanocrystals,[1] (Quantum Dots, QDs) have become serious contenders as luminescent labels, beacons, and sensors for biological and sensing applications.[2] Indeed, QDs are well suited for the design and engineering of nanoscale hybrid materials for the functions mentioned above.[3-6] Firstly, their photophysical properties are in many aspects superior to those of organic chromophores or inorganic metal complexes. Broad absorption, narrow and symmetric emission spectra, high quantum yields, low photobleaching rates, and the size in the nanoscale regime make QDs an attractive choice as light sources for many applications.[7] Recently, new organic coatings of QDs have been synthesized to render the QDs stable in aqueous dispersions. Additionally, protocols for surface chemical derivatization were developed. These protocols allow one to couple various functional groups to the QD surface.[8] The functional groups range from simple functionalities, like hydroxyl or carboxyl, through short chain polymers, e.g. PEG and chromophores, to large biomacromolecules, e.g., proteins, DNA or enzymes.[2] In sensing applications, this new generation of QD-based optical probes is tailored to respond to specific chemical events, with the transduction occurring through energy or electron transfer mechanisms.[9,10] Although some progress has been made

in the recent years, there are still many synthetic and design challenges associated with such complex nanoscale materials. In particular, coating QDs with redox responsive molecules or polymers results in a new generation of molecular hybrids characterized by electrochemically controlled photophysical properties.[11] Such electroactive coatings can be used in sensing of redox processes, where changes of the electrochemical potential modulate or control the optical properties of the nanocrystals.[12-15] A challenge is to integrate the resulting materials into devices, which should be realized without loosing the recognition capability of the QDs. In this context, host-guest supramolecular chemistry is relatively unexplored. However, fabrication of supramolecular QD structures on surfaces provides a robust and flexible approach to the design of various sensing platforms.

1.2 Concept of the thesis

The research described in this thesis is concerned with the synthesis, characterization, and application of novel QD materials, and their integration into multilayer structures at interfaces. In particular, chemical engineering of the QD ligand shell with redox active molecules and molecules able to take part in supramolecular host-guest reactions is tackled. Thesis is focused on ferrocene as the redox molecule and on spectroscopic and electrochemical evaluation of the interactions between ferrocene and the QD. β-Cyclodextrin is explored as the molecular host for complexation reactions on the QD surface. Fluorescence Resonant Energy Transfer and Electron Transfer are explored as signal transduction mechanisms in surface bound QD-based supramolecular sensing platforms. A strategy for the functionalization of QDs with electroactive polymers is also discussed.

In Chapter 2 the basic definitions and concepts related to semiconductor nanocrystals are introduced. In particular, the structure, synthesis, and photophysical properties of QDs, as well as QD surface ligand exchange methods, are described. Analytical tools and characterization methods of QDs used in this thesis are briefly introduced. QD applications are highlighted, and sensing principles using electron and energy transfer as the transduction mechanisms are reviewed. Finally, methods for surface functionalization with QDs are briefly introduced.

Chapter 3 describes the synthesis and luminescence properties of ferrocene-coated QDs. The attachment of ferrocenyl thiols to the nanoparticle's surface has been probed by diffusion-

filtered ^{1}H NMR spectroscopy. The photoluminescence quenching of QDs by molecular ferrocene is studied experimentally by steady state absorption and emission spectroscopies. Ferrocene thiols are shown to quench the QD luminescence to a different degree depending on the length of the alkyl chain (6, 8 and 11 carbon units) separating ferrocene from the QD surface. A charge transfer mechanism is postulated to be responsible for the observed quenching.

In Chapter 4 the electrochemical properties of CdSe/ZnS QDs in a non-aqueous solution and of QDs modified with redox-active ferrocenyl thiol are described. The energies of the valence and conduction bands are determined and the electrochemical band gap of the QDs is estimated from the anodic and cathodic redox peaks. The value of the bandgap is in good agreement with the value obtained from optical spectroscopy. The presence of the ferrocene ligand on the surface of the QDs remarkably influences the electrochemical response of the nanocrystals. The QD redox peaks are shifted or diminished and the ferrocene-coated QDs display features of a "molecular hybrid".

Reversible phase transfer of ferrocene-modified QDs between an organic solvent and water is described in Chapter 5. The phase transfer has been achieved by formation of host-guest complexes between the ferrocenes located on the surface of QDs and the cavity of β-cyclodextrin. Importantly, the reversibility of the phase transfer is demonstrated by addition of molecules that strongly bind to the β-CD cavity.

Chapter 6 describes the preparation of supramolecular multilayer structures made of QDs functionalized at their periphery with β-CD, in combination with adamantyl terminated dendrimeric "glues". Two different fabrication methods are shown to result in robust multilayer structures. The surface-immobilized QDs are capable to form host-guest complexes with other molecules of interest via the vacant binding cavities of β-CD. Complex formation with ferrocene-functionalized molecules leads to partial quenching of the luminescence emission of the QDs, as expected according to the results presented in Chapter 3.

Chapter 7 is dedicated to the fabrication of a surface-bound sensing platform where the molecular recognition occurs via supramolecular host-guest complex formation between the analytes and β-CD on the QD surface. Binding of a lissamine rhodamine is detected by means

of fluorescence resonant energy transfer (FRET) from the QD to the chromophores. FRET was also confirmed and evaluated by employing fluorescence lifetime imaging microscopy (FLIM).

Chapter 8 briefly describes the derivatization of QDs with electroactive poly(ferrocenyl silane) (PFS) polymers. The polymer is grafted to the surface of the QDs by a thiol-functionalized chain end. Two polymers differing in molar mass are used and the attachment of the polymeric ligands is monitored by diffusion-filtered ^{1}H NMR spectroscopy.

References

1. Alivisatos A. P. *Science* **1996**, *271*, 933-937.
2. Michalet, X.; Pinaud, F. F.; Bentolila, L. A.; Tsay, J. M.; Doose, S.; Li, J. J.; Sundaresan, G.; Wu, A. M.; Gambhir, S. S.; Weiss, S. *Science* **2005**, *307*, 538-544.
3. Huynh, W. U.; Dittmer, J. J.; Alivisatos, A. P. *Science* **2002**, *295*, 2425-2427.
4. Rajeshwar, K.; Tacconi, N. R.; Chenthamarakshan, C. R. *Chem. Mater.* **2001**, *13*, 2765-2782.
5. Niemeyer, C. M. *Angew. Chem. Int. Ed.* **2001**, *40*, 4128-4158.
6. Rosi, N. L.; Mirkin, C. A. *Chem. Rev.* **2005**, *105*, 1547-1562.
7. Trindade, T.; O'Brien, P.; Pickett, N. L. *Chem. Mater.* **2001**, *13*, 3843-3858.
8. Querner, C.; Reiss, P.; Bleuse, J.; Pron, A. *J. Am. Chem. Soc.* **2004**, *126*, 11574-11582.
9. Raymo, F. M.; Yildiz, I. *PCCP* **2007**, *9*, 2036-2043.
10. Somers, R. C.; Bawendi, M. G.; Nocera, D. G. *Chem. Soc. R*ev. **2007**, *36*, 579-591.
11. Colvin, V. L.; Schlamp, M. C.; Alivisatos, A. P. *Nature* **1994**, *370*, 354-357.
12. Yildiz, I.; Tomasulo, M.; Raymo, F. M. *Proc. Nat. Acad. Sci.* **2006**, *103*, 11457-11460.
13. Medintz, I. L.; Pons, T.; Trammell, S. A.; Grimes, A. F.; English, D. A.; Blanco-Canosa, J. B.; Dawson, P. E.; Mattoussi, H. *J. Am. Chem. Soc.* **2008**, *130*, 16745-16750.
14. Galian, R. E.; de la Guardia, M.; Perez-Prieto J. *J. Am. Chem. Soc.* **2009**, *131*, 892-897.
15. Anderson, N. A.; Lian, T. *Annu. Rev. Phys. Chem.* **2005**, *56*, 491-519.

Chapter 2

Semiconductor Quantum Dots: Properties, Surface Engineering, Characterization and Applications

This chapter gives a general overview of terms and definitions concerning semiconductor Quantum Dots. The QD structure, photophysical properties, and synthetic approaches are reviewed, with a particular emphasis on surface ligand exchange reactions, design and fabrication of QD hybrid materials, and chemical engineering of the ligand periphery. Analytical tools for QD characterization and manipulation are also introduced. Applications of QDs in biology and optoelectronics are briefly reviewed, and the use of QDs as optical signal transducers in sensing applications is highlighted. Finally, methods for the immobilization of QDs on surfaces are described.

2.1 INTRODUCTION

Quantum Dots (QDs) are semiconductor nanocrystals with unique optical and electronic properties.[1] These properties are the result of the confinement of electronic wavefunctions and can be manipulated by controlling the size of the QDs. To observe the confinement effects, the size of the nanocrystals has to be in the range of nanometers. QDs, as tunable, nanoscale light sources have found numerous applications in biology, bioanalytics, and optoelectronics.[2-12] Many of these applications require engineering of the QD surface in order to obtain novel materials with functional ligands. The development of methods to obtain well-defined QD hybrid materials having functional coatings with controlled physicochemical properties is therefore an active field of research. For instance, for QDs to be useful in biology, initial research directions have targeted water dispersability of the nanocrystals.[6,13,14] Additionally, specific functional groups for sensing and optoelectronics were developed. Nowadays, the QD coatings have grown in their chemical complexity, and very specific research targets related to QD functionality and function are pursued. In particular, it has been demonstrated that specific QD coatings can be used to control the QD optical properties. This is often exploited in sensors applications.[15,16] Direct surface modification of the nanocrystals with stimuli responsive molecules also allows one to control the physicochemical properties of the QDs, including colloidal stability in different solvents, and QD surface character.

This chapter briefly introduces the terms, and definitions related to semiconductor nanocrystals, which will be used throughout this thesis. The synthesis, structure, and photophysical properties of QDs are reviewed, with a particular emphasis on the surface ligand exchange methods, fabrication of QD hybrid materials, and chemical engineering of the ligand periphery. The main characterization methods of QDs are described. This chapter presents also some of the applications of QDs and describes the use of QDs as optical signal transducers in sensing applications. The transduction mechanisms may include electron or energy transfer. Finally, methods for substrate functionalization with QDs are also introduced.

2.2 PHYSICAL PROPERTIES OF QUANTUM DOTS

2.2.1 Structure and General Properties of QDs

Quantum Dots are semiconductor nanocrystals, which due to the size quantization effects (see below) exhibit many interesting electronic and optical properties. The most common QDs are elemental (Ge, Si) or are comprised of a combination of elements (e.g. CdSe, PbSe, CdS, ZnO, InAs, InSb, GaAs). Like all semiconductors, QDs can be characterized by an energy bandgap between the valance and conduction bands, and the associated highest occupied (HOMO) and the lowest unoccupied (LUMO) molecular orbitals. When QDs are excited with energies above the bandgap (E_g), an electron is promoted from the valence band to the conduction band, leaving behind a hole in the valence band of the semiconductor. The bound state of the electron and the hole is called an exciton. The characteristic size of the exciton is often referred to as the Bohr radius a_B, which is given by:

$$a_B = \frac{\hbar^2 \varepsilon}{e^2}\left(\frac{1}{m_e^*} + \frac{1}{m_h^*}\right) \tag{2.1}$$

where e is the elementary charge, ε is the bulk dielectric constant, m_e^* and m_h^* are the effective masses of the electrons and holes, respectively. A three-dimensional confinement of the electrons and holes in the QDs arises when the size of the nanocrystals decreases below the Bohr radius.[17,18] The consequence of this confinement is that the energy levels in the conduction and valence bands become discreet. Additionally, the absolute energy level positions vary as a function of the degree of confinement, and therefore as a function of the nanocrystals' size.[19] The energy difference between the valence and conduction bands increases with the increase of confinement. The change in the width of the bandgap, comparing to its bulk value, as a function of the size of the nanocrystals can be expressed as:[20]

$$\Delta \mathrm{E} = \frac{\hbar^2 \pi^2}{2R^2}\left(\frac{1}{m_e^*} + \frac{1}{m_h^*}\right) - \frac{1.8e^2}{\varepsilon R} \tag{2.2}$$

where R is the nanoparticle radius. By choosing a semiconductor material and a particular size of the nanocrystals one can therefore tune the electronic properties of the QDs.

The electron and the hole can recombine with each other and this process can give rise to emission of light. The radiative recombination process of electrons and holes directly from the conduction and valence bands is known as the “band edge” emission. If there are defects in the crystal structure or on the crystal’s surface, the photoexcited electrons and holes can be trapped. Recombination from these traps results in shifted emission. The presence of defects in nanocrystals plays therefore a crucial role in defining the electronic and optical properties of the QDs. The quality of QDs, and the efficiency of luminescence, can be expressed in terms of quantum yield (QY). QY is defined as the ratio between the number of emitted photons and the number of photons absorbed. Usually QY values for QDs are between 5-50%; a higher QY indicates a better quality of the nanocrystals.

2.2.2 Core-shell CdSe/ZnS QDs

Since the QD electronic bandgap is material- and size-dependent, it is possible to synthesize QDs emitting at different wavelengths by simply varying the QD size. Alternatively, one can tune the emission by changing the chemistry and composition of the QDs. Throughout this thesis we use QDs made of a CdSe core and a ZnS shell.[1] The core-shell structure of these QDs is shown in Figure 2.1. The horizontal lines represent the valence and conduction bands of the semiconductor materials. This type of band alignment is called Type I alignment, in which the energy levels of the core are effectively confined by the shell. Due to the energy difference between the two semiconducting materials this alignment results in a confinement of the photoexcited electrons and holes mainly to the QD core.[17,18] The shell passivates additionally the core surface defects by lattice matching between the two semiconductors. As a result, QDs with such a core-shell composition exhibit relatively high QYs in combination with enhanced chemical as well as photochemical stability.

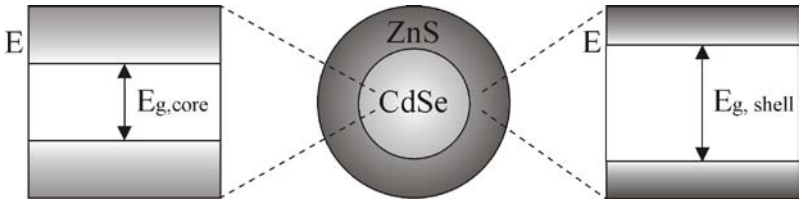

Figure 2.1 Schematic structure of core-shell CdSe/ZnS QDs with the corresponding energy levels of the core and the shell. The CdSe core is confined energetically by the ZnS shell.

Figure 2.2 shows luminescence from solutions of CdSe/ZnS QDs with sizes ranging from 2 to 6 nm. For this size range and material composition the QDs emit over the whole range of the electromagnetic spectrum, from the blue (2 nm QDs) to the red (6 nm QDs).

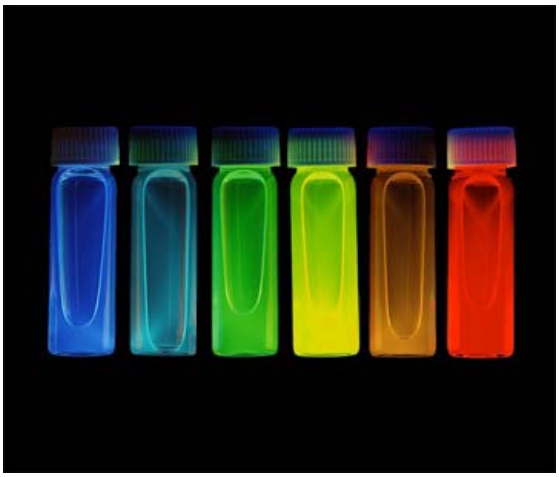

Figure 2.2 CdSe/ZnS QDs solutions under UV lamp irradiation emitting different colors, from the blue to the red, depending on their size (from 2 to 6 nm).[21]

Due to the presence of discrete energy levels in the valence and conduction bands, a monodisperse sample of QDs would have very narrow emission spectra. However, perfectly homogenous samples are difficult to obtain, and size distribution in addition to defects broadens the emission spectrum of the QDs.[22] Nowadays, QDs with emission spectra with full widths at half maximum (fwhm) values of 20-50 nm can be routinely synthesized, and fwhm values below 20 nm are being reported in the literature. High QY and narrow emission lines are therefore main figures of merit determining many applications of the QDs.

In comparison with bulk semiconductors usually having a uniform absorption spectrum, the QD absorption spectrum shows a series of overlapping peaks. Due to the discrete nature of the electronic energy levels in the nanocrystals, each peak corresponds to an electronic transition between the discrete levels.[22-25] QDs do not absorb light at wavelengths longer than the first excitonic peak, which is also referred to as the absorption onset. The wavelength value of the first excitonic peak (and of all subsequent peaks) is a function of the composition and of the size of the QDs. Smaller QDs have the first excitonic peak at shorter wavelengths (Figure 2.3).

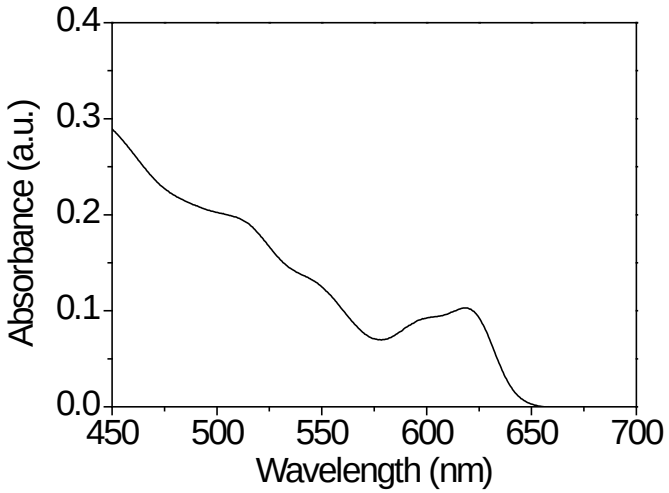

Figure 2.3 Typical absorption spectra of CdSe/ZnS QDs in toluene solution, with the first excitonic peak at ~620 nm.

In addition to the unique optical properties, such as the narrow, size-dependent emission, QDs have also other attractive properties, comparing to organic fluorophores. QDs display a much higher luminescence stability under excitation and much lower photobleaching rates. The absorption profiles of quantum dots are also broad compared to conventional dyes. Broad absorption spectra allow for the excitation of multiple QDs of different size with a single excitation wavelength. These optical properties make QDs excellent candidates for numerous applications in life science, diagnostics, and sensing.

2.3 CHEMISTRY OF QUANTUM DOTS

2.3.1 Synthesis of Semiconductor QDs

The synthesis of CdSe/ZnS QDs is usually carried out by thermal decomposition of organometallic precursors in the presence of a coordinating solvent, which provides a micelle-like ligand shell that controls the growth of the particles. Such a procedure provides high quality nanocrystals due to a discrete, homogeneous nucleation followed by slow growth and annealing.[26] Over the years, many improvements and refinements to methods based on organometallic precursors have been made. However, already in the early 80's Murray, Norris and Bawendi synthesized CdE (E= S, Se, Te) QDs with a relatively high QY and narrow size distribution. The reported method is also suitable to grow core-shell structures. Coating the CdSe core with a wider band gap semiconductor shell (e.g. ZnS) results in an enhancement of the luminescence quantum yields by 50-100%.[27-29] This is accompanied by increased photochemical stability. Besides the popular CdSe/ZnS core/shell quantum dots, QDs made of other materials, as well as multi-shell systems and doped nanocrystals have also been obtained.[30-38] A more detailed discussion about the synthesis of QDs can be found in dedicated reviews.[39]

Due to the high surface area of the nanocrystals, colloidal solutions of QDs are unstable and proper surface functionalization with suitable ligands is necessary. Since the ligand interacts with the nanocrystal surface, it also influences the luminescent properties of the QDs. The choice of the ligand is therefore crucial. Due to the synthesis procedures described above, the surface of CdSe/ZnS QDs is covered by a capping layer, usually a small organic molecule, or a polymer, which binds to the surface of the QD. This capping layer stabilizes the nanoparticles in solutions and prevents aggregation and precipitation of the QDs. CdSe/ZnS quantum dots are often stabilized by trioctylphosphine (TOP) or trioctylphosphine oxide (TOPO) ligands, which bind preferentially to the Cd or Zn atoms of the nanocrystals' surface. The alkyl chains simultaneously stabilize the QDs in nonpolar solvents, e.g., toluene or chloroform. Fortunately, one can rather easily replace TOPO with other molecules during the so-called ligand exchange reactions. The choice of the new ligand will depend on the QD applications and dispersion media.

2.3.2 Colloidal Stability of Semiconductor QDs

QD surface ligands prevent aggregation of the nanoparticles and control the growth of the nanocrystals during synthesis. In general, the choice of the stabilizing ligand depends on the solvent, size of the QD and its surface chemistry. Molecules binding strongly to the nanocrystal surface form stable ligand layers, which stabilize the QDs in solution. Chemisorption, electrostatic or hydrophobic interactions provide usually strong binding of the ligand to the nanoparticles surface. The most common examples of binding groups are thiols, phosphines, and amines (Figure 2.4). Polar and charged molecules provide good dispersability of the QDs in aqueous media while nanocrystals with hydrophobic ligands are only soluble in nonpolar organic solvents. In aqueous media, charged carboxylate, or hydroxylate groups stabilize effectively the QDs at specific pH values and concentrations. However, even in a good solvent the passivating ligand dynamically binds and unbinds to and from the QD surface.[40-42] Due to this dynamic process the passivating ligand molecules can desorb, e.g., by excessive washing or by competition with another molecule able to bind to the QD surface. This might compromise the stability of the nanoparticles in a given solvent and cause aggregation and precipitation. Some ligands may also desorb due to chemical reactions. For example, irradiation with light can cause photo-oxidation of thiols, what may result in desorption of the ligands followed by aggregation.[43-45]

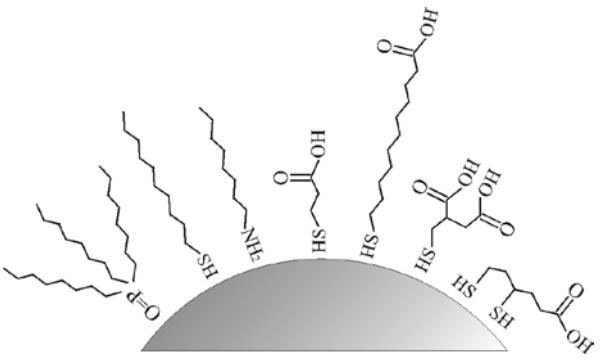

Figure 2.4 Common hydrophobic and hydrophilic ligands stabilizing QDs. Ligands for nonpolar solvents: trioctylphosphine oxide (TOPO), dodecanethiol (DDT), octylamine (OA); ligands for aqueous solutions: mercaptopropionic acid (MPA), mercaptoundecanoic acid (MUA), mercaptosuccinic acid (MSA), dihydrolipoic acid (DHLA).

2.3.3 Surface Modification of QDs via Ligand Exchange Reaction

To endow the QDs with a desired functionality or to improve the QD stability in solution, the original surface ligands can be exchanged for new ligands, as discussed above, which should be able to bind to the QD surface and provide good dispersability for the QDs in a given solvent.

Over the last two decades, a large number of ligand exchange procedures with different ligands have been reported.[6,14,46-48] The most common strategy is to mix the nanocrystals with excess of a new ligand followed by intensive stirring or sonication. The reaction is usually carried out at moderate temperatures. The time needed for the ligand exchange to occur depends on the type and size of the new ligand and its binding affinity, comparing to the ligand already present on the QD surface.[48-51] From available ligand chemistries, thiol groups are considered to have the highest affinity to the nanocrystal surfaces. Usually, ligand exchange reactions with ligands having bulky functional groups proceed longer in comparison with smaller molecules.[47]

The ligand chemistry is not restricted to small organic molecules. Polymeric ligands are often used to stabilize nanoparticles in solutions. The derivatization of QDs with polymers is of major importance for applications in biology and optoelectronics. The colloidal stability of the nanoparticles in solution is dictated by the formation of a stable ligand shell on the QD surface. Polymer-coated QDs were found to be more stable in comparison to QDs functionalized with small organic molecules. By using polymers, multiple and diverse functionalities can be introduced to the QD surface.[52-54] Different strategies to obtain polymer-coated QDs were developed involving direct attachment of macromolecules onto the QD surface via multivalent or single bonds (so called “grafting to” approaches),[55-61] or growth of the polymer chains from the QD surface (“grafting from” approaches) (Figure 2.5).[62-78] Unfortunately, the latter methods often require an intermediate step of ligand exchange and often lead to changes in the photophysical properties of the QDs.

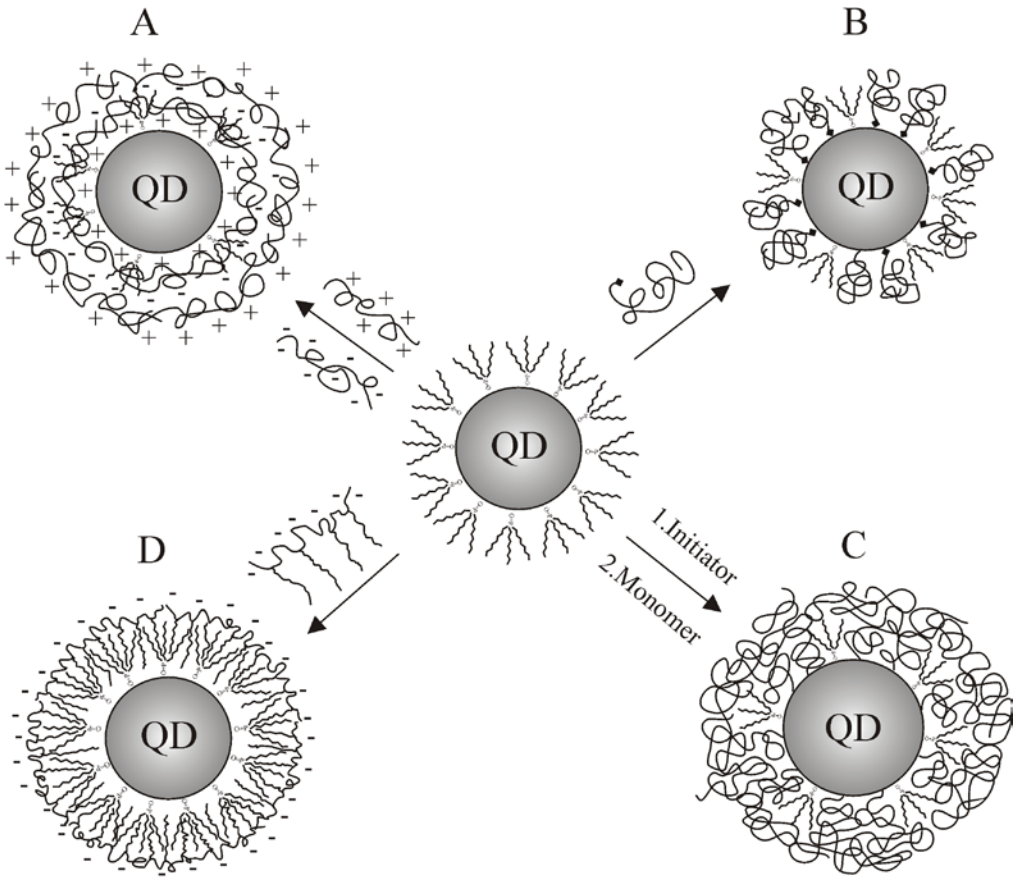

Figure 2.5 Different methods of coating the QDs with polymers. (A) Electrostatic layer-by-layer assembly, (B) "grafting to" approach, (C) "grafting from" approach, (D) amphiphilic polymeric coatings. For (A) and (C) an intermediate ligand exchange step is needed.

Another approach includes the assembly of polymers on the surface of QD via an electrostatic layer-by-layer technique, in which the QDs are modified stepwise with positively and negatively charged polyelectrolytes.[69-71] This procedure might also cause changes in the optical properties of the QDs. Hydrophobic interactions between the nanocrystals' surface ligands, usually TOPO or other ligands having hydrophobic alkyl chains, and polymers, can be used to coat the QDs with a thin polymeric shell.[8,72,73] This method does not involve ligand exchange reactions and thus does not affect the QD optical properties.

2.3.4 Phase Transfer of QDs

Phase transfer refers to a process during which the nanoparticles are transferred between solvents of markedly different polarities. For QDs this usually involves the transfer of QDs to water, since most of the QD synthesis is performed in organic solvents. Transfer of QDs to water is mainly motivated by the QD applications in biology. QD dispersability in aqueous solution, e.g., in biological buffers, is a prerequisite for their use as biological labels and probes. There are, however, also instances when the nanoparticles are required to be compatible with an organic solvent but the synthesis was carried out in aqueous solution; such circumstances are however rare, since one can synthesize high quality nanocrystals directly in organic solvents. Several strategies exist to perform phase transfer.[76-78] The most commonly applied method is based on ligand exchange, where the molecules stabilizing the nanocrystal in one phase are replaced by new ligands (Figure 2.6). Other methods include chemical modification or introducing additional coating layers on top of the original ligand shell.

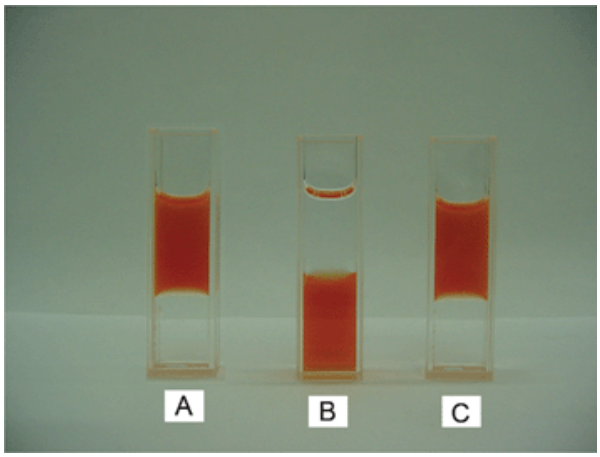

Figure 2.6 Photographs of CdTe QDs before and after reversible phase transfer under daylight (A, B, C). A: CdTe aqueous solution with the addition of chloroform; B: after phase transfer of CdTe NCs from the aqueous to the chloroform phase; C: after the reversible phase transfer of CdTe NCs from chloroform back to the aqueous phase.[79]

The transfer of TOP/TOPO-coated CdSe/ZnS quantum dots to aqueous solutions can be achieved by replacing the phosphine-based hydrophobic ligands with a hydrophilic thiol-based molecule, often having carboxyl or hydroxyl groups. One can also derivatize the

surface with multiple functionalities in order to create a mixed monolayer on the top of the QDs. The same concept is applied to transferring the nanocrystals stabilized with hydrophilic ligands to the organic phase. It seems that phase transfer of QDs from the aqueous to the organic phase is more difficult, primarily because already a strong binding ligand is used in aqueous solutions.[80-83] In order to facilitate the contact of the nanoparticles with the phase boundary, additional components can be added to the solution.

Modifications of the existing ligand using electrostatic, hydrophobic/hydrophobic, or host-guest interactions are some of the alternative approaches to transfer QDs between different phases. Recently, methods based on amphiphilic polymeric coatings were developed.[84-92] Refinement of these methods allows one not only to transfer the QDs to water but also to endow the QDs with a specific functionality. Complex block copolymers including hydrophobic parts interacting with the TOPO layer and hydrophilic parts providing interactions with water are synthesized for this purpose. The methods based on amphiphilic polymers result in QDs with increased colloidal stability through the multivalent attachment of the polymers to the QDs. Another advantage compared to ligand exchange is that the optical properties of the original QDs are largely retained.

Reversibility of the phase transfer is an issue, and not many examples are available in the literature. One of the examples of such phase transfer is the application of host-guest chemistry of cyclodextrins allowing reversible transfer of nanoparticles between two phases - a topic discussed in more detail in Chapter 5.

2.4 FABRICATION OF QUANTUM DOT FUNCTIONALIZED SURFACES

2.4.1 Immobilization of QDs on Surfaces

Immobilization of QDs onto planar surfaces is important in fabrication of photonic devices and in the design of various sensing platforms. There are two main methods for the deposition of QDs on surfaces. The first method involves covalent coupling between the chemical groups present on the substrate and the functional groups located at the QD surface. The second method is based on non-specific interactions between the substrate and the surface of the nanoparticles e.g. physisorption, electrostatic layer-by-layer assembly (LbL) etc.

Covalent attachment of nanoparticles is irreversible and usually stable QD layers are obtained. An example of this approach is the coupling of carboxylate-functionalized QDs to amine-terminated glass substrates resulting in a relatively dense QD film (Figure 2.7).[93,94]

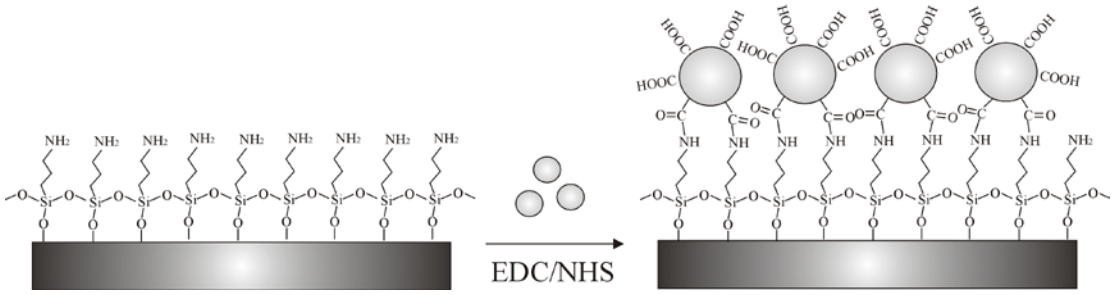

Figure 2.7 Immobilization of quantum dots on a substrate via covalent attachment.[93]

Functionalization of substrates with QDs using non-covalent attachment results in less stable structures. However, non-covalent attachment usually does not require functionalization of QDs and the substrate with very specific and complementary functional groups. More often than not, the presence of many functional groups needed for covalent coupling results in poor QD stability in a given solvent. Non-covalent attachment methods are reversible. This allows for the correction of defects in the QD layers. Non-covalent attachment was realized, among others, by electrostatic layer-by-layer assembly,[95,96] hydrogen bond formation,[97] or supramolecular host-guest chemistry. In the case of the latter, cyclodextrins or biomacromolecules have been usually employed to fabricate 2/3D QD assemblies.

Owing to the simplicity of electrostatic assembly this method has been widely used to fabricate multilayered structures including QDs (Figure 2.8). To be able to use QDs in LbL assembly, the QDs need to be functionalized with charged ligands.[96] Polyelectrolytes are usually the second component of the assemblies. The difference in size, morphology, and effective charge density between the multilayer components significantly affects the fabrication process. Additionally, the electrostatically assembled structures are very sensitive to pH, ionic strength, hydrogen bonding, and to the concentration of the nanoparticles and of the polyelectrolyte.

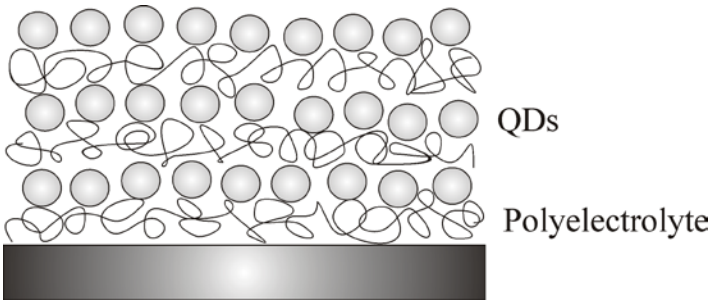

Figure 2.8 The electrostatic assembly of quantum dots in a composite layer-by-layer film.[95]

2.4.2 Surface Patterning of QDs

Fabrication of substrates patterned with QDs often requires the use of a combination of "top-down" and "bottom up" fabrication techniques. Using different lithographic and patterning techniques the nanocrystals can be immobilized on the surface in localized areas. Photolithography is a method widely used in fabrication of patterned substrates. In this technique the substrate is exposed radiation, e.g. UV or X-ray, through a mask with pre-patterned features (for example by e-beam lithography). For instance, selective immobilization of CdSe/CdS QDs on a substrate was achieved by selective photoactivation of the surface to provide amine functionality (Figure 2.9). The QDs underwent a ligand exchange reaction and were bound to the amine groups.[98]

Soft lithography patterning techniques like microcontact printing (μCP), nanoimprint lithography, or scanning probe based lithography are particularly attractive because they are simple to perform, and do not require clean-room facilities (therefore they are very cost effective). In microcontact printing an elastomeric "stamp" is molded from a previously fabricated silicon master. The stamps are often made of elastomers, e.g., crosslinked poly(dimethylsiloxane) (PDMS). PDMS has been used as a stamp to transfer many different nanoparticles, including QDs, onto various substrates.[99,100] QD deposition on surfaces using μCP is based on simple inking of the PDMS stamp with a QD solution and making a conformal contact between the inked stamp and the substrate. The concentration of the nanoparticles in the solution, inking time, and contact time are the primary parameters, which one can tune to obtain high-quality prints. To modify the interactions with the QD ink, the PDMS stamp can be oxidized to render its surface hydrophilic.

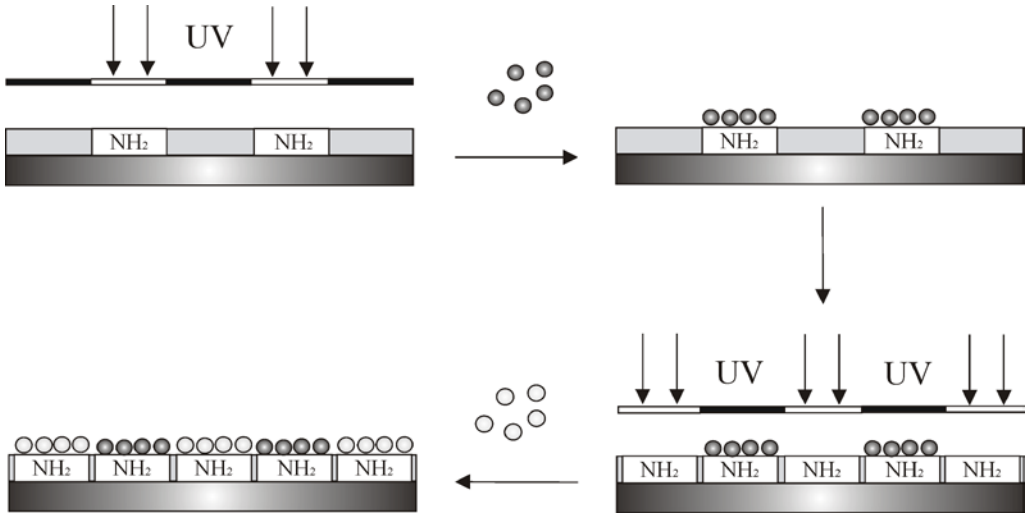

Figure 2.9 Scheme of the stepwise preparation of multicomponent QD arrays by using photolithography and surface ligand exchange.

2.5 APPLICATIONS OF QUANTUM DOTS

2.5.1 Technical Applications

QDs have found many applications in such diverse fields like optoelectronics, nanophotonics, sensing or biology.[2-12,15,16] These application, stem from the attractive electronic and optical properties of QDs and from their nanometer-scale size. Developments in the synthesis and handling of QD materials have improved tremendously the performance of QDs in these applications. For example, novel core/shell nanocrystals have enhanced quantum yields and therefore brighter biolabels are obtained, while higher stability to photo-oxidation results in increased device lifetimes. In optoelectronics the QDs are therefore employed as active components of light emitting diodes (LEDs) (Figure 2.10),[2,100-103] transistors,[104] solar cells and lasers.[105-107]

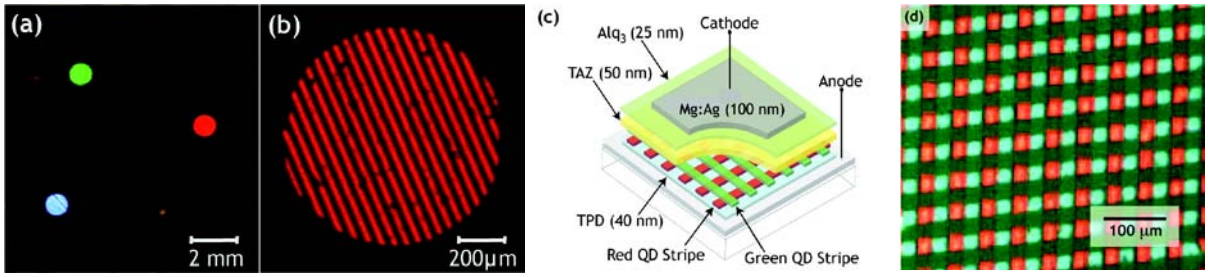

Figure 2.10 (a) Electroluminescent red and green QD-LED pixels are fabricated on the substrate. (b) Electroluminescent QD-LED pixel is patterned with 25 µm wide stamp features. (c) Scheme of the QD-LED device. (d) Schematic diagram showing the structure of a QD-LED with an emissive layer consisting of 25 µm wide stripes of green and red QD monolayers.[100]

2.5.2 Applications in Life Science

The advances in QD surface functionalization have resulted in novel QD materials displaying functional ligands on the surface. These ligands could be responsive to an external stimulus to provide sensors, or be able to bind to relevant biomolecules to provide luminescent biomarkers. QDs are widely used as fluorescent probes and labels in biology.[108] Due to the size-tunable and narrow emission spectra combined with broad absorption spectra, quantum dots are often used in multiplexed detection where a single excitation light source is used, and light from multiple labels of different target biomolecules or cellular compartments is spectrally filtered and collected (Figure 2.11).[14,109-113]

For applications under physiological conditions in biologically relevant environments, appropriate surface modification and functionalization of the QDs is crucial to maintain nanocrystal stability. The long-term stability of luminescence against photobleaching/photooxidation and bio-inertness make QDs superior compared to organic dyes and fluorescent proteins.[8,112] Furthermore, the difference in fluorescen lifetimes enables nanocrystals to be distinguished from cellular autofluorescence by fluorescence lifetime imaging (FLIM).[114] QDs have successfully been used in immunocytochemistry,[6,7] DNA microarrays,[115] imaging of live cells,[8,14,116] or imaging in-vivo of the blood flow.[117] A key

issue in medical applications, and indeed in any *in vivo* or living-cell research, is the potential toxicity of the quantum dots, however the issue is far from settled.[118]

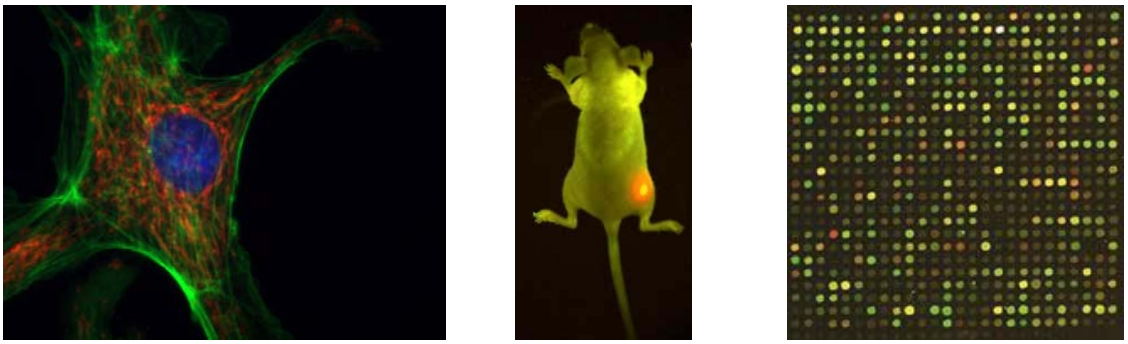

Figure 2.11 Application of QDs in life sciences. Multiple labeling of cellular compartments (left), tumor targeting in medical imaging (middle) and microarray technology for immunodiagnostics and DNA screening (right).[119-121]

2.5.3 Detection and Sensing

The applications of QDs as optical transducers in sensing have clearly benefitted from the advances in chemical surface engineering. QDs have been used in the detection of biomolecules, simple organic molecules, like TNT, or inorganic molecules e.g. cyanide and metal ions, as well as sensors of temperature and pH.[122-126] QDs have also been used as tracers in flow velocimetry in microfluidic devices,[127] or as gas sensors.[128] Most of these sensing applications are based on signal transduction via fluorescence resonance energy transfer (FRET) or photoinduced electron transfer (PET) phenomena, which are briefly described below.[15,16]

Electron Transfer. Electron transfer processes play a crucial role in molecular signaling in biological systems, in solar energy harvesting in natural and artificial systems, or in photocatalysis. Regarding QDs, solar cell, photocatalysis and sensing applications have been actively explored in connection with PET. Upon light excitation both the electron in the conduction band and the hole in the valence band can take part in electron transfer processes.[129] Due to PET, the QD luminescence is effectively quenched. This modulation of the luminescence by PET can be exploited in sensing applications.[15,16,129] For instance, using a PET process, a maltose-binding protein (MBP) can be engineered to manipulate the

luminescence of a QD. In this example a ruthenium complex donor is placed close to the surface of the nanocrystal and transfers efficiently electrons to the QD upon excitation (Figure 2.12). In consequence, the luminescence of the QD decreases. Upon addition of maltose to the system, the conformation of the protein changes significantly, shifting the ruthenium complex away from the quantum dot surface; consequently, the electron transfer efficiency decreases leading to an increase of the luminescence QY. Similar concepts of modulation of ET via conformational changes driven by a molecular recognition event is explored in various QD sensing schemes.[130]

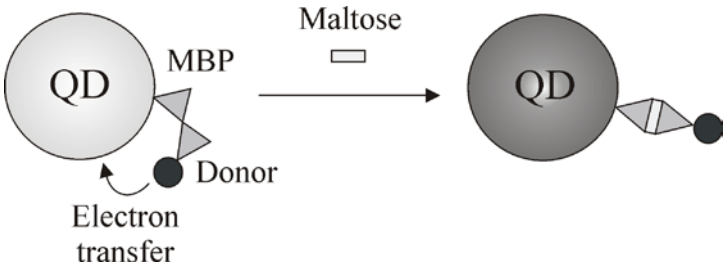

Figure 2.12 Association of MBP with maltose moves the ruthenium electron donor away from the CdSe quantum dot, preventing the electron transfer process to occur and switching-on the luminescence of the nanoparticle.

Energy Transfer. Another class of QD-based sensors is based on fluorescence resonant energy transfer (FRET). In FRET the excitation energy from a donor species is transferred to an acceptor species. QDs in the FRET donor-acceptor couple can act as donors or acceptors.[15,16 ,133] For the energy transfer to occur the donor and the acceptor need to be in close proximity to each other and the emission of the donor must overlap with the absorption of the acceptor. The FRET process is strongly distance-dependent. Theoretically, the sensing principle can be based on the physical separation between the donor and acceptor as well as on their spectral overlap. Hence, the energy transfer efficiency and the nanocrystals' luminescence intensity can be manipulated by the interaction of analytes with the QDs. The presence of analytes can be actuated into a detectable optical signal. For example, CdSe/ZnS quantum dots were derivatized with thiol terminated oligonucleotide strands. Upon hybridization with complementary DNA strands labeled with a chromophore, a FRET signal is detected (Figure 2.13) due to the energy transfer from the quantum dot to the organic dye. The luminescence switching mechanism based on FRET can also be exploited in the detection of small organic molecules.[122] CdSe/ZnS QDs conjugated to an antibody were able

to specifically recognize 2,4,6-trinitrotoluene (TNT) via the formation of a complex with the antibody located at the nanocrystal surface and subsequent modulation of FRET between QDs and a chromophore initially bound to the antibody.

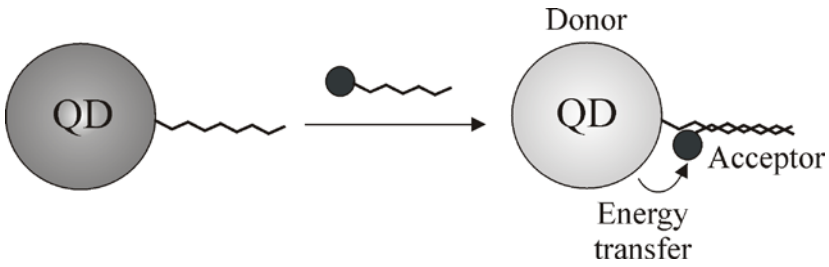

Figure 2.13 Hybridization of an oligonucleotide-labeled QD with an oligonucleotide labeled with a complementary energy acceptor results in energy transfer. The red-shifted emission of the energy acceptor is then detected.

2.6 CHARACTERIZATION OF QUANTUM DOTS

The QD characterization methods can be divided into three main groups: (1) methods used to characterize the QD composition, morphology and size, (2) methods used to characterize the ligand shell, and (3) methods used to characterize the optical and electronic properties of the QDs. QD size is easily accessible by transmission electron microscopy (TEM) or atomic force microscopy (AFM). Characterization of the ligand shell is more problematic and is usually tackled by using NMR. Related NMR methods, discussed below, allow one to follow ligand exchange reactions and provide proof for the ligand exchange. Spectroscopy and electrochemistry are relatively straightforward methods, which give direct information on a number of important QD parameters, like QYs, emission wavelength, or redox potentials. The QD samples are always heterogeneous by size and composition. It should be therefore remembered that average values alone could be misleading in interpreting the results. Whenever this is possible, widths of the parameter distributions should be assessed.

2.6.1 Microscopy

Transmission electron microscopy. Transmission electron microscopy (TEM) is a primary characterization tool used to investigate QDs and allows for the direct evaluation of the size of the nanoparticles and their crystal structure (Figure 2.14). The contrast in TEM is usually

high enough for materials with high electron densities, limiting TEM to nanoparticles made of inorganic materials. The organic ligands on the surface of QDs are usually not well-resolved, but can be stained by addition of heavy metal salts to the sample.[8] To obtain the average size and size distribution of QDs from TEM images one has to evaluate many nanoparticles. In practice this means that many TEM images at a desired magnification have to be acquired to obtain statistically relevant results. Sometimes, it is possible to image nanocrystals coated with polymers, having thick and dense coatings on the top of the QDs. However, due to the sample preparation protocols, all the solvent is evaporated causing usually shrinkage of the organic shell compared to its state in a solvent.

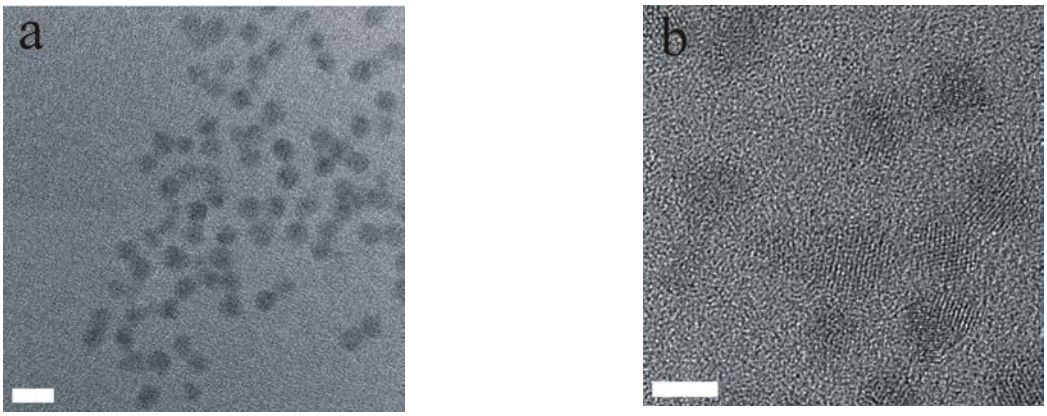

Figure 2.14 Transmission electron microscope images of individual TOPO-coated CdSe/ZnS nanocrystals. The scale bars are (a) 10 nm and (b) 5 nm. The crystal structure of the QDs is visible on (b).

Scanning probe microscopy. Scanning probe microscopy, including AFM (atomic force microscopy), is an indispensable tool to characterize nanoparticles immobilized onto flat surfaces.[132-134] The topography images obtained during AFM data acquisition give information on the sample morphology and homogeneity (Figure 2.15). They also allow one to determine the surface coverage (particle density per surface area), nanoparticle dimensions etc. These experiments are limited mainly by the size of the probe used to scan the surface. Probe diameters are usually in the range of 4-40 nm; characterization of the probe radius is rather troublesome and therefore the step height information, which is independent of the probe radius, rather than the lateral dimensions, is used to evaluate the nanoparticles[*]. A

[*] There is the assumption of an accessible reference plane made here.

combination of AFM and fluorescence microscopy is a powerful tandem characterization technique for patterned surfaces. The emission from the patterns can be directly correlated with the presence of nanoparticles. In an extreme case, fluorescence from single QDs coupled with topographical information allows for the identification of QDs exhibiting differences in QYs, but more importantly to indentify "dark" QD fractions, i.e., the fraction of QD, which does not emit light, lowering the ensemble value of QY.[135]

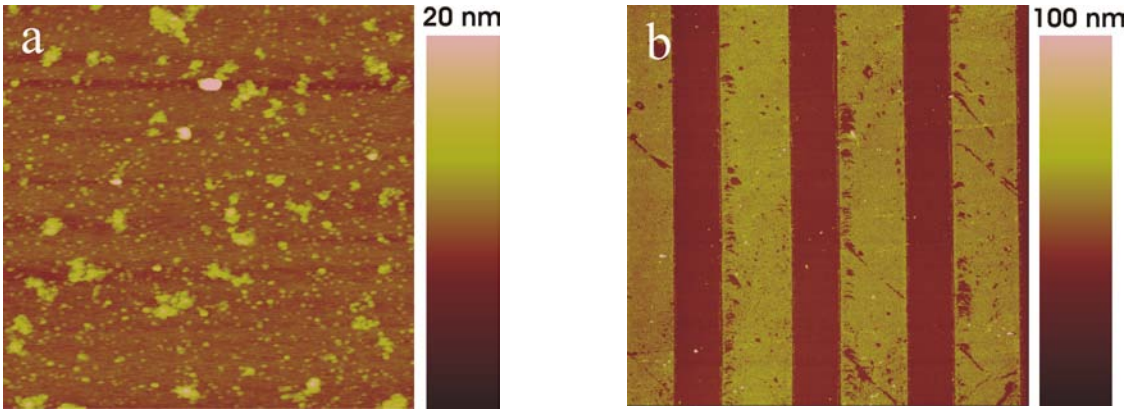

Figure 2.15 (a) AFM height image of CdSe/ZnS quantum dots deposited on a glass substrate. The scan size is 2×2 μm. (b) AFM height image of a QD pattern obtained by using microcontact printing. The scan sizes are 50×50 μm.

2.6.2 Spectroscopy

NMR spectroscopy. Analysis of QD surfaces represents a considerable challenge. NMR is often used in the characterization of the QD organic ligand shells as it gives unique information on the chemical identity of the ligand molecules and on the molecular mobility in complex inhomogeneous systems. Additionally, it has been also used to identify the chemical bonds between the ligands and the QD surface, and to follow ligand exchange reactions. NMR is in principle a non-destructive analytical method and allows for long-term studies of QDs. Unlike in electron and scanning probe microscopies, NMR can be performed in liquids without disturbing the surface ligand molecular conformation.

Pulsed field gradient stimulated echo (PFGSE) NMR techniques are often used for the selective observation of spectral features arising from organic molecules or polymer chains bound to the nanoparticle surfaces. Ligand identification was demonstrated in the literature

for thiol- and TOPO-coated QDs.[44,136-138] The method is based on the fact that species which have smaller hydrodynamic radius are diffusing faster. This difference in the characteristic diffusion constants allows one to discriminate between free ligands and ligands attached to QDs. From the diffusion decays, a self-diffusion coefficient, D_s, can be estimated. The hydrodynamic radius of the nanoparticles in solution R_h can be calculated by using the Stokes-Einstein relation:[139]

$$D_s = \frac{k_B T}{6\pi\eta R_h} \tag{2.3}$$

where k_B is the Boltzmann constant and η is the solution viscosity at a temperature T. In summary, diffusion ordered NMR spectroscopy (DOSY) based on PFGSE NMR is a technique able to distinguish between unbound ligand molecules diffusing freely in the solution and molecules adsorbed on the nanocrystal surface, and it is used throughout this thesis to evaluate ligand exchange reactions and size of the assemblies.

UV-VIS and fluorescence spectroscopy. The QD absorption and emission spectra are related to the electronic structure of the semiconductor nanoparticles and depend on the QD size due to the spatial confinement of the electronic wave functions of the electron and the hole (Figure 2.16). Optical spectroscopy is therefore a simple and relatively easy tool used to characterize the confinement effects in QDs. Additionally, since the absorption and luminescence of QDs depend on the ligand shell and on the QD surroundings (e.g. polarity, dielectric constant, presence of quenchers) spectroscopic methods can be used to study the ligand shell and various processes happening in the vicinity of the QDs.

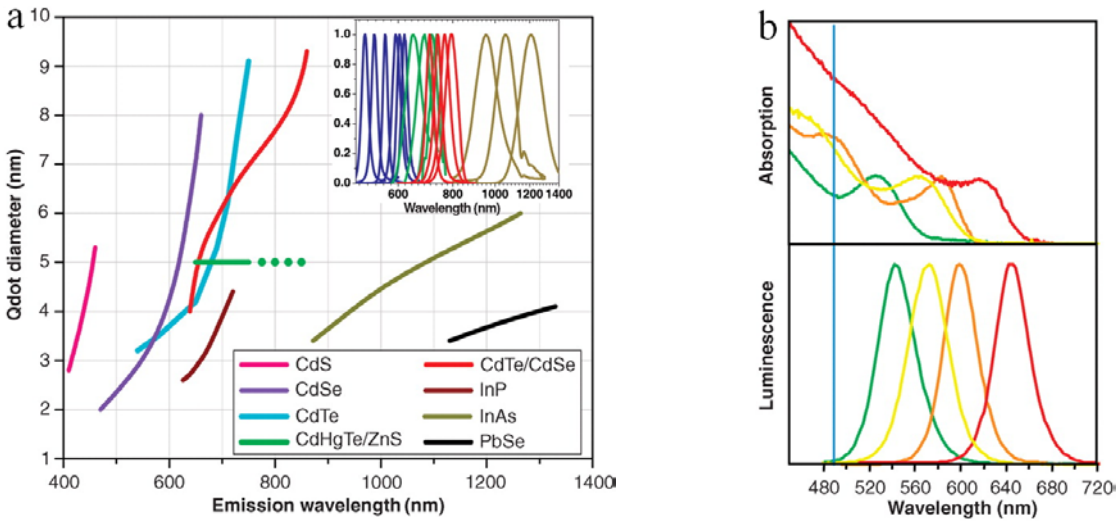

Figure 2.16 (a) Relation between the size of the QD and its peak emission wavelength for QDs of different chemical composition. (b) Absorption (upper curves) and emission (lower curves) spectra of four CdSe/ZnS QDs samples. The blue line shows the 488 nm excitation line. One can efficiently excite all the QDs simultaneously.[10]

By analysis of the spectral curves and applying an empirical formula one can estimate the average size D of the QD in solution:[140]

$$D = (1.6122 \times 10^{-9})\lambda^4 - (2.6575 \times 10^{-6})\lambda^3 + (1.6242 \times 10^{-3})\lambda^2 - (0.4277)\lambda + (41.57) \qquad (2.4)$$

where λ is the wavelength of the first excitonic absorption peak. The extinction coefficient ε can be obtained from:

$$\varepsilon = 1600\Delta E(D)^3 \qquad (2.5)$$

where ΔE is the energy of the first excitonic peak in units of eV. If the absorption spectrum is obtained for a low-concentration sample (to avoid reabsorption), and the distribution of the nanoparticle diameters is not broad, one can obtain the concentration of the QDs in the solution directly from the Lambert-Beer equation:

$$A = \varepsilon L c \qquad (2.6)$$

where A is the absorbance value at the first excitonic peak, and L is the path length of the measuring cell. The average diameter of the QDs can be estimated directly from TEM images and usually a good correlation between TEM and the optical methods is observed. For core-shell nanocrystals the method is still valid, however the ZnS shell is not taken into account since it absorbs at much higher energies. The thickness of the shell can be estimated from the synthetic protocol and the size of the nanoparticles obtained from TEM. The luminescence spectrum provides information on the emission wavelength, size distribution, presence of surface traps, and of course on the bandgap energy value. From the luminescence emission one can calculate the QD luminescence QY by employing an appropriate fluorescence standard R of known QY.[141,142]

$$QY = QY_R \times \frac{I}{I_R}\frac{A_R}{A}\frac{n^2}{n_R^2} \tag{2.7}$$

where I is the integrated area of the emission peak, A is the absorbance at the excitation wavelength, and n is the refractive index of the solvent.

The influence of the ligand exchange on the optical properties of QDs can be measured using spectroscopic techniques. The spectral shifts in the absorption and emission spectra of QDs can be also caused by changes in the ligand environment or solvent composition and are usually detectable with spectroscopic methods. Optical spectroscopy is therefore employed as a universal detection tool in sensing applications.

2.6.3 Electrochemistry of QDs

Cyclic voltammetry. Cyclic voltammetry (CV) is a well-known electrochemical technique widely used to obtain qualitative and quantitative information on redox reactions. It provides information on the thermodynamics and kinetics of electron transfer processes, it allows for the detection of adsorption processes and it is indispensable in the evaluation of redox potentials of electroactive species in solution or absorbed on electrodes. The CV experimental setup is a simple electrode system where the potential between the working electrode (WE), at which the electrochemical oxidation and reduction reactions of electroactive species occur, is measured with respect to a reference electrode (RE) (Figure

2.17). The third electrode, the counter electrode (CE), is added to complete the current loop with the working electrode.[143]

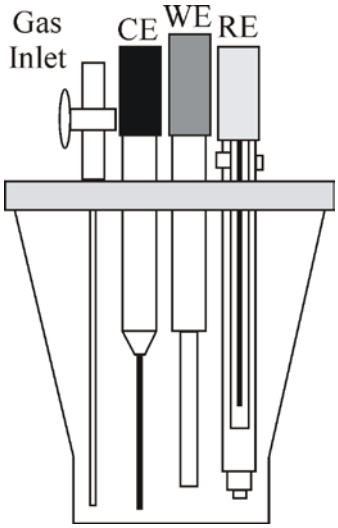

Fugure 2.17 Scheme of a standard electrochemical cell with three-electrode configuration and a gas inlet for purging the electrolyte solution.

Conducting media in the form of a supporting electrolyte solution are added to the electrochemical cell. During CV experiments the potential of the working electrode is scanned linearly using a triangular potential form. During the potential sweep, a potentiostat measures the current resulting from the applied potential. The resulting current-potential plot is called a cyclic voltammogram. Peaks, which appear on the voltammogram, correspond to oxidation and reduction reactions of electroactive species at the electrode surface. Analysis of the cyclic voltammograms gives the following qualitative and quantitative information: (1) reversibility of the redox system, (2) formal potential of the redox processes, and (3) reaction mechanisms.

In the context of QDs the electron reactions are expected to occur through the valence and conduction bands. CV can be used to estimate the highest occupied molecular orbital (HOMO) and the lowest unoccupied molecular orbital (LUMO) of semiconducting materials (Figure 2.18). Importantly, as compared to spectroscopy, the absolute positions of the band potentials can be obtained by electrochemical methods. Since in QDs the valence and conduction band positions shift as a function of QD size, CV can be used to probe the effects of confinement on the energetics of the HOMO and LUMO bands directly.[144-161] This

"electrochemical bandgap" can be correlated with the bandgap estimated by spectroscopic methods or calculated theoretically from the QD size (obtained e.g. from TEM).

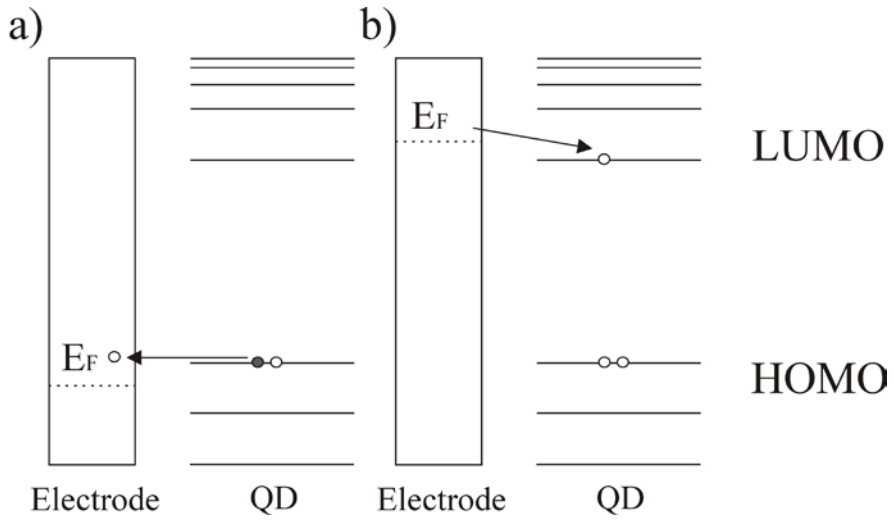

Figure 2.18 Electrochemical oxidation (a) and reduction (b) of a QD at the electrode surface. a) A positive potential is applied and the electron transfer from the QD HOMO to the electrode occurs. b) A negative potential is applied and the electron transfer occurs from the QD LUMO to the electrode.[162]

CV just recently has been applied to the study of QDs, and there are still many experimental and theoretical challenges. The interpretation of cyclic voltammograms is far from simple. Additionally, the QD samples are not homogeneous, and the different synthetic procedures to obtain the same type of QDs may lead to different electrochemical responses. Poor solubility of QDs in electrolytic solutions and electrochemical corrosion processes are other experimental hurdles. In this thesis we describe QDs functionalized with redox-active molecules for applications as redox-responsive switches, optical beacons or in redox sensing systems for nanoelectronics and nanophotonics. In this context, electrochemistry can become an important tool for the study of such complex redox responsive systems and contribute to the fundamental understanding of electron transfer mechanisms on the nanoscale.

2.7 CONCLUSIONS

Quantum Dots, due to their unique optical and electronic properties, are excellent candidates as nanoscale emitters in various applications. However, for many applications, surface chemical engineering of the nanocrystals' ligand periphery is essential. Presence of new ligands results in changed physical and chemical properties of the QDs. This can be exploited in QD phase transfer reactions, or surface functionalization with QDs. Depending on the nature of the functional ligand, the QD hybrid materials can be employed in nanophotonics, biomedicine or sensing. In sensing, the transduction mechanism may include electron or energy transfer. Functional hybrid QD materials can be characterized by various analytical techniques. In particular, NMR is a suitable tool to characterize the QD surface ligands and to monitor ligand exchange reactions, and electrochemical approaches, like cyclic voltammetry, are employed to characterize QDs coated with electroactive ligands.

2.8 REFERENCES

1. Alivisatos A. P. *Science* **1996**, *271*, 933-937.
2. Colvin, V. L.; Schlamp, M. C.; Alivisatos, A. P. *Nature* **1994**, *370*, 354-357**.**
3. Klein, D. L.; Roth, R.; Lim, A. K. L.; Alivisatos, A. P.; McEuen, P. L. *Nature* **1997**, *389*, 699-701.
4. Coe, S.; Woo, W.-K.; Bawendi, M.; Bulovic, V. *Nature* **2002**, *420*, 800-803.
5. McDonald, S. A.; Konstantatos, G.; Zhang S.; Cyr, P. W.; Klem, E. J. D.; Levina, L.; Sargent E. H. *Nat. Mater*. **2005,** *4*, 149-152.
6. Chan, W. C. W.; Nie S. *Science* **1998**, *281*, 2016-2018.
7. Bruchez, M. Jr.; Moronne, M.; Gin, P.; Weiss, S.; Alivisatos, A. P. *Science* **1998**, *281*, 2013-2016.
8. Dubertret, B.; Skourides, P.; Norris, D. J.; Noireaux, V.; Brivanlou, A. H.; Libchaber, A. *Science* **2002**, *298*, 1759-1760.
9. Gao, X.; Cui, Y.; Levenson, R. M.; Chung, L. W. K.; Nie, S. *Nat. Biotechnol.* **2004**, *22*, 969-976.
10. Michalet, X.; Pinaud, F. F.; Bentolila, L. A.; Tsay, J. M.; Doose, S.; Li, J. J.; Sundaresan, G.; Wu, A. M.; Gambhir, S. S.; Weiss, S. *Science* **2005**, *307*, 538-544.

11. Medintz, I. L.; Clapp, A. R.; Mattoussi, H.; Goldman, E. R.; Fisher, B.; Mauro, J. M. *Nat. Mater.* **2003**, *2*, 630-638.
12. Anikeeva, N.; Lebedeva, T.; Clapp, A. R.; Goldman, E. R.; Dustin, M. L.; Mattoussi, H.; Sykulev, Y. *Proc. Nat. Acad. Sci.* **2006**, *103*, 16846-16851.
13. Pathak, S.; Choi, S.; Arnheim, N.; Thompson, M. E. *J. Am. Chem. Soc.* **2001,** *123*, 4103-4104.
14. Jaiswal, J. K.; Mattoussi, H.; Mauro, J. M.; Simon, S. M. *Nat. Biotechnol.* **2003**, *21*, 47-51.
15. Raymo, F. M.; Yildiz, I. *PCCP* **2007**, *9*, 2036-2043.
16. Somers, R. C.; Bawendi, M. G.; Nocera, D. G. *Chem. Soc. Rev.*, **2007**, *36*, 579-591.
17. Brus, L. E. *J. Chem. Phys.* **1983**, *79*, 5566-5571.
18. Brus, L. E. *J. Chem. Phys.* **1984**, *80*, 4403-4409.
19. Efros, A. L.; Rosen, M. *Annu. Rev. Mater. Sci.* **2000**, *30*, 475-521.
20. Brus L. E. *J. Phys. Chem.* **1986**, *90*, 2555-2560.
21. www.nanoe.ece.drexel.edu
22. Brus, L. E.; Efros, A. I.; Itoh, T. J. *Luminesc.* **1996**, *70*, R7.
23. Li, L. S.; Hu, J.; Yang, W.; Alivisatos, A. P. *Nano Lett.* **2001**, *1*, 349-352.
24. Leatherdale, C. A.; Bawendi, M. G. *Phys. Rev. B* **2001**, *6316*, 165315.
25. Guyot-Sionnest, P.; Shim, M.; Matranga, C.; Hines, M. *Phys. Rev. B* **1999**, *60*, R2181.
26. Murray, C. B.; Norris, D. J.; Bawendi, M. G. *J. Am. Chem. Soc.* **1993**, *115*, 8706-8715.
27. Hines, M. A.; Guyot-Sionnest, P. *J. Phys. Chem.* **1996,** *100*, 468-471.
28. Dabbousi, B. O.; Rodriguez-Viejo, J.; Mikulec, F. V.; Heine, J. R.; Mattoussi, H.; Ober, R.; Jensen, K. F.; Bawendi, M. G. *J Phys Chem B* **1997**, *101*, 9463-9475.
29. Peng, X.; Schlamp, M. C.; Kadavanich, V.; Alivisatos, A. P. *J. Am. Chem. Soc.* **1997**, *119*, 7019-7029.
30. Mokari, T.; Banin, U. *Chem. Mater.* **2003**, *15*, 3955-3960.
31. Cao, Y.-W.; Banin, U. *Angew. Chem. Int. Ed.* **1999**, *38*, 3692-3694.
32. Kim, S.; Fisher, B.; Eisler, H.-J.; Bawendi M. *J. Am. Chem. Soc.* **2003**, *125*, 11466-11467.
33. Reiss, P.; Carayon, S.; Bleuse, J.; Pron, A. *Synth. Met.* **2003**, *139*, 649-652.
34. Talapin, D. V.; Mekis, I.; Götzinger, S.; Kornowski, A.; Benson, O.; Weller, H. *J. Phys. Chem. B* **2004**, *108*, 18826-18831.

35. Xie, R.; Kolb, U.; Li, J.; Basche, T.; Mews, A. *J. Am. Chem. Soc.* **2005**, *127*, 7480-7488.
36. Aharoni, A.; Mokari, T.; Popov, I.; Banin, U. *J. Am. Chem. Soc.* **2006**, *128*, 257-264.
37. Mikulec, F. V.; Kuno, M.; Bennati, M.; Hall, A. D.; Griffin, R. G.; Bawendi M. G *J. Am. Chem. Soc.* **2000**, *122*, 2532-2540.
38. Kwak, W. C.; Sung, Y. M.; Kim, T. G.; Chae, W. S. *Appl. Phys. Lett.* **2007**, *90*, 173111.
39. Embden, J. V.; Jasieniak, J.; Gomez, D. E.; Mulvaney, P.; Giersig, M. *Austr. J. Chem.* **2007**, *60*, 457-471.
40. Love, J. C.; Estroff, L. A.; Kriebel, J. K.; Nuzzo, R. G.; Whitesides, G. M *Chem. Rev.* **2005**, *105*, 1103-1169.
41. Dollefeld, H.; Hoppe, K.; Kolny, K.; Schilling, K.; Weller, H.; Eychmüller, A. *PCCP* **2002**, *4*, 4747-4753.
42. Ji, X.; Copenhaver, D.; Sichmeller, C.; Peng, X. *J. Am. Chem. Soc.* **2008**, *130*, 5726-5735.
43. Clarke, S. J.; Hollmann, C. A.; Zhang, Z.; Suffern, D; Bradforth, S. E.; Dimitrijevic, N.; W. G. Minarik, W. G.; Nadeau J. L. *Nat. Mater.* **2006**, *5*, 409-417.
44. Aldana, J.; Wang, Y. A.; Peng, X. *J. Am. Chem. Soc.* **2001**, *123*, 8844-8850.
45. Aldana, J.; Lavelle, N.; Wang, Y.; Peng, X. *J. Am. Chem. Soc.* **2005**, *127*, 2496-2504.
46. Pathak, S.; Choi, S.; Arnheim, N.; Thompson, M. E. *J. Am. Chem. Soc.* **2001,** *123*, 4103-4104.
47. Querner, C.; Reiss, P.; Bleuse, J.; Pron, A. *J. Am. Chem. Soc.* **2004**, *126*, 11574-11582.
48. Dubois, F.; Mahler, B.; Dubertret, B.; Doris, E.; Mioskowski, C. *J. Am. Chem. Soc.* **2007**, *129*, 482-483.
49. Wuister, S. F.; Donega, C. D.; Meijerink A. *J. Phys. Chem. B* **2004**, *108*, 17393-17397.
50. Bullen, C.; Mulvaney, P. *Langmuir* **2006**, *22*, 3007-3013.
51. Kalyuzhny, G.; Murray, R. W. *J. Phys. Chem. B* **2005**, *109*, 7012-7021.
52. Kim, S.; Bawendi, M. G. *J. Am. Chem. Soc.* **2003**, *125*, 14652-14653.
53. Kim, S. W.; Kim, S.; Tracy, J. B.; Jasanoff, A.; Bawendi, M.G. *J. Am. Chem. Soc.* **2005**, *127*,4556-4557.
54. Yang, C. H.; Bhongale, C. J.; Chou, C. H.; Yang, S. H.; Lo, C. N.; Chen, T. M.; Hsu, C. S. *Polymer* **2007**, *48*, 116-128.

55. Potapova, I.; Mruk, R.; Hübner, C.; Zentel, R.; Basché, T.; Mews, A. *Angew. Chem. Int. Ed.* **2005**, *44*, 2437-2440.

56. Querner, C.; Benedetto, A.; Demadrille, R.; Rannou, P.; Reiss, P. *Chem. Mater.* **2006**, *18*, 4817-4826.

57. Wang, X. S.; Dykstra, T. E.; Salvador, M. R.; Manners, I.; Scholes, G. D.; Winnik, M. A. *J. Am. Chem. Soc.* **2004**, *126*, 7784-7785.

58. Wang, M. F.; Dykstra, T. E.; Lou, X. D.; Salvador, M. R.; Scholes, G. D.; Winnik, M. A. *Angew. Chem. Int. Ed.* **2006**, *45*, 2221-2224.

59. Wang, M.; Oh, J. K.; Dykstra, T. E.; Lou, X.; Scholes, G. D.; Winnik, M. A. *Macromolecules* **2006**, *39*, 3664-3672.

60. Skaff, H.; Emrick, T. *Chem. Commun.* **2003**, 52-53.

61. Milliron, D. J.; Alivisatos, A. P.; Pitois, C.; Edder, C.; Fréchet, J. M. J. *Adv. Mater.* **2003**, *5*, 58-61.

62. Wang, J. S.; Matyjaszewski, K. *J. Am. Chem. Soc.* **1995**, *117*, 5614-5615.

63. von Werne, T.; Patten, T. E. *J. Am. Chem. Soc.* **1999**, *121*, 7409-7410.

64. Sill, K.; Emrick, T. *Chem. Mater.* **2004**, *16*, 1240-1243.

65. Carrot, G.; Rutot-Houzé, D.; Pottier, A.; Degée, P.; Hilborn, J.; Dubois, P. *Macromolecules* **2002**, *35*, 8400-8404.

66. Skaff, H.; Emrick, T. *Angew. Chem. Int. Ed.* **2004**, *43*, 5383-5386.

67. Skaff, H.; Sill, K.; Emrick, T. Q. *J. Am. Chem. Soc.* **2004**, *126*, 11322-11325.

68. Skaff, H.; Ilker, M. F.; Coughlin, E. B.; Emrick, T. *J. Am. Chem. Soc.* **2002**, *124*, 5729-5733.

69. Jaffar, S.; Nam K. T.; Khademhosseini, A.; Xing, J.; Langer, R. S.; Belcher, A. M. *Nano. Lett.* **2004**, *4*, 1421-1425.

70. Schneider, G.; Decher, G. *Nano. Lett.* **2004**, *4*, 1833-1839.

71. Potapova, I.; Mruk, R.; Prehl, S.; Zentel, R.; Basché, T.; Mews, A. *J. Am. Chem.* Soc. **2003**, *125*, 320-321.

72. Yu, W. W.; Chang, E.; Falkner, J. C.; Zhang, J. Y.; Al-Somali, A. M.; Sayes C. M.; Johns, J.; Drezek, R.; Colvin, V. L. *J. Am. Chem. Soc.* **2007**, *129*, 2871-2879.

73. Luccardini, C.; Tribet, C.; Vial, F.; Marchi-Artzner, V.; Dahan, M. Langmuir **2006**, *22*, 2304-2310.

74. Uyeda, H. T.; Medintz, I. L.; Jaiswal, J. K.; Simon, S. M.; Mattoussi, H. *J. Am. Chem. Soc.* **2005**, *127*, 3870-3878.

75. Kim, S.; Bawendi, M. G *J. Am. Chem. Soc.* **2003**, *125*, 14652-14653.

76. Algar, W. R.; Krull, U. J. *ChemPhysChem* **2007**, *8*, 561-568.
77. Kumar, I. G.; Mandale, A. B.; Sastry, M. *Langmuir* **2000**, *16*, 9299-9302.
78. Liu, W.; Howarth, M.; Greytak, A. B.; Zheng, Y.; Nocera, D. G.; Ting, A. Y.; Bawendi, M. G. *J. Am. Chem. Soc.* **2008**, *130*, 1274-1284.
79. Jiang, H.; Jia, J. *J. Mater. Chem.* **2008**, *18*, 344 - 349
80. Nann, T. *Chem. Commun.* **2005**, 1735-1736.
81. Lin, W.; Fritz, K.; Guerin, G.; Bardajee, G. R.; Hinds, S.; Sukhovatkin, V.; Sargent, E. H.; Scholes, G. D.; Winnik M. A. *Langmuir* **2008**, *12*, 2304 – 2310.
82. Zhang, T.; Ge, J.; Hu, Y.; Yin, Y. *Nano Lett.* **2007**, *7*, 3203-3207.
83. Tian, Y.; Fendler, J. H. *Chem. Mater.* **1996**, *8*, 969-974.
84. Zhang, H.; Cui, Z.; Wong, Y.; Zhang, K.; Lu, X. J. C.;B. Yang, B.; Gao, M. *Adv. Mater.* **2003**, *15*, 777-780.
85. Petruska, M. A.; Bartko, A. P.; Klimov, V. I. *J. Am. Chem. Soc.* **2004**, *126*, 714-715.
86. Luccardini, C.; Tribet, C.; Vial, F.; Marchi-Artzner, V.; Dahan, M. *Langmuir* **2006**, *22*, 2304-2310.
87. Anderson, R. E.; Chan W. C. W. *ACS Nano* **2008**, *2*, 1341-1352.
88. Snee, P. T.; Somers, R. C.; Nair, G.; Zimmer, J. P.; Bawendi, M. G.; Nocera, D. G. *J. Am. Chem. Soc.* **2006**, *128*, 13320-13321.
89. Kairdolf, B. A.; Mancini, M. C.; Smith, A. M.; Nie, S. *Anal. Chem.* **2008**, *80*, 3029-3034.
90. Kairdolf, B. A.; Smith, A. M.; Nie, S. *J. Am. Chem. Soc.* **2008**, *130*, 12866-11286.
91. Pellegrino, T.; Manna, L. S.; Kudera, S.; Liedl, T.; Koktysh, D.; Rogach, A. L.; Keller, S.; Rädler, J.; Natile, G.; Parak, W. J. *Nano Lett.* **2004**, *4*, 703-707.
92. Di Corato, R.; Quarta, A.; Piacenza, P.; Ragusa, A.; Figuerola, A.; Buonsanti, R.; Cingolani, R.; Manna, L.; Pellegrino, T. *J. Mater. Chem.* **2008**, *18*, 1991-1996.
93. Shavel, A.; Gaponik, N.; Eychmuller, A. *ChemPhysChem.* **2005**, *6*, 449-453.
94. Xu, H.; Hong, R.; Lu, T.; Uzun, O.; Rotello V. M. *J. Am. Chem. Soc.* **2006**, *128*, 3162-3167.
95. Kotov, N. A.; Dekany, I.; Fendler, J. H. *J. Phys. Chem.* **1995**, *99*, 13065-13069.
96. Jaffar, S.; Nam, K. T.; Khademhosseini, A.; Xing, J.; Langer, R. S.; Belcher, A. M. *Nano Lett.* **2004**, *4*, 1421-1425.
97. Baron, R.; Huang' C. H.; Bassani, D. M.; Onopriyenko, A.; Zayats, M.; Willner, I. *Angew. Chem. Int. Ed.* **2005**, *44*, 4010-4015.

98. Vossmeyer, T.; Jia, S.; Delonno, E.; Diehl, M. R.; Kim, S.-H.; Peng, X.; Alivisatos, A. P.; Heath, J. R. *J. Appl. Phys.* **1998**, *84*, 3664-3666.

99. Pattani, V. P.; Li, C.; Desai, T. A.; Vu, T. Q. *Biomed. Microdev.* **2008**, *10*, 367–374.

100. Kim, L.; Anikeeva, P. O.; Coe-Sullivan, S. A.; Steckel, J. S.; Bawendi, M. G.; Bulovic, V. *Nano Lett.* **2008**, *8*, 4513–4517.

101. Dabbousi, B. O.; Bawendi, M. G.; Onotsuka, O.; Rubner, M. F. *Appl. Phys. Lett.* **1995**, *66*, 1316.

102. Schlamp, M. C.; Peng, X.; Alivisatos, A. P. *J. Appl. Phys.* **1997**, *82*, 5837-5842.

103. Rizzo, A.; Li, Y. Q.; Kudera, S.; Della Sala, F.; Zanella, M.; Parak, W. J.; Cingolani, R.; Manna, L.; Gitransistor, G.; Roth, R.; Lim, A. K. L.; Alivisatos, A. P.; McEuen, P. L. *Nature* **1997**, *389*, 699-701.

104. Nozik, J. *Physica E* **2002**, *14*, 115-120.

105. Plass, R.; Pelet, S.; Krueger, J.; Grätzel, M.; Bach, U. *J. Phys. Chem. B* **2002**, *106*, 7578-7580.

106. Huynh, W. U.; Dittmer, J. J.; Alivisatos, A. P. *Science* **2002**, *295*, 2425-2427.

107. Wang, P.; Abrusci, A.; Wong, H. M.; Svensson, M.; Andersson, M. R.; Greenham, N. C. *Nano Lett.* **2006**, *6*, 1789-1793.

108. Smith, A. M.; Duan, H.; Mohs, A. M.; Nie, S. *Adv. Drug Delivery Rev.* **2008**, *60*, 1226-1240.

109. Tada, H.; Higuchi, H.; Wanatabe, T. M.; Ohuchi, N. *Cancer Research* **2007**, *67*, 1138-1144.

110. Liu, W.; Howarth, M.; Greytak, A. B.; Zheng, Y.; Nocera, D. G.; Ting, A. Y.; Bawendi, M. G. *J. Am. Chem. Soc.* **2008**, *130*, 1274-1284.

111. Wu, M. X.; Liu, H.; Liu, J.; Haley, K. N.; Treadway, J. A.; Larson, J. P.; Ge, N.; Peale, F.; Bruchez, M. P. *Nat. Biotech.* **2003**, *21*, 41-46.

112. Jayagopal, A.; Russ, P. K.; Haselton, F. R. *Bioconjugate Chem.* **2007**, *18*, 1424-1433.

113. Thorne, R. G.; Nicholson C. *Proc. Nat. Acad. Sci.* **2006**, *103*, 5567-5572.

114. Dahan, M.; Laurence, T.; Pinaud, F.; Chemla, D. S.; Alivisatos, A. P.; Sauer, M.; Weiss, S. *Opt. Lett.* **2001**, *26*, 825-827.

115. Giraud, G.; Schulze, H.; Bachmann, T. T.; Campbell, C. J.; Mount, A. R.; Ghazal, P.; Khondoker, M. R.; Ross, A. J.; Ember, S. W. J.; Ciani, I.; Tlili, C.; Walton, A. J.; Terry, J. G.; Crain, J. *Int. J. Mol. Sci.* **2009**, *10*, 1930–1941.

116. Dahan, M.; Levi, S.; Luccardini, C.; Rostaing, P.; Riveau, B. A.; Triller, A. *Science* **2003**, *302*, 442-445.

117. Larson, D. R.; Zipfel, W. R.; Williams, R. M.; Clark, S. W.; Bruchez, M. P.; Wise, F. W.; Webb, W. W. *Science* **2003**, *300*, 1434-1436.
118. Derfus, A. M.; Chan, W. C. W.; Bhatia, S. N. *Nano Lett.* **2004**, *4*, 11-18.
119. www.invitrogen.com.
120. www.ieeeghn.org.
121. www.wi.mit.edu.
122. Goldman, E. R.; Medintz, I. L.;Whitley, J. L.; Hayhurst, A.; Clapp, A. R.; Uyeda, H. T.; Deschamps, J. R.; Lassman, M. E.; Mattoussi, H. *J. Am. Chem. Soc.* **2005**, *127*, 6744-6751.
123. Jin, W. J.; Fernandez-Argüelles, M. T.; Costa-Fernandez, J. M.; Pereiro, R.; Sanz-Medel A. *Chem. Commun.* **2005**, 883-885.
124. Fernandez-Argüelles, M. T.; Jin, W. J.; Costa-Fernandez, J. M.; Pereiro, R.; Sanz-Medel, A. *Anal. Chim. Acta* **2005**, *549*, 20-25.
125. Guasto, J.; Huang, P.; Breuer, K. *Exp. Fluids* **2006**, *41*, 869-872.
126. Guasto, J.; Breuer, K. *Exp. Fluids* **2008**, *45*, 157-161.
127. Tomasulo, M.; Yildiz, I.; Kaanumalle, S. L.; Raymo, F. M. *Langmuir* **2006**, *22*, 10284-10290.
128. Nazzal, A. Y.; Qu, L.; Peng, X.; Xiao, M. *Nano Lett.* **2003**, *3*, 819-822.
129. Burda, C.; Chen X.; Narayanan, R.; El-Sayed, M. A. *Chem Rev.* **2005**, 105,1025-1102.
130. Sandros, M. G.; Gao, D.; Benson, D. E. *J. Am. Chem. Soc.* **2005**, *127*, 12198-12201.
131. Clapp, A. R.; Medintz I. L.; Mattoussi, H. *ChemPhysChem* **2006**, *7*, 47-51.
132. Howarth, M.; Liu, W. H.; Puthenveetil, S.; Zheng, Y.; Marshall, L. F.; Schmidt, M. M.; Wittrup, K. D.; Bawendi, M. G.; Ting, A. Y. *Nat. Meth.* **2008**, *5*, 397-399.
133. Ebenstein, Y.; Nahum, E.; Banin, U. *Nano Lett.* **2002**, *2*, 945-950.
134. Nehilla, B. J. ; Vu, T. Q. ; Desai, T. A. *J. Phys. Chem. B* **2005**, *109*, 20724-20730.
135. Ebenstein, Y.; Mokari, T.; Banin, U. *Appl. Phys. Lett.* **2002**, *80*, 4033-4037.
136. Majetich, S. A.; Carter, A. C.; Belot, J.; McCullough R. D. *J. Phys. Chem.* **1994**, *98*, 13705-13710.
137. Sachleben, J. R.; Colvin, V.; Emsley, L.; Wooten, E. W.; Alivisatos, A. P. *J. Phys. Chem. B* **1998**, *102*,10117-101028.
138. Hens, Z.; Moreels, I.; Martins, J. C. *ChemPhysChem* **2005**, *6*, 2578-2584.
139. Moreels, I.; Fritzinger, B.; Martins, J. C.; Hens, Z. *J. Am. Chem. Soc.* **2008**, *130*, 15081-15086.

140. Yu, W. W.; Qu, L.; Guo, W.; Peng, X. *Chem. Mater.* **2003**, *15*, 2854-2860.

141. Montalti, M.; Credi, A.; Prodi, L.; Gandolfi, M. T. *Handbook of Photochemistry*, 3rd. Ed., CRC Press, **2006**, pp. 572-576.

142. Lakowicz, J. R. *Principles of Fluorescent Spectroscopy*, 2nd Ed., Kluwek Academic Plenum Press, **1999**, pp. 10-12.

143. Isutsu, K. *Electrochemistry in Non-aqueous Solutions*; Wiley: **2002**, ISBN 978-3-527-30516-2.

144. Quener, C.; Reiss, P.; Sadki, S.; Zagorska, M.; Pron A. *PCCP* **2005**, *7*, 3204-3209.

145. Ogawa, S.; Hu, K.; Fan, F. F.; Bard, A. J. *J. Phys. Chem. B* **1997**, *101*, 5707-5711.

146. Haram, S. K.; Quinn, B. M.; Bard, A. J. *J. Am. Chem. Soc.* **2001**, *123*, 8860-8861.

147. Ding, Z.; Quinn, B. M.; Haram, S. K.; Pell, L. E.; Korgel, B. A.; Bard A. J. *Science* **2002**, *296*, 1293-1295.

148. Myung, N.; Ding, Z. F.; Bard, A. J. *Nano Lett.* **2002**, *2*, 1315-1319.

149. Kucur, E.; Reigler, J.; Urban, G. A.; Nann, T. *J. Chem. Phys.* **2003**, *119*, 2333-2337.

150. Bae, Y.; Myung, N.; Bard, A. J. *Nano Lett.*, **2004**, *4*, 1153-1161.

151. Myung, N.; Lu, X.; Johnston K. P.; Bard A. J. *Nano Lett.* **2004**, *4*, 183-185.

152. Kucur, E.; Bucking, W.; Giernoth, R.; Nann, T. *J. Phys. Chem. B* **2005**, *109*, 20355-20360.

153. Poznyak, S. K.; Osipovich, N. P.; Shavel, A.; Talapin, D.V.; Gao, M.; Eychmuller, A.; Gaponik, N. *J. Phys. Chem. B* **2005**, 109, 1094-1100.

154. Ren, T.; Xu, J. Z.; Tu, Y. F.; Xu, S.; Zhu, J. J. *Electrochem. Commun.* **2005**, *7*, 5-9.

155. Bard, A. J.; Ding, Z.; Myung, N. *Struc. Bond*. **2005**, *118*, 1-57.

156. Li, Y.; Zhong, H.; Li, R.; Zhou, Y.; Yang, C.; Li, Y. *Adv. Funct. Mater.* **2006**, *16*, 1705-1716.

157. Kucur, E.; Bucking, W.; Arenz, S.; Giernoth, R.; Nann, T. *ChemPhysChem* **2006**, *7*, 77-81.

158. Osipovich, N. P.; Shavel, A.; Poznyak, S. K.; Gaponik, N.; Eychmuller, A. *J. Phys. Chem. B* **2006**, *110*, 19233-19237.

159. Inamdar, S. N.; Ingole, P. P.; Haram, S. K. *ChemPhysChem* **2008**, *9*, 2574-2579.

160. Kucur, E.; Bucking, W.; Nann, T. *Microchim. Acta* **2008**, *160*, 299-308.

161. Gaponik, N.; Poznyak, S. K.; Osipovich, N. P.; Shavel, A.; Eychmuller, A. *Microchim. Acta* **2008**, *160*, 327-334.

162. Cameron P. J., Nanoparticles at the Interfaces: the Electrochemical and Optical Properties of Nanoparticles Assembled into 2D and 3D Structures at Planar Electrode

Surfaces, in “Surface Design: Applications in Bioscience and Nanotechnology”, Förch, R.; Schönherr, H.; Jenkins, A. T. A, Eds.; Wiley: **2009**, ISBN: 978-3-527-40789-7.

Chapter 3

Photoluminescence Quenching of CdSe/ZnS Quantum Dots by Ferrocene Moieties*

Photoluminescence quenching of CdSe/ZnS quantum dots (QD) by molecular ferrocene and ferrocenyl thiols was investigated by steady state absorption and emission spectroscopy. Modification of QD surfaces with ferrocenyl thiols exhibiting different lengths of the alkyl chains (6, 8 and 11 carbon units) was performed by means of a ligand exchange reaction. These alkyl chains function as spacer between the QDs and ferrocene. Diffusion-filtered NMR spectroscopy was applied to characterize the surface of the modified nanoparticles. Ferrocene and ferrocenyl thiols bound to the QD surface efficiently quenched the QD photoluminescence. Charge transfer between the photoexcited QD and ferrocene is described as a possible quenching mechanism. At maximum surface coverage the quenching efficiency of ferrocenyl thiols at the QD surface depends on the hydrocarbon spacer length.

* Part of this Chapter has been published in: (a) Dorokhin, D.; Tomczak, N.; Velders, A. H.; Reinhoudt, D. N.; Vancso G. J. *J. Phys. Chem. C* **2009**, *113*, 18676-18680. (b) Dorokhin, D.; Tomczak, N.; Han, M. Y.; Reinhoudt, D. N.; Velders, A. H.; Vancso, G. J. *Polym. Mater. Sci. Eng.* **2009**, *101*, 1254-1255.

3.1 INTRODUCTION

Surface engineering of semiconductor nanocrystals (quantum dots, QDs) with inorganic and organic capping layers allows one to obtain tailored hybrid QDs for specific applications in sensors,[1] optoelectronics,[2,3] biolabelling,[4,5] and biodiagnostics.[6,7] In these applications the chemical and physicochemical nature of the capping layer plays a detrimental role. The surface ligands control the colloidal, chemical and photochemical stability, influence the photophysical properties of the QDs and define the (bio)chemical affinity to proteins,[8] carbon nanotubes,[9] or cell membranes.[10] There is particular interest to engineer the surface ligands such that they become responsive to external stimuli or to the molecular composition of the environment. This would allow one to fabricate QD optical "switches" [11] and "beacons" controllable by these stimuli.[1,2] In particular, the interactions between QDs and redox(electro)-active molecules are investigated in the context of biosensing[5,12-17] and fundamental nanoscale charge transfer processes.[18-21] Placing redox molecules in proximity to the QDs may have many advantages. Firstly, the redox species involved in the transfer of charges to and from the QDs can modulate the photoluminescence of the QDs.[13,17,22,23] Secondly, the redox state of redox-active ligands can be tuned by application of an external potential or by introducing oxidizing/reducing agents.[14,24] Thirdly, the photogenerated charges in the QD can take part in reduction/oxidation reactions with the species present in the nanoparticle shell.[12-14,25-29] In principle, all these approaches can be used in a variety of sensing schemes.[12-14,17,24,30-32]

Nanoparticles,[33,34] dendrimers[35,36] or inorganic clusters,[37] functionalized with multiple ferrocene units have attracted attention due to possible applications in sensing,[5,33,34,36] catalysis,[37,38] or in optoelectronic devices.[39] Ferrocenes are well-studied, thermally and chemically stable molecules in their oxidized, as well as reduced forms of the reversible Fc/Fc^{+} redox couple. Regarding the effects of ferrocene and its derivatives on the luminescence of QDs reports in the literature are somewhat confusing. For different ferrocenes and QDs little effect on fluorescence,[17,39] quenching [39-41] as well as fluorescence enhancement[39,40] were reported.

This chapter describes the quenching of QD photoluminescence by molecular ferrocene and ferrocenyl thiols in chloroform solutions. The surface of the QDs was modified via ligand exchange reactions with ferrocenyl thiols of variable spacer lengths, with 6, 8, and 11 carbon

units, changing therefore the distance between the ferrocene and the QD surface. The ferrocenyl-thiol quenching efficiency was found to depend on the linker length and it sharply increases when reducing the number of CH_2 units in the linker between the QD surface and the ferrocene.

3.2 RESULTS AND DISCUSSION

3.2.1 Characterization of CdSe/ZnS QDs

Core-shell CdSe/ZnS QDs were synthesized by decomposition of organometallic precursors at high temperature in the presence of a coordinating ligand[42] trioctylphosphine oxide (TOPO) as described by Jańczewski et al.[43] The ZnS shell grown on top of the CdSe core improves the photophysical properties of the QDs by passivating CdSe surface defects, which may act as traps for photogenerated holes or electrons.[44,45] The purified QDs have their first absorption peak located at ~580 nm and a symmetric emission peak located at ~605 nm with a full width at half maximum equal to 31 nm (Figure 3.1). The relatively narrow emission peak is a signature of a narrow distribution of QD diameters. The size of the QD CdSe core is estimated to be ~3.8 nm by using the empirical relationship as reported.[46] TEM imaging (Figure 3.1a) revealed a mean value of the diameter of the QDs of ~4.2 nm. From these values, and from the synthetic procedure, it is estimated that the CdSe cores are coated with ~2 monolayers of ZnS, but likely a distribution of ZnS shell thickness is present in the sample.

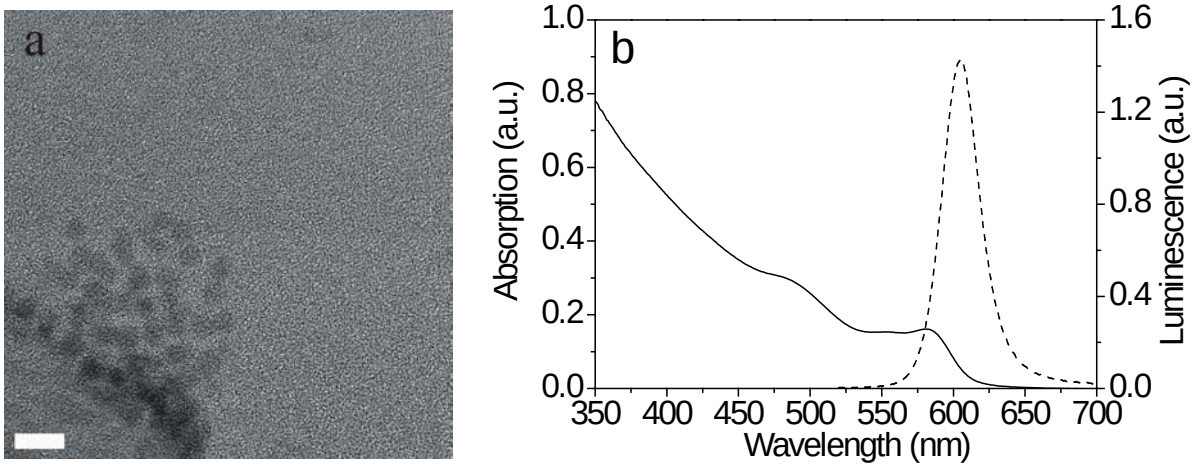

Figure 3.1 a) TEM image of CdSe/ZnS TOPO-coated QDs. Scale bar is 10 nm. b) Absorption (solid) and emission (dash) spectra of TOPO-coated CdSe/ZnS QD in

chloroform. The first absorption peak is located at ~580 nm, and the maximum of the emission is located at 605 nm (with 31 nm full width at half maximum value).

3.2.2 Luminescence Quenching of QDs with Molecular Ferrocene

Before proceeding with QD surface functionalization the influence of ferrocene on the luminescence emission of the CdSe/ZnS QDs was investigated. To this end, the steady state luminescence of QDs as a function of the ferrocene concentration and temperature (at 25 °C and 35 °C) was measured. The results of these experiments are presented in Figure 3.2 in the form of a Stern-Volmer (SV) plot. Figure 3.2 shows that upon addition of ferrocene to the solution of CdSe/ZnS/TOPO the luminescence of the QDs sharply decreases. Although the initial part of the quenching curve ([Fc]<4×10^{-7}M) is almost linear, at higher concentrations the curve bends upwards. The nonlinear behavior indicates that both static and dynamic quenching mechanisms are operative in the system. Static quenching is often attributed to binding of the quenchers to the surface of the QDs and passivation of surface charge traps, especially for core-only QDs, which leads to a "complex" formation between the luminophore and the quencher. Dynamic quenching at higher concentrations, on the other hand, is related to the diffusion of the quencher in the vicinity of the luminophore.[47] Upon increasing the temperature to 35 °C the same quenching efficiency is achieved at lower ferrocene concentrations. This is a typical behavior when dynamic quenching is responsible for the luminescence decrease. [47]

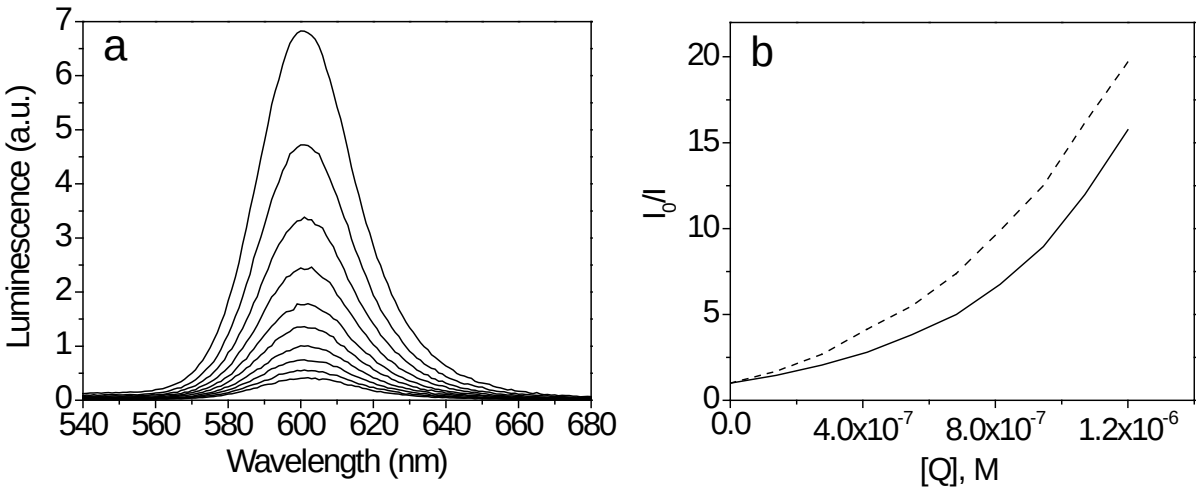

Figure 3.2 (a) Luminescence quenching of TOPO-coated CdSe/ZnS quantum dots upon

stepwise addition of ferrocene. b) Integrated emission intensity, extracted from (a), as a function of quencher concentration [Q] at two different temperatures 25 °C (solid) and 35 °C (dash).

For the static component some adsorption of ferrocene onto the QDs should be possible. While ferrocene does not have any coordinating group that could effectively displace TOPO from the QD surface, it is not possible to rule out that some of the ferrocene adsorbs directly onto TOPO, or to a defect site in the ligand shell.[48] It should be noted that the shape of the SV plot obtained in this study is different from the usually reported quenching saturation at higher concentrations.[49] Such saturation behavior was explained by exhaustion of possible passivation sites on the QD surface by the quencher and was mainly observed for, but not limited to,[49] core-only QDs.

Quenching by ferrocene can occur by either energy or electron transfer processes.[50] For the energy transfer to occur the absorption of ferrocene must overlap with the emission of the QD. Figure 3.3 shows the absorption of ferrocene and compounds **1-3** used in this study. Ferrocene and ferrocenyl thiols exhibit a broad absorption band around 440 nm. Exciting the QDs above the absorption band of the ferrocene ensures that the ferrocene remains in the ground state and there will be no conditions for the energy transfer from the QDs to the ferrocene to occur. Thus, excitation of the samples at 510 nm minimizes the probability for the energy transfer as a possible path for the deactivation of the QD excited state. On the other hand, electron transfer from the ferrocene to the QDs is not feasible for the same reason i.e. the excitation wavelength of 510 nm is above the absorption band of the ferrocene.

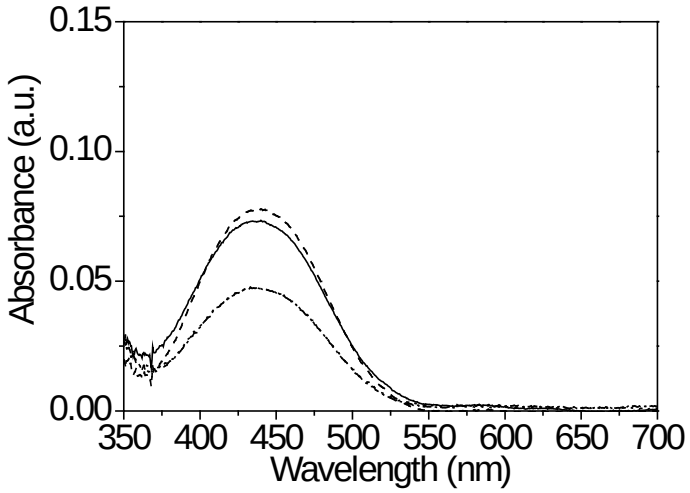

Figure 3.3 Absorption spectra of Fc (solid) and ferrocenyl thiols FcHT (dash), FcOT (dot) and FcUT (dash dot) in chloroform.

Therefore, photoinduced electron transfer from the ferrocene to QDs is not energetically favorable. No changes in the emission peak and spectral shape indicate that no new emission centers were formed. It is unlikely (although it cannot be ruled out entirely) that ferrocene displaces TOPO from the QD surface leading to the formation of new charge trapping centers at the QD surface. Therefore interactions between excited QDs and ground state ferrocene were probed. The observed photoluminescence quenching was ascribed to a photoinduced hole transfer between the QD and ferrocene.[25,48,51,52] The excitation light is being absorbed exclusively by the CdSe/ZnS QDs and the ferrocene species behave like outer-sphere electron donors.[15,22,25-27,53] A thermodynamically feasible electron transfer from the ferrocene to the valence band of the photoexcited QDs results in the formation of a nonluminescent, charged QD,[20,54] which is consistent with the observed decrease in luminescence. This happens despite the higher bandgap of the ZnS and TOPO coatings.[20,48] Additionally, Grela *et al.* have demonstrated that e.g. the photocatalytic oxidation of aromatic compounds does not require the direct attachment of the donors to the QDs surface and can proceed directly through electron transfer mechanisms.[22]

Thus, the results in this study show that ferrocene is a relatively strong quencher of the CdSe/ZnS luminescence and that the probable mechanism involves a photoinduced hole transfer. Ferrocene-coated QDs should therefore provide an attractive nanoparticle system with a redox active shell.

3.2.3 Synthesis and Characterization of Ferrocene-coated QDs

To place the ferrocene permanently in the vicinity of the QD the initial TOPO ligands were exchanged with three different ferrocenyl thiols (Figure 3.4). The chemical structure of the thiols varies in the number of the CH_2 units between the ferrocene and the thiol functionality, i.e. the distance between the thiol and the ferrocene is controlled by the alkyl spacer. Thiols were demonstrated to effectively displace TOPO from a ZnS surface by several ligand exchange reactions.[55] Taking into account the geometrical size of the nanoparticles and the surface coverage of a ferrocene sulfide monolayer on gold[56] the molar ratio between the ferrocenyl thiols and the QDs during the reaction was chosen as 1:100. Chloroform was used as the reaction medium as it is a good solvent for the TOPO-coated QDs and for ferrocene.

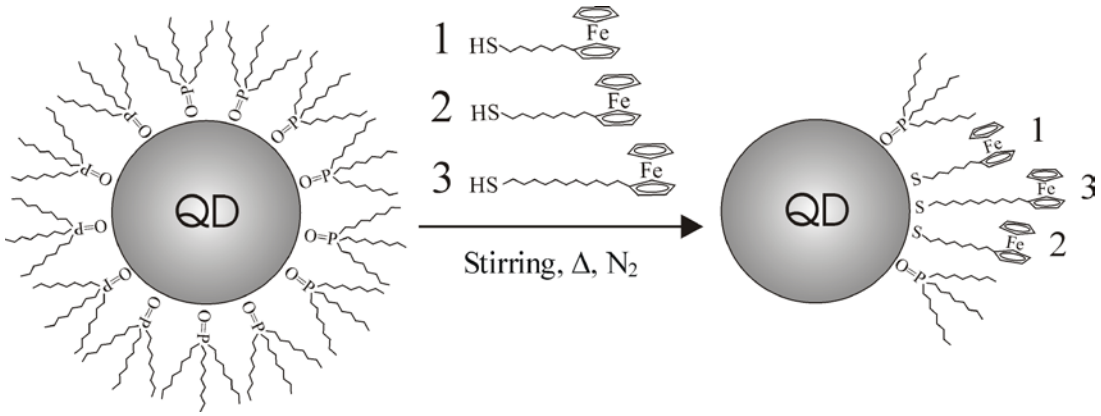

Figure 3.4 Ligand exchange reaction between TOPO-coated CdSe/ZnS QDs and ferrocenyl thiols **1-3**. The thiols differ in the number of CH_2 units (6, 8, and 11 units for compound **1**, **2**, and **3**, respectively) in the alkyl spacer.

For all thiols **1-3** the reaction volume, temperature, and time, and the molar ratio between the substrates were kept the same. The ferrocene-coated QDs could be conveniently purified by centrifugation. The purified samples were clear and transparent with no visible signs of aggregation or precipitation.

NMR spectroscopy was employed to prove that the ligand exchange reaction takes place, and that the new ligand binds to the surface of the quantum dots. Solution-state ^{1}H NMR spectroscopy is a powerful tool for the characterization and investigation of nanoparticles, including semiconducting nanocrystals.[57-60] In particular, the use of pulsed field gradient

(PFG) spectroscopy is a most valuable tool for the investigation of these relatively large systems that show relatively broad signals. PFG experiments allow the discrimination of small and larger molecules, using the different self-diffusion coefficients of the molecules. Discrimination of differently sized molecules can be obtained by performing the so-called DOSY experiments, yielding pseudo 2D plots where NMR signals from a mixture of compounds in solution are spread along a diffusion-coefficient axis.[61] Another, faster, easy-to-perform method is using the 1D sequence of a bipolar stimulated echo experiment with a fixed gradient strength and fixed diffusion time, which then acts like a filter. Signals of small solvent molecules, like toluene or water, and small organic molecules like TOPO or Fc thiols, can so readily be filtered out, leaving a clear spectrum of the functionalized QDs.

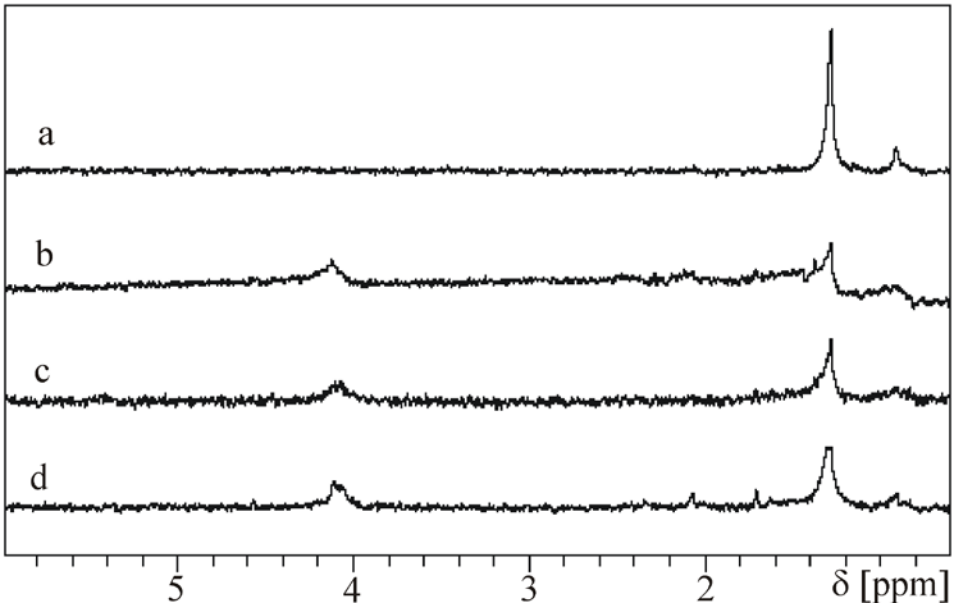

Figure 3.4 Diffusion-filtered NMR spectra of TOPO-coated CdSe/ZnS quantum dots (a) and functionalized with FcHT (b), FcOT (c) and FcUT (d) in deuterated chloroform. Peaks between 4-4.5 ppm correspond to the protons of the ferrocene cyclopentadienyl rings, peaks at 0.5-2 ppm correspond to the alkyl chains of TOPO and ferrocenyl thiol alkyl spacer.

In Figure 3.4 the diffusion-filtered ^{1}H spectra of QDs are shown. The used pulse sequence emphasizes the signals of relatively large molecules, suppressing those of small molecules, like residual protonated toluene, water, impurities, uncapped TOPO etc. In fact, the intense signals at high field in a normal experiment, almost completely vanish in the diffusion-weighted experiment. In Figure 3.4 the diffusion-filtered ^{1}H NMR spectra of FcHT, FcOT

and FcUT modified QDs are compared to the native TOPO-capped QDs. The TOPO-capped nanocrystals exhibit characteristic peaks of the alkyl chains with chemical shifts in the range of 1-2 ppm, but do not show peaks in the range of 4-5 ppm. The spectra of the FcHT, FcOT and FcUT modified QDs on the other hand show a broad peak in the range of 4-5 ppm, which can be attributed to the ferrocene protons of the FcHT, FcOT or FcUT ligands linked to the CdSe/ZnS QDs. The broad peaks around 1.5 ppm are related to the alkyl protons of the remaining TOPO, still present on the surface, and from the alkyl protons of the FcHT, FcOT or FcUT chains.

The ^{1}H NMR data of TOPO-capped QDs and the ferrocene-derivatized QDs unambiguously prove that ligand exchange reaction between TOPO and ferrocene thiols indeed has occurred. The lines of the ^{1}H NMR for the ferrocene region, were however, too broad to obtain reliable results for the molar ratios between the TOPO and Fc ligands present on the QD surface. Previous NMR studies have shown that during the ligand exchange reactions with thiols the TOPO ligands are replaced between 85 to 95 %.[62]

The progress (kinetics) of the ligand exchange reaction was monitored by recording changes in the luminescence spectra in time. In Figure 3.5 a plot of I/I_0 as a function of time is shown. The initial QD photoluminescence QY value is equal to 33 %. After addition of ferrocene thiols **1-3** the QY decreases in time. The characteristic times of the decays obtained from exponential decay fits (solid lines in Figure 3.5) are equal to 20.2+/-1.5 min, 14.7 +/-1.1 min and 14.2 +/- 1.1 min for FcUT, FcOT and FcHT, respectively. These results are one order of magnitude smaller than those reported earlier e.g. by Breus et al. for TOPO exchange with thiols.[49] To achieve complete coverage for each ligand the reaction continued for an additional 3 days, however the QY remained essentially the same as after 60 minutes reaction time. Interestingly, the quenching curves display slightly different kinetics depending on the ferrocenyl thiol ligand used (Figure 3.5). The FcHT molecules quench the luminescence most efficiently, followed by FcOT and FcUT. The QY obtained for each thiol coated QDs is equal to 1.7 %, 3.6 %, and 7.5 % for FcHT, FcOT and FcUT, respectively.

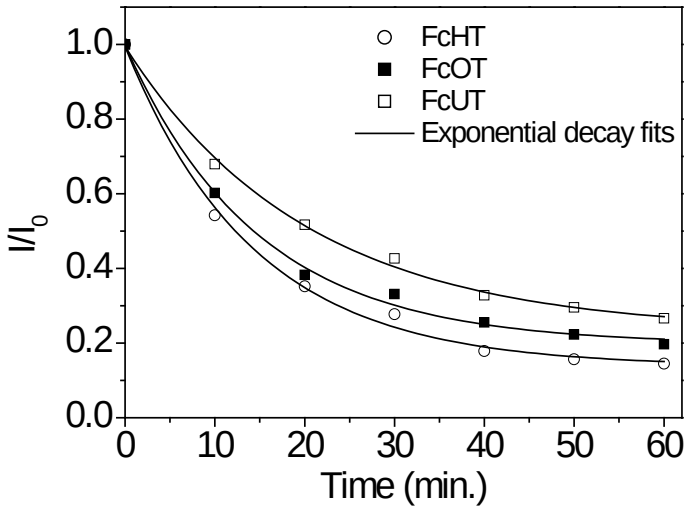

Figure 3.5 Integrated luminescence intensities normalized to the initial intensity I_0 and recorded in time during the ligand exchange reaction between CdSe/ZnS QDs and different ferrocenyl thiols. The solid lines are exponential decay fits to the experimental data.

3.2.4 Effects of Ferrocene Thiol Ligands on QD Luminescence

Only relatively minor changes are found in the absorption spectra of the modified QDs after the ligand exchange (Figure 3.6a). Thus one can exclude charge transfer to surface defect states[17] or structural transformation of the nanocrystals[63] as the possible reasons for the luminescence decrease. The ferrocene-coated samples are stable in solution under dark conditions for a period of months during which no changes in the absorption are visible. This indicates that no photoerosion of the CdSe cores takes place.

The mechanism for the quenching is likely the same as for molecular ferrocene. Unlike for uncapped CdSe, where the holes and electrons can occupy surface traps, passivation with ZnS should result in a confinement of the carriers to the core. The effect of the ligand passivating surface traps is therefore less pronounced. Indeed, ligand exchange reactions on ZnS-capped CdSe change the luminescence quantum yields much less comparing to surface modified CdSe.[64,65] Exchanging TOPO to thiols has been reported to either quench or enhance the luminescence of CdSe/ZnS QDs, however much smaller effects were reported than the quenching observed here. The role of the thiols will be therefore to passivate the ZnS surface without directly intercepting photoinduced charge carriers. Thus, in ferrocenyl thiol

coated QDs the photogenerated holes are directly intercepted by the ferrocene, resulting in a strongly reduced photoluminescence.

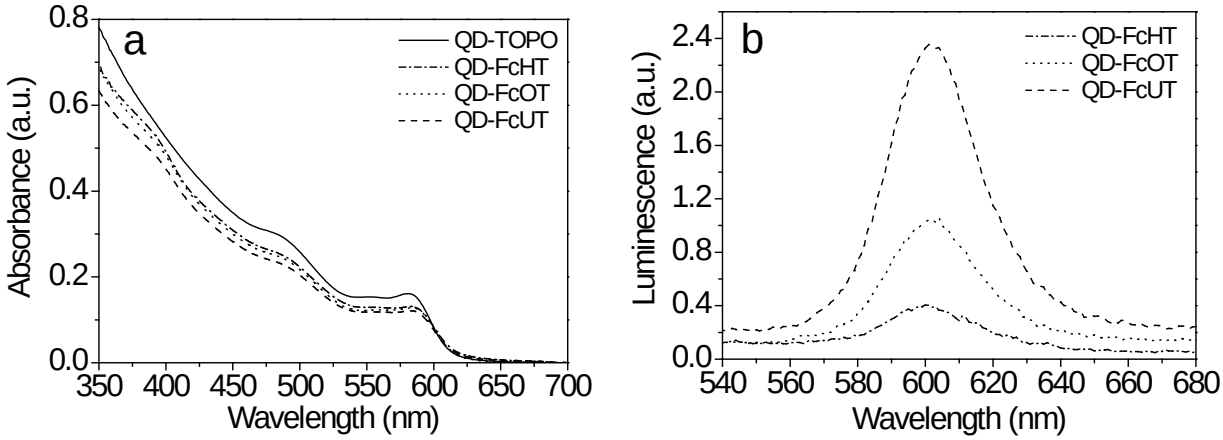

Figure 3.6 Absorption (a) and emission spectra (b) of CdSe/ZnS quantum dots modified with FcUT (dash), FcOT (dot) and FcHT (dash-dot) in chloroform. The excitation wavelength was 510 nm. The absorption spectrum of TOPO-caped QDs is also shown in (a) (solid).

The luminescence emission spectra of compounds **1**-**3** show different quenching effects (Figure 3.6b). The degree of quenching varies with the length of the alkyl chain. FcHT is the most efficient quencher, followed by the longer FcOT and then the longest FcUT derivative. The lengths of the thiols are estimated to be 12 Å, 15 Å, 19 Å for FcHT, FcOT, and FcUT, respectively. Quenching of QDs by ferrocene occurs therefore at relatively small distances and decays fast as a function of distance. The rate of the charge transfer processes is expected to fall off rapidly as a function of distance.[21,30,66] For ferrocenyl thiol longer than the TOPO ligand (~13 Å) the quenching efficiency is still pronounced. Molecular ferrocene diffusing in the solution or adsorbed to the TOPO layer could therefore also easily quench the QD luminescence, as reported in this study. The distance between the redox active center and the QDs is crucial in applications involving charge transfer.[30] For example, additional spacer layers are usually needed to prevent charge transfer processes to occur in favor of e.g. FRET.[24]

Although it is clear that the quenching is dominated by the presence of the ferrocene, subtle differences in the composition of the shell could also contribute to the observed differences in the QD photoluminescence quenching. Several studies have shown that the progress of the ligand exchange reaction may depend on the size of the thiol[67] and on the bulkiness of the

end-group.[68] The efficiency to replace TOPO from the surface of QDs for the ferrocenyl thiol having longer chain would be higher. Thus, the efficiency of the displacement of TOPO by the ferrocene derivatives should be of the following order FcUT>FcOT>FcHT. Finally, the changes in the hydrophobicity in the QD ligand shell, as reported,[69] should not play a role as the experiments were performed in chloroform rather than in aqueous medium.

3.3 CONCLUSIONS

Ferrocenyl thiols with variable length of the alkyl thiol were coated on the surface of CdSe/ZnS QDs. The presence of ferrocenyl thiols at the surface of QD was proven by diffusion-ordered NMR spectroscopy. The ligand exchange reaction was followed in time by monitoring the decrease of the luminescence efficiency of the nanocrystals. The QDs modified with ferrocene thiols show variable QYs depending on the length of the alkyl linker between ferrocene and the surface of the nanoparticles. With decrease of the alkyl spacer length the quenching efficiency increased. The quenching mechanism involves a hole transfer between the photoexcited QD and the ferrocene.

3.4 EXPERIMENTAL

Materials. Core-shell CdSe/ZnS semiconductor nanocrystals were synthesized by decomposition of organometallic precursors in an organic coordinating solvent as described by Janczewski *et al.*[43] Ferrocenyl-thiols, 6-ferrocenyl-1-hexanethiol (FcHT) (**1**), 8-ferrocenyl-1-octanethiol (FcOT) (**2**) and 11-ferrocenyl-1-udecanethiol (FcUT) (**3**), were obtained from Dojindo (Dojindo Europe, Amsterdam, The Netherlands) and used as received. Analytical grade chloroform and *d*-chloroform, as well as ferrocene were obtained from Aldrich.

Synthesis of ferrocenyl thiol-coated QD. The chloroform stock solutions of TOPO-coated QDs were purified by precipitation with methanol and centrifugation at 10000 rpm for 10 minutes. After decantation, the precipitated solid containing the QDs was re-dissolved in chloroform. Purified QDs (0.5mL, 2.72×10^{-6}M) and the chloroform solutions of ferrocenyl thiols (FcHT: 41.1μL, 3.3×10^{-3}M; FcOT: 44.91μL, 3.03×10^{-3}M; FcUT: 55.6μL, 2.69×10^{-3}M) were mixed in a three-neck flask equipped with a condenser and a thermometer. The reaction was carried out for 3 days at 40°C in nitrogen atmosphere. Following the reaction the solution was cooled down and the QDs were purified by precipitation in methanol and centrifugation at 10000 rpm for 5 minutes.

The progress of the reaction was monitored separately by placing the CdSe/ZnS QDs (2mL, 1.4×10^{-7}M) in a spectroscopic cuvette equipped with a stirring bar. The ferrocenyl thiol solutions (FcHT: 8.5μL, 3.31×10^{-3}M; FcOT: 9.2μL, 3.03×10^{-3}M; FcUT: 10μL, 2.69×10^{-3}M) were added to the QDs and the cuvette was placed in a 40^0C mineral oil bath. The emission was recorded in 10 minute intervals, and the progress of the reaction was monitored for 1 hour. The same procedure was applied to each of the ferrocenyl thiols **1-3**.

Luminescence of CdSe/ZnS in presence of molecular ferrocene. Purified QDs were dissolved in 1mL of chloroform (1.4×10^{-7}M) and placed in a quartz cuvette. Luminescence spectra were recorded by a fluorimeter during a stepwise addition of 5μL of a ferrocene solution (2.7×10^{-5}M) to the solution containing the QDs. The solution was excited at 510 nm and the emission spectra were recorded between 540 and 680 nm. The ratios I_0/I, where I_0 and I are the integrated emissions without and with ferrocene, respectively, were calculated after each addition of ferrocene. The experiments were performed at 25+/-2 °C and 35 +/-2 °C.

Methods. Transmission electron microscopy (TEM) images were obtained with a Philips CM300ST-FEG. For imaging, a drop of quantum dot solution in toluene was placed directly onto a copper grid and subsequently dried in air. At least 100 QDs were imaged to obtain statistically relevant results. The absorption spectra of quantum dot solutions in toluene and water were measured using a Varian Model Cary 300 UV-vis spectrophotometer. The photoluminescence spectra were recorded on an Edinburg XE-900 spectrofluorometer. The luminescence quantum yield (QY) for the substrates and products was estimated by comparing the integrated luminescence intensities to the $[Ru(bpy)_3]^{2+}$ complex standard (QY = 0.028).[70,71] Nuclear magnetic resonance spectra were recorded on a Bruker Avance II 600 MHz NMR spectrometer at room temperature, using an SEI 2.5 mm probe head equipped with z-axis gradient system. Appropriate 2.5 mm tubes were used to limit convection during the pulsed field gradient (PFG) experiments. Pseudo-2D DOSY experiments and 1D diffusion-filtered 1H experiments were performed using the bipolar stimulated echo sequence with typically a diffusion time (Δ) of 100 ms, and gradients between 5 and 95 % of maximum 35 Gauss.

3.5 REFERENCES

1. Murphy, C. J. *Anal. Chem.* **2002**, *74*, 520-526.
2. Colvin, V. L.; Schlamp, M. C.; Alivisatos, A. P. L. *Nature* **1994**, *370*, 354-357.
3. Klein, D. L.; Roth, R.; Lim, A. K. L.; Alivisatos, A. P.; McEuen, P. L. *Nature* **1997**, *389*, 699-701.
4. Medintz, I. L.; Uyeda, H. T.; Goldman, E. R.; Mattoussi, H. *Nat. Mater.* **2005**, *4*, 435-446.
5. Katz, E.; Willner, I.; Wang, J. *Electroanalysis* **2004**, *16*, 19-44.
6. Rosi, N. L.; Mirkin, C. A. *Chem. Rev.* **2005**, *105*, 1547-1562.
7. Michalet, X.; Pinaud, F. F.; Bentolila, L. A.; Tsay, J. M.; Doose, S.; Li, J. J.; Sundaresan, G.; Wu, A. M.; Gambhir, S. S.; Weiss, S. *Sience* **2005**, *307*, 538-544.
8. Chan, W. C. W.; Nie, S. *Science* **1998**, *281*, 2016-2018.
9. Hu, L.; Zhao, Y. L.; Ryu, K.; Zhou, C.; Stoddart, J. F. *Adv. Mater.* **2008**, 20, 939-940.
10. Lidke, D. S.; Nagy, P.; Heintzmann, R.; Arndt-Jovin, D. J.; Post, J. N.; Grecco, H. E.; Jares-Erijman, E. A. *Nature Biotechnology* **2004,** 22 , 198-203.
11. Zhang, R.; Wang, Z.;e Wu, Y.; Fu, H.; Yao, J. *Org. Lett.* **2008**, *10*, 3065-3068.
12. Clarke, S. J.; Hollmann, C. A.; Zhang, Z.; Suffern, D.; Bradforth, S. E.; Dimitrijevic, N. N.; Minarik, W. G.; Nadeau, J. L. *Nat. Mater.* **2006**, *5*, 409-417.
13. Yildiz, I.; Tomasulo, M.; Raymo, F. M. *Proc. Natl. Acad. Sci.* **2006**, *103*, 11457-11460.
14. Gill, R.; Freeman, R.; Xu J.-P.; Willner, I.; Winograd, S.; Shweky, I.; Banin, U. *J. Am. Chem. Soc*. **2006**, *128*, 15376.
15. Pardo-Yissar, V.; Katz, E.; Wasserman, J.; Willner, I. *J. Am. Chem. Soc*. **2003**, *125*, 622-623.
16. Han, G.; Mokari, T.; Ajo-Franklin, C.; Cohen, B. E. *J. Am. Chem. Soc.* **2008**, *130*, 15811-15815.
17. Medintz, I. L.; Pons, T.; Trammell, S. A.; Grimes, A. F.; English, D. A.; Blanco-Canosa, J. B.; Dawson, P. E.; Mattoussi, H. *J. Am. Chem. Soc.* **2008**, *130*, 16745-16750.
18. Adams, D. M.; Brus, L.; Chidsey, C. E. D.; Creager, S; Creutz, C.; Kagan, C. R.; Kamat, P. V.; Lieberman, M.; Lindsay, S; Marcus, R. A.; Metzger, R. M.; Michel-Beyerle, M. E.; Miller, J. R.; Newton, M. D.; Rolison, D. R.; Sankey, O.; Schanze, K. S.; Yardley, S.; Zhu, X. *J. Phys. Chem. B* **2003**, *107*, 6668-6697.

19. Scholes G. D. *ACS Nano* **2008**, *2*, 523-537
20. Gooding, A. K.; Gomez, D. E.; Mulvaney P. *ACS Nano* **2008**, *2*, 669-676.
21. Anderson, N. A.; Lian, T. *Annu. Rev. Phys. Chem.* **2005**, *56*, 491-519.
22. Grela, M. A.; Brusa, M. A.; Colussi, A. J. *J. Phys. Chem. B*, **1999**, *103*, 6400-6402.
23. Galian, R. E.; de la Guardia, M.; Perez-Prieto J. *J. Am. Chem. Soc.*, **2009**, *131*, 892-897.
24. Freeman, R.; Gill R.; Shweky, I.; Kotler, M.; Banin, U.; Willner I. *Angew. Chem. Int. Ed.* **2009**, *48*, 309-310.
25. Schmelz, O.; Mews, A.; Basche, T.; Herrman, A.; Müllen, K. *Langmuir* **2001**, *17*, 2861-2865.
26. Sharma, S. N.; Pillai, Z. S.; Kamat, P. V. *J. Phys. Chem. B* **2003**, *107*, 10088-10093.
27. Blackburn, J. L.; Selmarten, D. C.; Ellingson, R. J.; Jones, M.; Micic, O.; Nozik, A. J. *J. Phys. Chem. B* **2005**, *109*, 2625-2631.
28. Huang, J.; Stockwell, D.; Huang, Z.; Mohler, D. L.; Lian, T. *J. Am. Chem. Soc.* **2008**, *130*, 5632-5633.
29. Boulesbaa, A.; Issac, A.; Stockwell, D.; Huang, Z.; Huang, J.; Guo, J.; Lian, T. *J. Am. Chem. Soc.* **2007**, *129*, 15132-15133.
30. Sandros, M. G.; Goa, D.; Benson, D. E. *J. Am. Chem. Soc.* **2005**, *127*, 12198-12199.
31. Ipe, B. I.; Niemeyer, C. M. *Angew. Chem. Int. Ed.* **2006,** *45*, 504-506.w
32. Fruk, L.; Rajendran, V.; Spengler, M.; Niemeyer, C. M. *ChemBioChem* **2007**, *8*, 2195-2198.
33. Qiu, J.-D.; Guo, J.; Liang, R.-P.; Xiong, M. A. *Electroanalysis* **2007**, *19*, 2335-2341.
34. Labande, J. R.; Ruiz, J.; Astruc, D. *J. Am. Chem. Soc.* **2002**, *124*, 1782-1789.
35. Ornelas, C.; Ruiz, J.; Belin, C.; Astruc, D. *J. Am. Chem. Soc.* **2009**, *131*, 590-601.
36. Kaifer A. E. *Eur. J. Inorg. Chem.* **2007**, 5015-5027.
37. Ingram, R. S.; Hostetler, M. J.; Murray, R. W. *J. Am. Chem. Soc.* **1997**, *119*, 9175-9178.
38. Budny, A.; Novak, F.; Plumere, N.; Schetter, B.; Speiser, B.; Straub, D.; Mayer, H. A.; Reginek, M. *Langmuir* **2006**, *22*, 10605-10611.
39. Cyr, P. W.; Tzolov, M.; Hines, M. A.; Manners, I.; Sargent, E. H.; Scholes, G. D. *J. Mater. Chem.* **2003**, *13*, 2213-2219.
40. Chandler, R. R.; Coffer, L. J.; Atherton, S. J.; Snowden, P. T. *J. Phys. Chem.* **1992**, *96*, 2713-2717.
41. Palaniappan, K.; Hackney, S. A.; Liu, J. *Chem. Commun.* **2004**, 2704-2705.

42. Murray, C. B.; Norris, D. J.; Bawendi, M. G. *J. Am. Chem. Soc.*, **1993**, *115*, 8706-8715.

43. Jańczewski, D.; Tomczak, N.; Khin, Y. W.; Han, M. Y.; Vancso G. J. *Eur. Pol. J.* **2009**, *45*, 3-9.

44. Hines, M. A.; Guyot-Sionnest, P. *J. Phys. Chem.* **1996**, *100*, 468-471.

45. Peng, X. G.; Schlamp, M. C.; Kadavanich, A. V.; Alivisatos, A. P. *J. Am. Chem. Soc.* **1997**, *119*, 7019-7023.

46. Yu, W. W.; Qu, L.; Guo, W.; Peng, X. *Chem. Mater.* **2003**, *15*, 2854-2860.

47. Lakowicz, J. R *Principles of fluorescent spectroscopy*, 2nd Ed., Kluwek Academic/ Plenum Press 1999, p 237-264.

48. Vinayakan, R.; Shanmugapriya, T.; Nair, P. V.; Ramamurthy, P.; Thomas, K. G. *J. Phys. Chem. C* **2007**, *111*, 10146-10149.

49. Breus, V. V.; Heyes, C. D.; Neinhaus, G. U. *J. Phys. Chem. C* **2007**, *111*, 18589-18594.a

50. Fergy-Forgues, S.; Delavaux-Nicot, B. *J. Photochem. Photobiol. A* **2000**, *132*, 137-159.

51. Sykora, M.; Petruska, M. A.; Alstrum-Acevedo, J.; Bezel, I.; Meyer, T. J.; Klimov, V. I. *J. Am. Chem. Soc.* **2006**, *128*, 9984-9985.

52. Zhang, Y.; Jing, P.; Zeng, Q.; Sun, Y.; Su, H.; Wang, Y. A.; Kong, X.; Zhao, J.; Zhang, H. *J. Phys. Chem. C* **2009**, *113*, 1886-1890.

53. Klimov, V. I.; Mikhailovsky, A. A.; McBranch, D. W.; Leatherdale, C. A.; Bawendi, M. G. *Phys. Rev. B* **2000**, *61*, R13349.

54. Wang, C.; Shim, M.; Guyot-Sionnest, P. *Science* **2001**, *291*, 2390-2392.

55. Querner, C.; Reiss, P.; Bleuse, J.; Pron, A. *J. Am. Chem. Soc.* **2004**, *126*, 11574-11582.

56. Beulen, M. W. J.; Veggel, F. C. J. M; Reinhoudt, D. N. *Chem. Commun.* **1999**, *6*, 503-505.

57. Berrettini, M. G.; Braun, G.; Hu, J. G.; Strouse, G. F. *J. Am. Chem. Soc.* **2004**, *126*, 7063-7070.

58. Voets, I. K.; De Keizer, A.; De Waard, P.; Frederik, P. M.; Bomans, P. H. H.; Schmalz, H.; Walther, A.; King, S. M.; Leermakers, F. A. M.; Cohen Stuart, M. A. *Angew. Chem. Int. Ed.* **2006**, *45*, 6673-6676.

59. Fery-Forgues, S.; Delavaux-Nicot, B. *J. Photochem. Photobiol. A* **2000**, *132*, 137-159.

60. Leatherdale, C. A.; Bawendi, M. G. *Phys. Rev. B* **2001**, *63*, 165315-165321.

61. Rekharsky, M. V.; Inoue, Y. *Chem. Rev.* **1998**, 98, 1875-1917.

62. Sachleben, J. R.; Wooten, E. W.; Emsley, L.; Pines, A.; Colvin, V. L.; Alivisatos, A.P. *Chem. Phys. Lett.* **1992**, *198*, 431-433.

63. Landes, C.; Braun, M.; Burda, C.; El-Sayed, M. A. *Nano Lett.* **2001**, *1*, 667-670.

64. Landes, C.; Burda, C.; Braun, M.; El-Sayed, M. A. *J. Phys. Chem. B* **2001**, *105*, 2981-2986.

65. Wuister, S. F.; de Mello Donega, C.; Meijerink A. *J. Phys. Chem. B* **2004**, *108*, 17393-17398.

66. Barbara, P. F.; Meyer, T. J.; Ratner, M. A. *J. Phys. Chem.* **1996**, *100*, 13148-13168.

67. Woehrle, G. H.; Brown, L. O.; Hutchison J. E. *J. Am. Chem. Soc.* **2005**, *127*, 2172-2183.

68. Hostetler, M. J.; Templeton, A. C.; Murray R. W. *Langmuir* **1999**, *15*, 3782-3789.

69. Blum, A. S.; Moore, M. H.; Ratna, B. R. *Langmuir* **2008**, *24*, 9194-9197.

70. Montalti, M.; Credi, A.; Prodi, L.; Gandolfi, M. T. *Handbook of Photochemistry*, 3rd. Ed., CRC Press, **2006**, pp. 572-576.

71. Lakowicz, J. R. *Principles of Fluorescent Spectroscopy*, 2nd Ed., Kluwek Academic/ Plenum Press, **1999**, pp. 10-12.

Chapter 4

Electrochemistry of Ferrocene-coated CdSe/ZnS Quantum Dots

Electrochemical properties of core-shell CdSe/ZnS Quantum Dots (QDs) in a non-aqueous solution are presented. Cathodic reduction and anodic oxidation processes involving the QD HOMO and LUMO levels as well as defect states were identified by cyclic voltammetry. The electrochemical bandgap was estimated from the anodic and cathodic redox peaks and found to match well the optical bandgap estimated from the absorption spectrum. Cyclic voltammetry showed that the redox potentials of the QDs are modified due to the presence of ferrocene on the surface of the QD. The QD oxidation peak decreased and the reduction peak shifted to more negative potentials. Concurrent shift of the ferrocene redox peaks indicates that the system displays features of a "molecular hybrid", where both the QD and the ligand influence each other.

4.1 INTRODUCTION

Nanoscale components of novel electronic device architectures for sensing or optoelectronic applications may be composed of single molecules or nanoparticles.[1,2] In this context, semiconductor nanocrystals (Quantum Dots, QD) offer unique optical and electronic properties. Most notably, the so-called confinement effects result in discrete energy levels, and size-tunable bandgaps.[3,4] Since QDs are expected to undergo electron transfer through the valence and conduction bands, this confinement results in size-dependent enhancement of the redox potentials for photoexcited electrons and holes through increase in the energy difference between the HOMO and LUMO energy levels.[5-7] Surface-bound redox-active molecules interfacing QDs with other device components or mediating the electron transfer between the QDs and species in solution find applications as redox-responsive optical beacons, switches or electron relays for sensing and nanoelectronics.[2,3,8-10] Investigating such systems is also important from the point of view of the understanding of fundamental aspects of electron transfer.[11-13] It has also been suggested that photodriven redox reactions on colloidal semiconductor nanoparticles could contribute to prebiotic synthesis.[14]

Although the synthesis of monodisperse QDs,[15,16] and their surface chemical derivatization have been well developed,[17] surface functionalization with redox-active molecules is relatively unexplored.[18-19] Electrochemistry has only recently been added to the list of characterization techniques, which are used to study QD materials. Photoelectrochemical investigations of QDs allow for the determination of absolute energetic positions of band edges and obtaining directly the electron affinity and ionization potentials of QDs as a function of their size.[19-43] Besides studies of the quantum confinement effects in QDs, electrochemistry has also been used to probe QD surface states and to monitor the evolution of these states during photochemical processing.[31,32,37]

It has been shown in chapter 3 that ferrocene (Fc), and its derivatives, act as quenchers of the QD luminescence via a process likely involving photoinduced electron transfer. QDs with surface-bound Fc ligands are therefore an interesting system to electrochemically study electron transfer processes.[19,44] This chapter describes the electrochemical characterization of CdSe/ZnS nanocrystals in non-aqueous solutions. The cyclic voltammetry allows for the estimation of electrochemical bandgaps of the QDs from the position of the anodic and cathodic redox peaks. The electrochemical bandgap correlates well with the optical bandgap.

The electrochemical response of QDs is sensitive to the presence of redox active species, like Fc, on their surface. In this study 6-ferrocenyl-1-hexanethiol (FcHT) was utilized as redox active mediator for QDs surface modification. A new electrochemical peak of ferrocene appears on the cyclic voltammograms and the anodic and cathodic redox peaks of the QD are shifted due to the presence of the Fc ligand.

4.2 RESULTS AND DISCUSSION

4.2.1 Modification of the QDs with 6-Ferrocen-1-hexanethiol

The QDs were synthesized by decomposition of organometallic precursors in the presence of a coordinating solvent (TOPO) according to the procedure mentioned in the chapter 3. The stock solution of TOPO-coated QD was purified by precipitation in a poor solvent, e.g. methanol, repeated centrifugation to remove the excess of TOPO, and redispersion in a good solvent, e.g. toluene. After purification the solutions were clear and transparent with no visible signs of aggregation or precipitation.

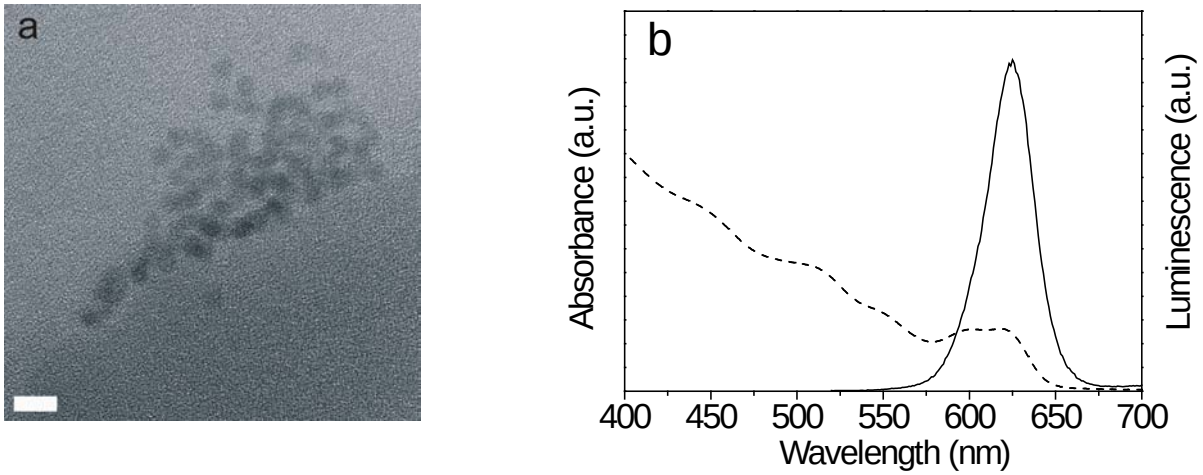

Figure 4.1. a) Transmission electron microscope image of individual QDs; the scale bar is 10 nm. The mean value of the diameter of the nanocrystals was ~ 5.2 nm. b) UV-vis absorption (dash) and photoluminescence spectra (solid) (λ_{ex} = 510 nm) of TOPO-coated CdSe/ZnS in toluene. The emission maximum is located at 625 nm; the value of the full width at half maximum is equal to 32 nm.

A representative TEM image of individual CdSe/ZnS nanocrystals is shown in Figure 4.1a. From the TEM images the mean value of the diameter of the QDs was estimated to be 5.2 nm. The absorption and emission spectra of the QDs are shown in Figure 4.1b. The first

absorption peak is located at ~618 nm. The emission spectrum peaks at ~ 625 nm and is relatively narrow with a full width at half maximum (fwhm) value equal to 32 nm. The quantum yield (QY) was estimated to be equal to 28 %.

For modification of QDs with FcHT the ligand exchange procedure described in detail in chapter 3 was used. However, a longer reaction time of 6 days was used. The unreacted ferrocene derivative and TOPO were removed from the reaction solution by ultracentrifugation.

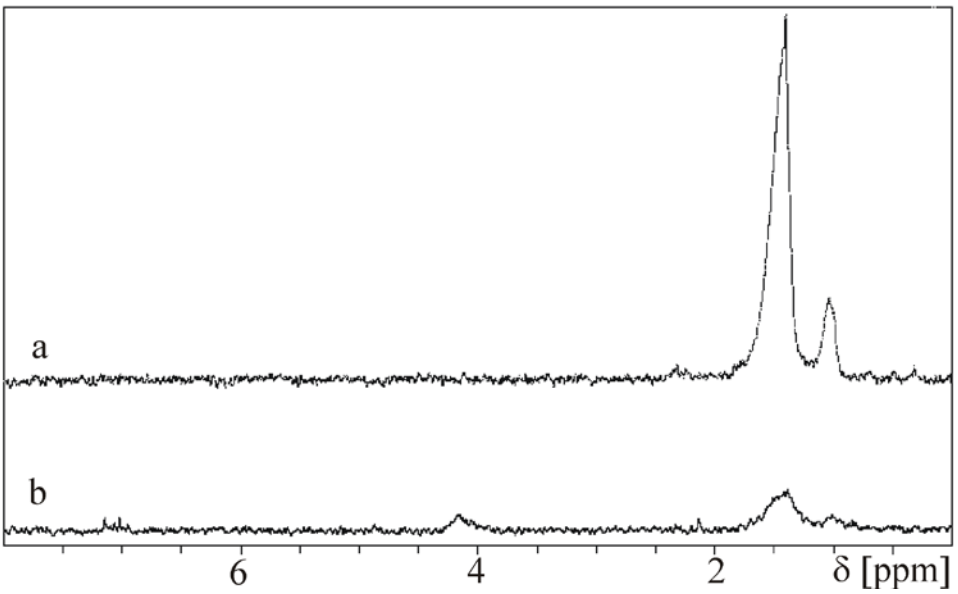

Figure 4.2. Diffusion-filtered ^{1}H NMR spectra of (a) CdSe/ZnS-TOPO and (b) CdSe/ZnS-FcHT in *d*-toluene. Chemical shifts in the range of 1-2 ppm are attributed to alkyl chains of TOPO and the ferrocene derivative. Peaks in the range of 4-4.5 ppm are attributed to the ferrocene protons of the FcHT ligands linked to the QD surface.

To obtain evidence that the ligand exchange reaction has been performed successfully and that the ferrocene thiols replaced TOPO from the QD surface, NMR spectroscopy was used. As it is described in chapter 3, NMR measurements allow one to prove that ligand exchange reactions occured. The diffusion-filtered ^{1}H spectra of FcHT-modified and unmodified nanoparticles are depicted in Figure 4.2.

The TOPO-capped nanocrystals exhibit characteristic peaks of the alkyl chains with chemicals shifts in the range of 1-2 ppm, but do not show peaks in the range of 4-5 ppm. On the other hand, the spectrum of QDs coated with FcHT shows a broad peak in the range of 4-5 ppm, which corresponds to the protons of the aromatic rings of the ferrocenyl thiol molecules. The alkyl protons of FcHT and those of the remaining TOPO on the surface of nanoparticles result in broad peaks positioned around 1.5 ppm. The data obtained with ^{1}H NMR spectroscopy prove that ligand exchange reaction between TOPO and ferrocene thiols indeed occurred.

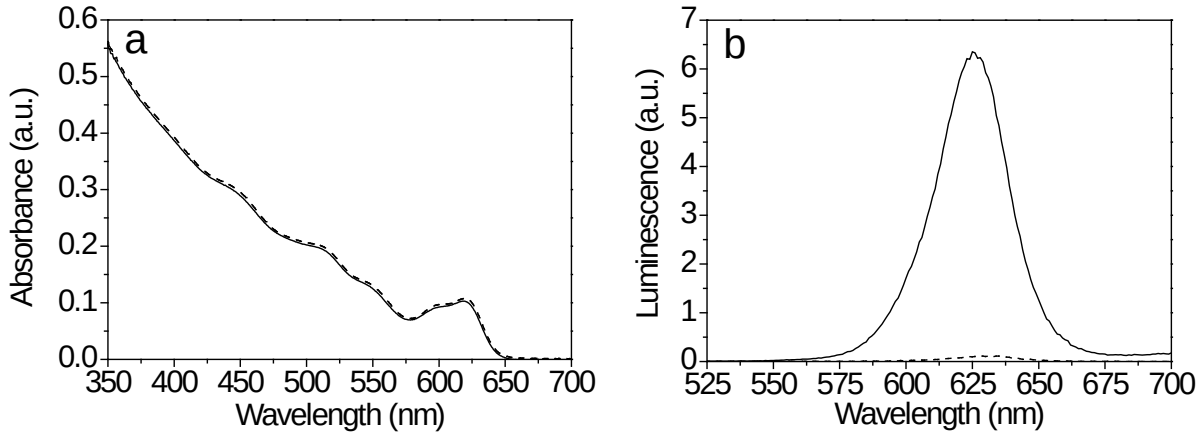

Figure 4.3. (a) Absorption and (b) emission spectra of QD-TOPO (solid) and QD-FcHT (dash) in toluene. Excitation wavelength was 510 nm.

Essentially no significant changes in the absorption profile of the UV-Vis spectra were found after the ligand exchange reaction in comparison to the original TOPO-coated QDs (Figure 4.3a). However, the luminescence of the QDs upon attachment of FcHT significantly decreased (Figure 4.3b). Excitation of the FcHT-modified QDs at 510 nm results in a relatively weak emission, and the QY of the QD-FcHT samples was estimated to be 0.89%. It is important to mention that the QY of Fc-coated QDs depended on the reaction time and, therefore, also on the surface coverage. Higher surface coverage and longer reaction times lead to lower QY (see chapter 3). Absence of significant changes in the absorption spectra between modified and unmodified QDs indicates that the decrease in luminescence is due to the presence of ferrocene rather than to changes in the QD composition or size due to long reactions times or higher reaction temperature.

4.2.2 Electrochemical Properties of TOPO-coated QDs and QDs Modified with 6-Ferrocen-1-hexanethiol

The electrochemical experiments were performed in a 5 mL electrochemical cell with a three electrode configuration. Glassy carbon electrodes were used in the measurements due to access to a wide potential window, chemical inertness, and low background current.[46] Furthermore, by the use of carbon electrodes possible chemisorption of the ferrocene thiols on the surface of the electrodes made of noble metals like Au or Pt could also be suppressed. The electrode potentials were recorded *versus* a reference Ag|AgCl electrode. The oxygen was removed from the system before each measurement by purging with N_2. The concentrations of TOPO-coated and FcHT-modified QDs were equal to 0.8×10^{-8} M and 1×10^{-8} M respectively, as estimated using the method described by Yu et al.[47] After addition of CdSeZnS QDs to the supporting electrolyte solution, a number of cathodic (C) and anodic (A) peaks appeared on the cyclic voltammogram (CV).

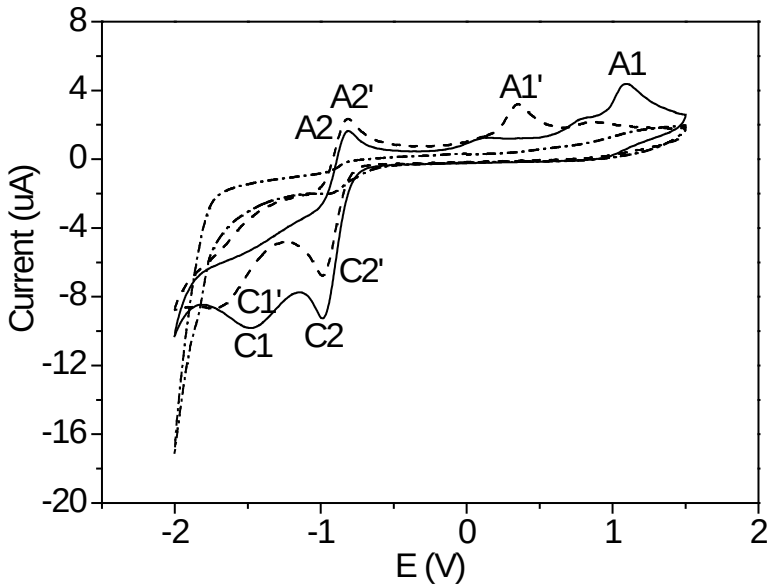

Figure 4.4 CV response of TOPO-capped CdSe/ZnS quantum dots (solid), FcHT modified QDs (dash) and baseline of the glassy carbon electrodes (dot dash). Potential scan rate was equal to 50 mV/s.

Scanning towards negative potentials gave two reduction peaks C1 and C2 with maximum values at -1.5 and -1 V, respectively (Figure 4.4). The anodic peaks were observed when the potentials were swept from the negative to the positive direction. Two well distinguished oxidation peaks A1 at 1 V and A2 at -0.8 V were visible. A number of broad peaks in the

region between -0.1 and 0.9 V are attributed to defect states of the QDs.[31,32] Apparently, the ZnS shell does not affect the charge injection to the CdSe core since electron injection occurs at potentials well below the predicted conduction energy level for ZnS.[48] The redox reactions are not reversible and constitute a multi-electron process, whereby the electrons are consumed by fast coupled chemical reactions leading to the decomposition of the QDs on the electrode or in its close proximity. Such behaviour was described earlier in the literature by Bard et. al.[24,34] Although the oxidation reactions should induce anodic decomposition of the clusters, the presence of the ZnS shell may prevent it. Additionally, a blue shift in the absorption spectrum was not observed. Thus the photocorrosion happens at the internal interface between CdSe and ZnS. The additional cathodic and anodic peaks A2 and C2 in the middle of the cyclic voltammogram are associated with these electrochemical processes.[24,29,33,49]

The reduction and oxidation peaks C1 and A1, respectively, are related to the electron and hole injection into the conduction and valence bands. Cyclic voltammetry thus allows to determine the E_{HOMO} (from $E_{ox.}$) and E_{LUMO} (from $E_{red.}$) values directly.[28] This complements nicely the optical spectroscopic techniques, which give only information on the energetic differences between electronic states. From the peak-to-peak separation between A1 and C1 the value of the electrochemical bandgap is estimated to be equal to 1.98 eV (CV potential scan rate equal to 50 mV/s), which is comparable to the bandgap of 1.92 eV calculated from the electronic spectra (see Table 4.1).

Table 4.1 TOPO-CdSe/ZnS nanocrystal oxidation and reduction potentials, absolute HOMO and LUMO energy levels, and energy bandgap values determined electrochemically and optically.

$E_{g,\,opt.}$ (eV)[a]	$E_{ox.}$ (V)[b]	$E_{red.}$ (V)[b]	E_{LUMO} (eV)[a]	E_{HOMO} (eV)[a]	$E_{g,\,el.}$ (eV)
1.92	1.03	-1.31	-3.60	-5.58	1.98

[a] Calculated by following the procedure described in [28].

[b] Estimated from the current peaks on the cyclic voltammograms obtained at a scan rate of 50 mV/s.

Electrochemical studies performed earlier showed that when decreasing the QD size the position of the oxidation and reduction peaks shifts toward higher and lower potential values,

respectively, resulting in higher electrochemical bandgaps.[24,28,32] The higher value of the electrochemical bandgap reported here as compared to the bulk (1.74 eV) is therefore a manifestation of a quantum confinement effect.[19,24,28,32] The result obtained in this study fits very well with the data presented by Querner et al. and Inamdar et al. showing the comparison between the results of the quantum confinement effect of CdSe QDs on the electrochemically estimated bandgap values taken from different studies.[19,38]

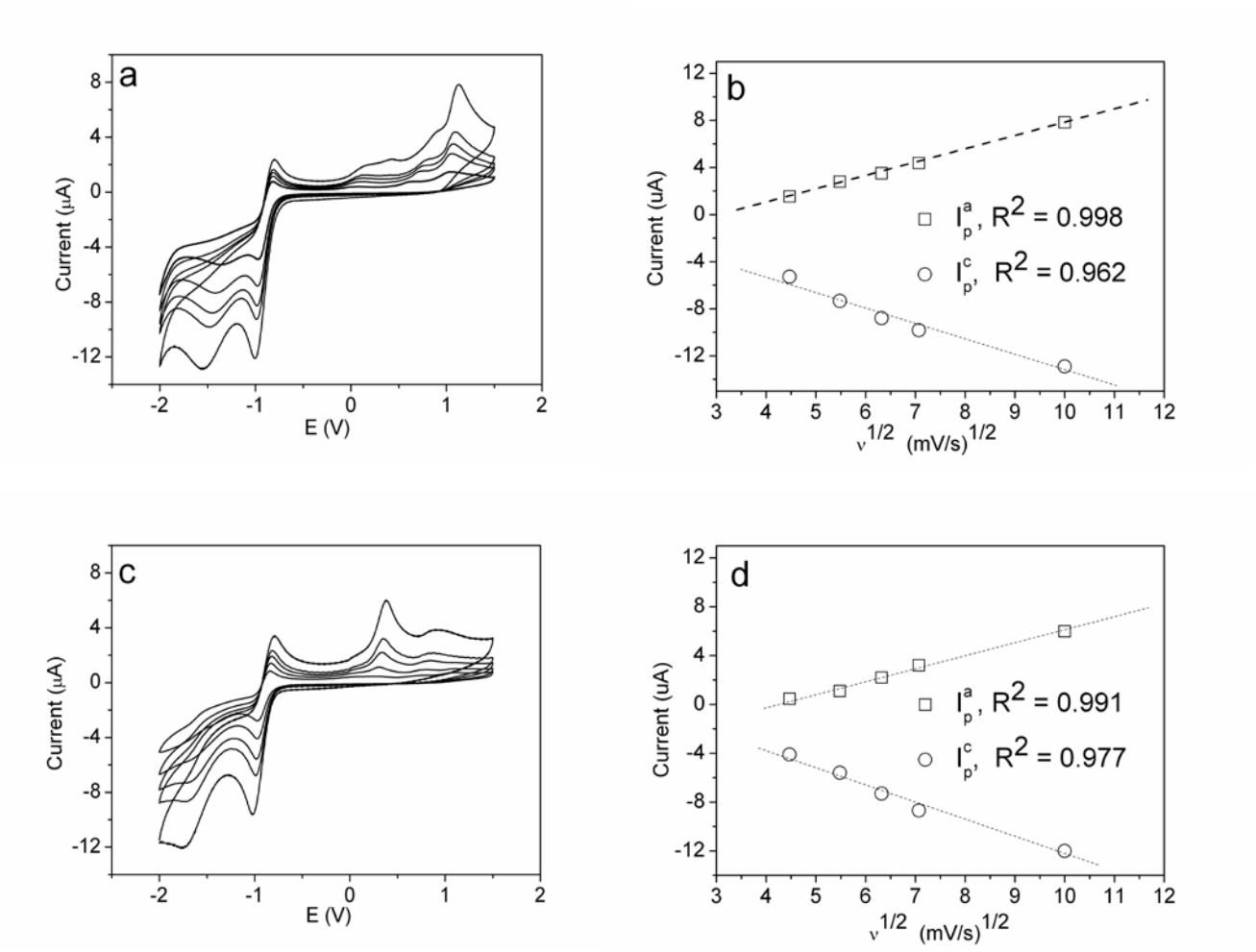

Figure 4.5 CV response of (a,b) TOPO-capped CdSe/ZnS and (c,d) FcHT-coated QDs at different scan rates 20, 30, 40, 50 and 100 mV/s. (c,d) Anodic I_p^a and cathodic I_p^c peak currents as a function of the square root of the scanning rate ν. The dashed lines are linear fits to the data; R is the correlation coefficient of the fits.

Cyclic voltammograms recorded at different scan rates *v* (20, 30, 40, 50 and 100 mV/s) are shown in Figure 4.5a and c. The peak positions shift and the anodic (I_p^a) and cathodic (I_p^c) peak currents increase with increasing scan rate. The linear relationships between the peak current as a function of $v^{1/2}$ (Figure 4.5b) indicate kinetic effects, and that the corresponding redox peaks are obtained for QDs diffusing in solution rather than from species adsorbed onto the electrodes. Similar kinetic effects are observed for nanoparticles coated with ferrocenyl thiols, i.e., the current is linearly proportional to the square root of the scan rate (Figure 4.5d). This result is rather puzzling since redox peaks in subsequent experiments following transfer of the electrodes to a clean electrolyte solution were also observed.

Electrochemical cyclic voltammograms obtained for QD-FcHT are shown in Figure 4.4 and Figure 4.5c, respectively. Introduction of electroactive ferrocene groups on the surface of the QDs substantially influences the voltammetric peak positions and their relative intensities. A new well pronounced peak A1' at 0.36 V appears which is associated with the oxidation of ferrocene to ferrocenium Fc/Fc^+. The Fc oxidation potential is shifted toward lower values compared to the oxidation peak value of pure FcHT compound (0.51 V) (Figure 4.6).

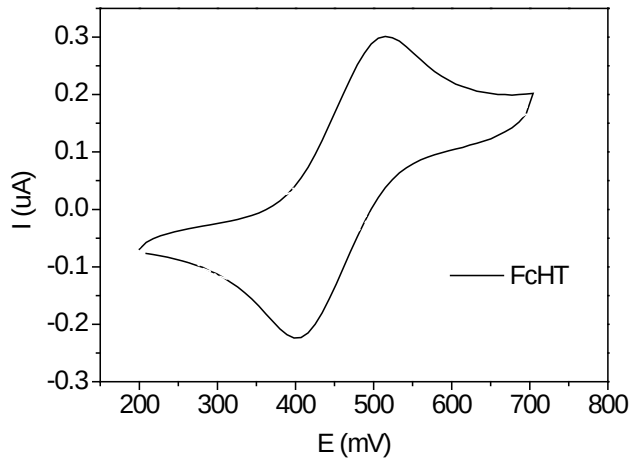

Figure 4.6 CV scan of FcHT in a solution of 0.1M $TBAPF_6$ in toluene/acetonitrile (5:1) at a potential scan rate equal to 50 mV/s.

The anodic oxidation peak A1 at 1V corresponding to an electron removal from the HOMO level, clearly diminished. The charging of the ferrocene ligand located on the surface of QDs may make the abstraction of an electron from the HOMO more difficult or impossible.

Concurrently, the anodic peak A1 may be shifted toward more positive potentials outside the probed potential window.[19] The presence of the FcHT ligand causes also a shift of the cathodic reduction peak toward more negative values by 0.15 V. The oxidation peak A2' and reduction peak C2' did not show any remarkable changes after coating the QDs with the new electroactive ligand. These peaks can therefore be assigned to redox reactions, which do not involve the ligand, corroborating the initial assertion. The QD-Fc system displays some features of a "molecular hybrid", where both the QD and the ligand influence each other, which results in shifted peak positions of the oxidation and reduction processes.[19] To get more insights into the nature of the electrochemical processes more investigations are needed. Raman spectroelectrochemistry and UV-Vis-NIR investigations may prove useful in this respect. The ferrocene is a suitable electroactive ligand for the manipulation of the electron transfer processes in CdSe/ZnS QDs.

4.3 CONCLUSIONS

Electrochemical characterization of core-shell CdSe/ZnS Quantum Dots in non-aqueous solution is presented. Cyclic voltammetry allowed for the detection of the cathodic reduction and anodic oxidation processes involving the QD HOMO and LUMO levels, as well as QD defect states. The electrochemical bandgap estimated from the HOMO and LUMO redox peaks was larger than the one in bulk material indicating quantum confinement effects on the redox potentials of CdSe/ZnS QDs. The electrochemical response of QDs was sensitive to the presence of Fc on their surface. A new electrochemical peak associated with oxidation of ferrocene appeared on the cyclic voltammograms and the anodic and cathodic redox peaks of the QDs were shifted due to the presence of the Fc ligand.

4.4 EXPERIMENTAL

Materials. Trioctylphosphine oxide (TOPO)-coated core-shell CdSe/ZnS QDs emitting at 625nm (QD625) were synthesized according to the method reported in [45]. For the modification of the QD surface 6-ferrocenyl-1-hexanethiol (FcHT) was obtained from Dojindo (Dojindo Europe, Amsterdam, The Netherlands) and used as received. Analytical grade solvents toluene, acetonitrile and d_8-toluene were obtained from Aldrich. Supporting electrolyte tetrabutylammonium hexafluorophosphate ($TBAPF_6$) was purchased from Aldrich.

Methods. Transmission electron microcopy (TEM) of quantum dots was performed using a Philips CM300ST-FEG instrument. The samples for TEM were prepared by putting a drop of QDs onto a carbon-coated copper grid and drying in air. To obtain statistically meaningful results 100 nanoparticles were imaged. A Varian spectrophotometer (model Cary 300) was employed to record the absorption spectra of QD solutions in toluene. To measure the photoluminescence spectra, an Edinburg XE-900 spectrofluorometer was used. The luminescence quantum yields (QY) of the substrates and products were estimated by comparing the integrated luminescence intensities to that of the $[Ru(bpy)_3]^{2+}$ complex standard (QY = 0.028).[50,51] Nuclear magnetic resonance spectra were recorded on a Bruker Avance II 600 MHz NMR spectrometer at room temperature, using an SEI 2.5 mm probe head equipped with z-axis gradient system. Appropriate 2.5 mm tubes were used to limit convection during the pulsed field gradient (PFG) experiments. Pseudo-2D DOSY experiments and 1D diffusion-filtered ^1H experiments were performed using the bipolar stimulated echo sequence with typically a diffusion time (Δ) of 100 ms, and gradients between 5 and 95% of maximum 35 G.

Cyclic voltammetry measurements were performed using a three-electrode electrochemical cell and an AUTOLAB PGSTAT 10 potentiostat purchased from ECO CHEMIE (Utrecht, The Netherlands). Potentials were recorded *versus* a double junction Ag|AgCl+3M KCl electrode (+0.201 V *vs* SHE) in a 0.1M $TBAPF_6$ solution of the supporting electrolyte. Glassy carbon working (Ø = 2mm) and counter (glassy carbon rod) electrodes were chosen for the measurements. Analytical grade solvents toluene and acetonitrile were used in all experiments. The electrolyte solutions (5 mL) containing the analytes were purged thoroughly for 15 min. with nitrogen before each measurement. A baseline was recorded for 5 mL of supporting electrolyte after purging with nitrogen (Figure 4.4). The experiments were performed at room temperature.

Synthesis of QD-FcHT nanoparticles. Prior to the synthesis, the CdSe/ZnS QDs were purified by precipitation with methanol and subsequent ultracentrifugation. The solid remaining after the centrifugation was dispersed in toluene. TOPO-coated QDs (4 mL, 4×10^{-6} M) were mixed in a two-neck flask with a toluene solution of the ferrocene thiol (1 mL, 3.3×10^{-3} M). The flask was equipped with a condenser and thermometer, immersed into an oil bath at a temperature of 40 ºC. The reaction was continued for six days under nitrogen flow. Ultracentrifugation (22000 rpm, 3 hours) was used to purify ferrocenyl-coated QDs after the reaction. The ultracentrifugation was repeated twice.

4.5 REFERENCES

1. Gittins, D. I.; Bethell, D.; Schiffrin, D. J.; Nichols, R. J. *Nature* **2000**, *408*, 67-69.
2. Klein, D. L.; Roth, R.; Lim, A. K. L.; Alivisatos, A. P.; McEuen, P. L. *Nature* **1997**, *389*, 699-701.
3. Banin, U.; Cao, Y.; Katz, D.; Millo, O. *Nature* **1999**, *400*, 542-544.
4. Alivisatos A. P. *Science* **1996**, *271*, 933-937.
5. Brus, L. *J. Chem. Phys.* **1983**, *79*, 5566-5571.
6. Nedeljkovic, J. M.; Nenadovic, M. T.; Micic, O. I.; Nozik, A. J. *J. Phys. Chem.* **1986**, *90*, 12-13.
7. Hoyer, P.; Weller, H. *Chem. Phys. Lett.* **1994**, *221*, 379-384.
8. Mulrooney, R. C.; Singh, N.; Kaur, N.; Callan J. F. *Chem. Commun.* **2009**, 686 – 688.
9. Willner, I.; Patolsky, F.; Wasserman, J. *Angew. Chem. Int. Ed.* **2001**, *40*, 1861-1864.
10. Liu, Q.; Lu, X.; Li, J.; Yao, X.; Li, J. *Biosens. Bioelectr.* **2007**, *22*, 3203-3209.
11. Anderson, N. A.; Lian, T. *Annu. Rev. Phys. Chem.* **2005**, *56*, 491-519.
12. Adams, D. M.; Brus, L.; Chidsey, C. E. D.; Creager, S.; Creutz, C.; Kagan, C. R.; Kamat, P. V.; Lieberman, M.; Lindsay, S; Marcus, R. A.; Metzger, R. M.; Michel-Beyerle, M. E.; Miller, J. R.; Newton, M. D.; Rolison, D. R.; Sankey, O.; Schanze, K. S.; Yardley, S.; Zhu, X. *J. Phys. Chem. B* **2003**, *107*, 6668-6697.
13. Bakkers, E.; Marsman, A. W.; Jenneskens, L. W.; Vanmaekelbergh, D. *Angew. Chem. Int. Ed.* **2000**, *39*, 2297-2299.
14. Zhang, X. V.; Ellery, S. P.; Friend, C. M.; Holland, H. D.; Michel, F. M.; Schoonen, M. A. A.; Martin, S. T. *J. Photochem. Photobiol. A: Chemistry* **2007**, *185*, 301-311.
15. Murray, C. B.; Norris, D. J.; Bawendi M. G. *J. Am. Chem. Soc*. **1983**, *115*, 8706-8715.
16. Peng, Z. A.; Peng, X. *J. Am. Chem. Soc.* **2001**, *123*, 183-184.
17. Tomczak, N.; Jańczewski, D.; Tagit, O.; Han, M. Y.; Vancso, G. J. Surface engineering of Quantum Dots with Designer Ligands, in: "Surface Design: Applications in Bioscience and Nanotechnology", Förch, R.; Schönherr, H.; Jenkins, A. T. A., Eds.; Wiley: **2009**, ISBN: 978-3-527-40789-7.
18. Torimoto, T.; Maeda, K.; Maenaka, J.; Yoneyama, H. *J. Phys. Chem.* **1994**, *98*, 13658-13664.
19. Quener, C.; Reiss, P.; Sadki, S.; Zagorska, M.; Pron A. *Phys. Chem. Chem. Phys.* **2005**, *7*, 3204-3209.

20. Ogawa, S.; Hu, K.; Fan, F. F.; Bard, A. J. *J. Phys. Chem. B* **1997**, *101*, 5707-5711.
21. Torimoto, T.; Nagakubo, S.; Nishizawa, M.; Yoneyama, H. *Langmuir*, **1998**, *14*, 7077-7081.
22. Torimoto, T.; Tsumura, N.; Miyake, M.; Nishizawa, M.; Sakata, T.; Mori, H.; Yoneyama, H. *Langmuir*, **1999**, *15*, 1853-1858.
23. Hickey, S. G.; Riley, D. J.; Lull, E. J. *J. Phys. Chem. B* **2000**, *104*, 7623-7626.
24. Haram, S. K.; Quinn, B. M.; Bard, A. J. *J. Am. Chem. Soc.* **2001**, *123*, 8860-8861.
25. Riley, D. J. *Curr. Op. Coll. Int. Sci.* **2002**, *7*, 186-192.
26. Ding, Z.; Quinn, B. M.; Haram, S. K.; Pell, L. E.; Korgel, B. A.; Bard A. J. *Science* **2002**, *296*, 1293-1295.
27. Myung, N.; Ding, Z. F.; Bard, A. J. *Nano Lett.* **2002**, *2*, 1315-1319.
28. Kucur, E.; Reigler, J.; Urban, G. A.; Nann, T. *J. Chem. Phys.* **2003**, *119*, 2333-2337.
29. Bae, Y.; Myung, N.; Bard, A. J. *Nano Lett.*, **2004**, *4*, 1153-1161.
30. Myung, N.; Lu, X.; Johnston K. P.; Bard A. J. *Nano Lett.* **2004**, *4*, 183-185.
31. Kucur, E.; Bucking, W.; Giernoth, R.; Nann, T. *J. Phys. Chem. B* **2005**, *109*, 20355-20360.
32. Poznyak, S. K.; Osipovich, N. P.; Shavel, A.; Talapin, D. V.; Gao, M.; Eychmuller, A.; Gaponik, N. *J. Phys. Chem. B* **2005**, 109, 1094-1100.
33. Ren, T.; Xu, J. Z.; Tu, Y. F.; Xu, S.; Zhu, J. J. *Electrochem Commun.* **2005**, *7*, 5-9.
34. Bard, A. J.; Ding, Z.; Myung, N. *Struc. Bond*. **2005**, *118*, 1-57.
35. Li, Y.; Zhong, H.; Li, R.; Zhou, Y.; Yang, C.; Li, Y. *Adv. Funct. Mater.* **2006**, *16*, 1705-1716.
36. Kucur, E.; Bucking, W.; Arenz, S.; Giernoth, R.; Nann, T. *ChemPhysChem* **2006**, *7*, 77-81.
37. Osipovich, N. P.; Shavel, A.; Poznyak, S. K.; Gaponik, N.; Eychmuller, A. *J. Phys. Chem. B* **2006**, *110*, 19233-19237.
38. Inamdar, S. N.; Ingole, P. P.; Haram, S. K. *ChemPhysChem* **2008**, *9*, 2574-2579.
39. Kucur, E.; Bucking, W.; Nann, T. *Microchim. Acta* **2008**, *160*, 299-308.
40. Gaponik, N.; Poznyak, S. K.; Osipovich, N. P.; Shavel, A.; Eychmuller, A. *Microchim Acta* **2008**, *160*, 327-334.
41. Aldakov, D.; Querner, C.; Kervella, Y.; Jousselme, B.; Demadrille, R.; Rossitto, E.; Reiss, P.; Pron, A. *Microchim. Acta* **2008**, *160*, 335-344.
42. Cameron P. J., Nanoparticles at the Interfaces: the Electrochemical and Optical Properties of Nanoparticles Assembled into 2D and 3D Structures at Planar Electrode

Surfaces, in “Surface Design: Applications in Bioscience and Nanotechnology”, Förch, R.; Schönherr, H.; Jenkins, A. T. A, Eds.; Wiley: **2009**, ISBN: 978-3-527-40789-7.

43. Querner, C.; Reiss, P.; Bleuse, J.; Pron, A. *J. Am. Chem. Soc.* **2004**, *126*, 11574-11582.
44. Chen, W.; Chen, S. W.; Ding, F. Z.; Wang, H. W.; Brown, L. E.; Konopelski, J. P. *J. Am. Chem. Soc.* **2008**, *130*, 12156-12160.
45. Janczewski, D.; Tomczak, N.; Khin, Y. W.; Han, M. Y.; Vancso G. J. *Eur. Pol. J.* **2009**, *45*, 3-9.
46. Isutsu, K. *Electrochemistry in Non-aqueous Solutions*; Wiley: **2002**, ISBN 978-3-527-30516-2.
47. Yu, W. W.; Qu, L.; Guo, W.; Peng, X. *Chem. Mater.* **2003**, *15*, 2854-2860.
48. Gooding, A. K.; Gomez, D. E.; Mulvaney P. *ACS Nano* **2008**, *2*, 669-676.
49. Chen, S.; Truax, L. A.; Sommers, J. M. *Chem. Mater.* **2000**, *12*, 3864-3869.
50. Montalti, M.; Credi, A.; Prodi, L.; Gandolfi, M. T. *Handbook of Photochemistry*, 3rd. Ed., CRC Press, **2006**, pp. 572-576.
51. Lakowicz, J. R. *Principles of Fluorescent Spectroscopy*, 2nd Ed., Kluwek Academic/ Plenum Press, **1999**, pp. 10-12.

Chapter 5

Reversible Phase Transfer of CdSe/ZnS Quantum Dots between Organic and Aqueous Solutions*

Phase transfer of ferrocene-modified QDs from organic solvents into water was achieved by complexation reactions with β-cyclodextrin (β-CD). The QDs coated with ferrocene thiols are soluble in nonpolar solvents and are transferred into the aqueous phase upon formation of host-guest complexes between the ferrocene units and the cavity of β-CD. The reversibility of the phase transfer was also demonstrated by addition of a naphthalene derivative to the aqueous phase containing QD-[Fc-CD] adduct.

* Part of this Chapter has been published in: (a) Dorokhin, D.; Tomczak, N.; Han M. Y.; Reinhoudt, D. N.; Velders, A. H.; Vancso G. J. *ACS Nano* **2009**, *3*, 661-667. (b) Dorokhin, D.; Tomczak, N.; Han, M. Y.; Reinhoudt, D. N.; Velders, A. H.; Vancso, G. J. *Polym. Mater. Sci. Eng.***2009**, *101*, 1254-1255.

5.1 INTRODUCTION

Hybrid organic-inorganic composite materials find numerous applications in optoelectronics,[1,2] nanocomposites,[3] biotechnology,[4] and biodiagnostics.[5] Due to attractive properties QDs are currently applied in fields of optoelectronics,[6-9] biolabelling,[10-14] and sensing.[15-17] For application of QDs in biological sensing, or biolabelling, the nanoparticles must be dispersible in aqueous solution and in relevant biological buffers.[18] Ligand exchange reactions, described in the previous chapters 2 and 3, have been widely used to modify the surface of quantum dots to tune the QD solubility[10,19] as well as to provide functionality for further coupling to biomacromolecules.[20] Phase transfer of QDs between solvents with markedly different polarity can be also achieved by coating the QDs with amphiphilic molecules *via* electrostatic,[21] hydrophobic/hydrophobic,[22,23] or host-guest interactions.[24-27] For some applications it is desirable to transfer the nanoparticles from the sensing medium and perform analysis in a new medium free from the interfering background molecules. Therefore there is a need to develop QD materials, which would undergo reversible phase transfer between solvents of markedly different polarity. This might be realized by employing stimulus responsive ligands, which upon external *stimuli* (temperature, pH, electric field) change their chemistry, and therefore the physicochemical properties of the QD surface, or by using ligands able to form supramolecular complexes with other molecules.

This chapter describes the reversible phase transfer of ferrocene-coated CdSe/ZnS quantum dots *via* host-guest interactions. TOPO-coated CdSe/ZnS QDs were functionalized with a ferrocenyl thiol with the alkyl chain length of 11 CH_2 units *via* the ligand exchange reaction. NMR spectroscopy proved the exchange of ligands at the QD surface. The presence of ferrocene causes a decrease of the luminescence quantum yields (QY) of QDs, as stated in previous chapters 3 and 4. Ferrocene-coated QDs are shown to undergo reversible phase transfer from chloroform to water (and *vice-versa*) upon formation/release of inclusion complexes of β-cyclodextrin with the ferrocene units on the surface of the QDs.

5.2 RESULTS AND DISCUSSION

5.2.1 Modification and Characterization of QDs

Two new batches of TOPO-coated CdSe/ZnS QDs having different size were chosen for the phase transfer experiment. The CdSe/ZnS QDs were characterized by UV-vis and spectrofluorometry. Adsorption and emission spectra of CdSe/ZnS QDs (QD595 and QD605) are shown in Figure 5.1. The maximum of the first absorption peak is located at 573 nm and 582 nm, respectively. The concentration of the nanocrystals was estimated by following the procedure of Peng *et al.*[28] The emission spectrum has a maximum located at 595 nm and 605 nm, and the full width at half maximum (FWHM) value of the emission peak is equal to 33 nm and 35 nm.

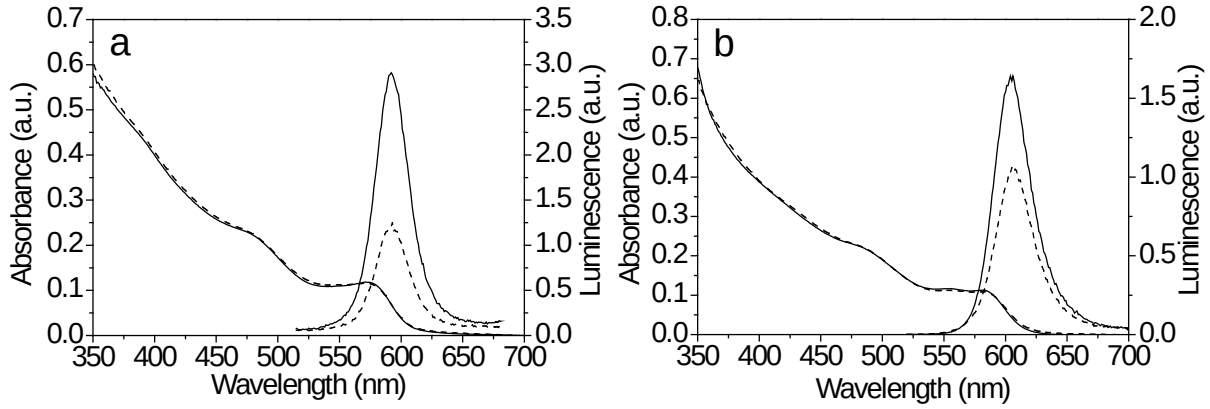

Figure 5.1 Absorption and photoluminescence spectra of CdSe/ZnS QDs (QD595(a) and QD605(b)) before (solid) and after (dash) modification with FcUT. Excitation wavelength is 510 nm.

The initial QDs coated with TOPO to stabilize them in an organic solvent were functionalized with 11-ferrocenyl-1-undecanethiol (FcUT). The ligand exchange reaction was chosen as a convenient and rapid method to modify the surface of TOPO-coated QDs. To perform the ligand exchange reaction the procedure described in chapter 4 was used. Briefly, TOPO-coated QDs were mixed with a large excess of the ferrocene derivatives. The molar ratio between the ferrocenyl thiols and QDs was 1:100. After the reaction centrifugation was applied to remove the untreated ferrocene derivative and TOPO from the solution.

As shown in chapter 3, to prove that ligand exchange reaction took place, i.e., that the TOPO ligands were displaced by the ferrocenyl thiols NMR spectroscopy was employed. The diffusion-filtered ^{1}H NMR spectrum of the FcUT modified QDs show a broad peak in the range of 4-4.5 ppm (Figure 5.2), which is attributed to the aromatic protons of the ferrocene linked to the CdSe/ZnS QDs. The broad peaks between 0.5-2 ppm are related to the alkyl chain protons of the remaining TOPO, still present on the surface, and to the alkyl protons of the ferrocenyl thiol. ^{1}H NMR spectroscopy proves unequivocally that the ligand exchange reaction between TOPO-coated QDs and the thiol derivatives was carried out successfully and that the thiol ligands attach onto the surface of CdSe/ZnS quantum dots.

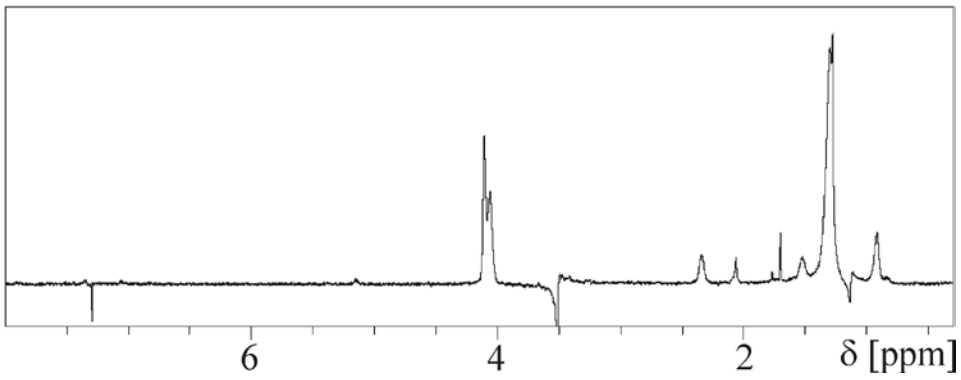

Figure 5.2 ^{1}H filtered NMR spectrum of CdSe/ZnS-FcUT quantum dots in chloroform-*d*. The broad peak close to 4 ppm corresponds to the ferrocene moiety. Peaks in the region between 3.5 ppm and 0.8 ppm corresponds to the alkyl chains of FcUT and TOPO.

5.2.2 Phase Transfer of QDs by Host-Guest Complexation with Cyclodextrin

Ferrocene is known to form complexes with β-cyclodextrin with a complexation constant K=1230 M^{-1}.[29] The chemical structure of β-CD forms a hydrophilic ring with hydrophobic cavity, which can interact with a suitable hydrophobic molecule that fits to the cavity. Therefore, transfer of ferrocene-coated QDs in and out of the aqueous phase upon complexation and decomplexation with β-CD can be achieved. The simulated lengths of FcUT and TOPO ligands are equal to 19 and 13 Å, respectively. In the complexation reactions with β-CD the access of the β-CD to the guest molecule is important. Additionally, the orientation of the guest in the β-CD cavity can affect the complexation behavior. The location of Fc moieties above the TOPO layer should in principle facilitate the complexation reaction. Thus, to demonstrate the complexation of ferrocene-coated QDs by β-CD, FcUT

ligands were chosen. Two series of experiments were performed using QD605 and QD595. The ligand exchange reaction times have been kept short in order to avoid steric hindrance of the ferrocene units during complexation with β-CD. The QY for unmodified and modified QDs was calculated to be 37,6% and 25,8%, and 39.3% and 17.9% for QD605 and QD595, respectively, indicating low surface coverage of ferrocene thiols for both QD samples. The schematic representation of the chemically driven phase transfer is depicted in Figure 5.3. Figure 5.4 shows two series of photographs of vials containing water and chloroform. Initially the QDs are present in the chloroform phase (Figure 5.4a and 5.4d). Upon addition of β-CD, complexation of the ferrocene units on the surface of QD occurs, and the nanocrystals migrate to the water phase (Figure 5.4b and 5.4e). This is accompanied by a noticeable emission from the water phase. Figure 5.5 shows the corresponding absorption and emission spectra of the chloroform phase before adding β-CD and of the water phase after adding β-CD.

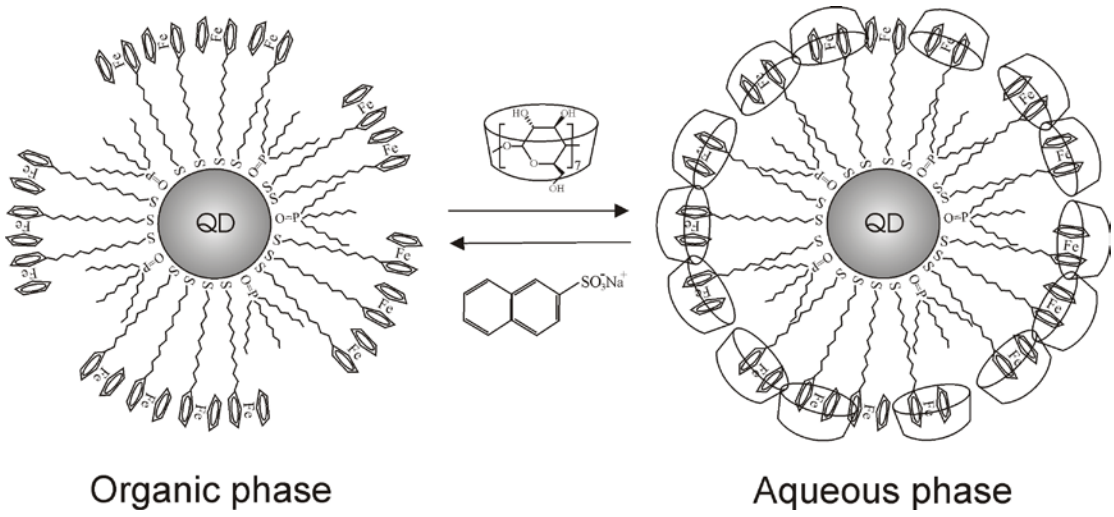

Figure 5.3 Phase transfer of ferrocenyl-coated QDs between organic and aqueous phases by formation of host-guest complexes with β-cyclodextrin and decomplexation by addition of a competitive guest.

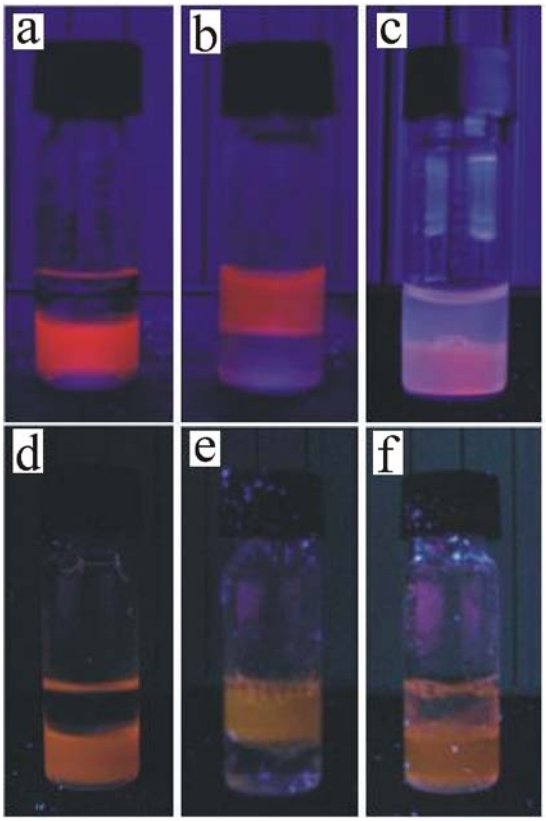

Figure 5.4 Photographs of the phase transfer experiments using QD605 (a,b,c) and QD595 (e,f,g,) quantum dots. The QDs-FcUT in the chloroform phase (a,d) are transferred to water (b,e) upon complexation of the ferrocene units with β-CD. Upon addition of sodium 2-nahpthalene sulfonate (c) and AdCOOH (f) the QDs migrate back to the chloroform phase.

The position of the first absorption peak for the organic and aqueous phases does not change noticeable for both QDs. There are, however, some minor changes in the profile of the absorption curve, which could be related to some aggregation of the nanoparticles in the aqueous medium. Dispersability of the QDs in water indicates that the complexation of the ferrocene units on the QD surface by β-CD was not prevented by steric hindrance. Due to short ligand exchange reaction times, the remaining TOPO ligands on the QD surface may serve as spacers between ferrocenyl thiol molecules. Additionally, deliberately, the FcUT ligands, which are longer than the TOPO molecules were chosen. Therefore an easy access for the β-CD molecules to the Fc units is created.

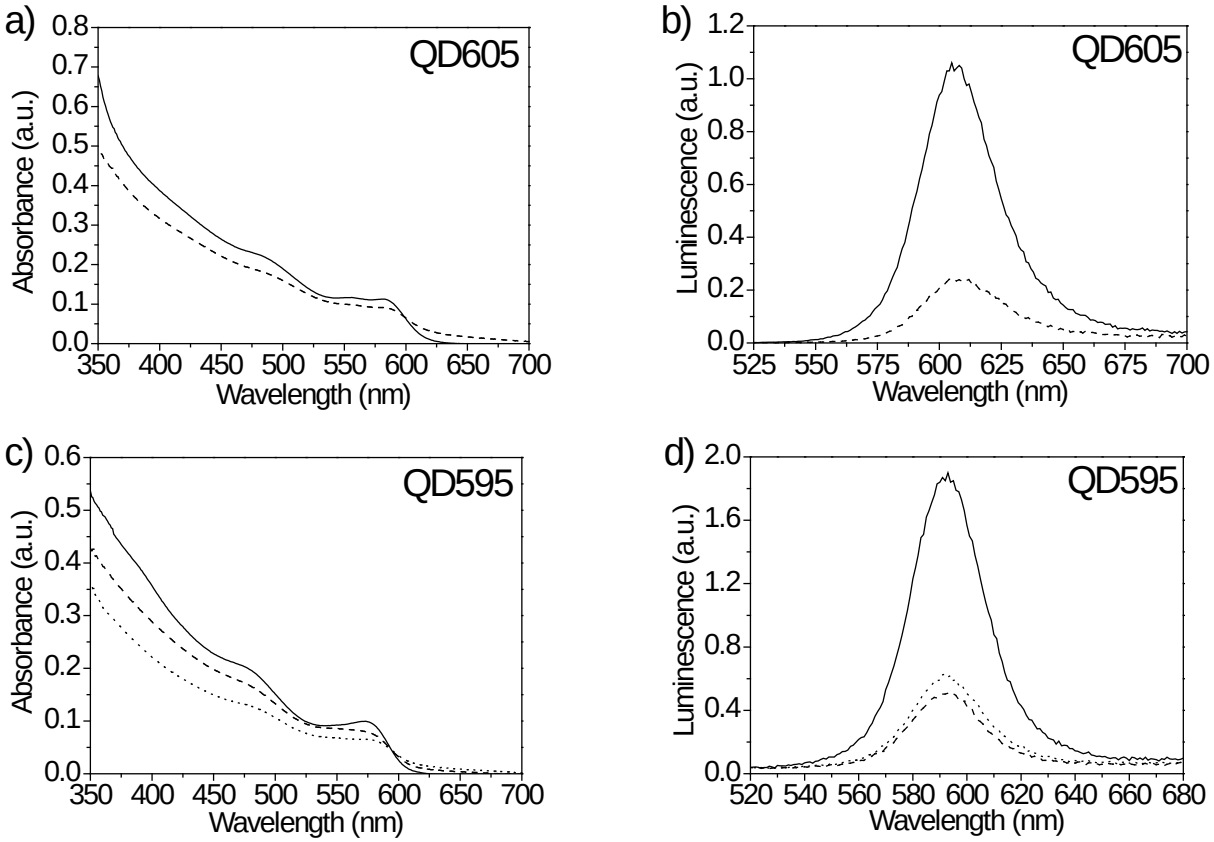

Figure 5.5 (a) Absorption spectra of QDs-FcUT (QD605) in chloroform solution (solid) and QDs-[FcUT-CD] complex in water (dash), (b) emission spectra of QDs-FcUT (QD605) in chloroform (solid) and QDs-[FcUT-CD] (dash) in water, (c) absorption spectra of QDs-FcUT (QD595) in chloroform solution (solid), QDs-[FcUT-CD] complex in water (dash) and chloroform after addition of AdCOOH (dot), (d) emission spectra of QDs-FcUT (QD595) in chloroform (solid), QDs-[FcUT-CD] in water (dash) and QDs-FcUT in chloroform after addition of AdCOOH (dot).

Based on the absorption spectrum one can estimate the efficiency of the β-CD driven phase transfer to be equal to ~ 80% for both QDs. The emission spectra (Figure 5.5b,d) clearly confirm the presence of QDs in the aqueous phases. Although the overall emission intensity decreased, no noticeable changes in the emission peak position are present. The reason for the luminescence decrease is unclear at present, but it is likely related to the presence of cyclodextrin and different media. Feng *et al*. reported cyclodextrin induced phase transfer performed for TOPO-derivatized CdSe/ZnS QDs.[25] In their work a 15 nm red shift after transfer of QDs to water was observed and it was related to the coordination of β-CD to the

surface of the QDs. During this study no shift in the emission was detected and direct attachment of β-CD to the ZnS surface is rather unlikely.

5.2.3 Reversible Phase Transfer of QD between Aqueous and Organic Phases

The formation of a host-guest complex between β-CD and ferrocene is usually reversible upon addition of molecules having a higher binding constant to the cavity of the β-CD.[29] In order to show that the phase transfer is reversible, sodium 2-naphthalene sulfonate (NAS), and adamantane carboxylate (AdCOOH), which are known to be effective in replacing ferrocene from the ring of β-CD, were added to the water phase.[29,30] To displace ferrocene from the β-CD cavity an excess of 10 times of NAS and 100 times of AdCOOH with respect to β-CD was added to the water phase.

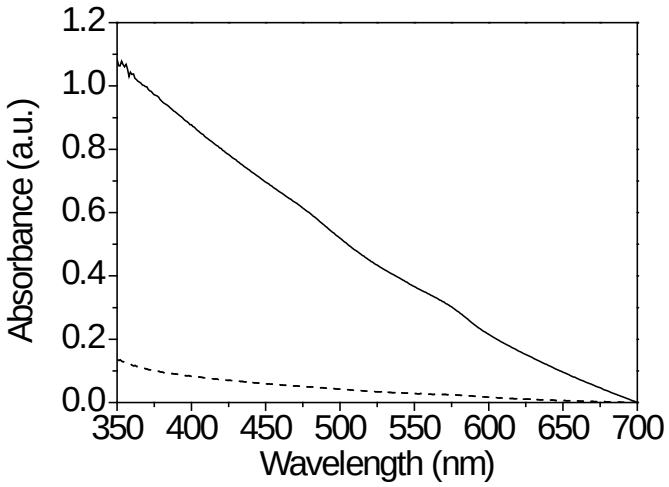

Figure 5.6 Absorption spectra of QDs-FcUT (QD605) in chloroform (solid) and aqueous phase (dash) after addition of sodium 2-naphthalene sulfonate.

Upon addition of the naphthalene salt and vigorous shaking the organic phase becomes luminescent under UV lamp illumination (Figure 5.4c). UV-vis spectroscopy of the aqueous and chloroform phases upon addition of the naphthalene salt is shown in Figure 5.6. Although the majority of the QDs transfer back to the chloroform phase, the changes in the absorption profiles indicate that some aggregation of the QD occurred and the solution turned slightly opaque. Probably not all β-CD molecules have been displaced before the QDs transferred into the chloroform phase. Aggregation of the QDs in chloroform phase can be largely avoided, when an adamantane derivate is used in the experiments. Similar to naphthalene, the majority

of the QDs transfer back to the chloroform phase upon addition of a large excess of AdCOOH. However, unlike in the experiments with naphthalene, upon addition of AdCOOH the chloroform QD phase is clear and transparent. Substantially diminished aggregation of the QDs is also visible on the absorption spectra of the chloroform phase after addition of AdCOOH (Figure 5.5a). Adamantane therefore is a more efficient complexating agent for β-CD on the surface of the QDs. Transfer of the QDs from water to chloroform is accompanied by a rise in fluorescence intensity. This observation complements to our initial statement that the cyclodextrin is largely responsible for the quenching of the emission of the QDs in the water phase. The release of β-CD from the QD surface leads to the formation of new host-guest complexes between respective complexating agents (naphthalene and adamantane) and β-CD molecules. In the case of naphthalene a weak blue emission from the water phase originating from the NAS-β-CD complex is clearly visible under UV-illumination. These data demonstrate that reversible phase transfer due to replacement of ferrocene by naphthalene or AdCOOH from the β-CD cavity does indeed occur. The choice of the competing complexating molecules seems however critical.

5.3 CONCLUSIONS

Reversible phase transfer to and from the aqueous phase was demonstrated using the complexation reaction of ferrocene on the surface of QDs with β-cyclodextrin and subsequent decomplexation *via* competitive reaction of β-cyclodextrin with naphthalene and adamantane derivatives. The emission of QDs in the water phase is quenched due to the presence of the cyclodextrin. The use of adamantane as the decomplexating agent results in clear and transparent solutions of QDs in the chloroform phase unlike for the case of naphthalene where aggregation of the QDs is observed. The choice of the decomplexating agent is therefore crucial to establish a reversible phase transfer of QDs from the aqueous to the organic phase.

5.4 EXPERIMENTAL

Materials. Core-shell CdSe/ZnS nanocrystals were synthesized as described in Janczewski *et. al.*[31] Two differently sized nanoparticles emitting at 605 nm (QD605) and 595 nm (QD 595) were chosen for this work. 11-Ferrocenyl-1-udecanethiol (FcUT) was obtained from Dojindo (Dojindo Europe, Amsterdam, The Netherlands) and used as received. Chloroform and deuterated chloroform were obtained from Aldrich (analytical grade). Phosphate buffer (Na_2HPO_4/NaOH, pH 11.6) was used to prepare solutions of β-cyclodextrin (CD, Aldrich). Sodium 2-naphtalenesulfonate (Fluka) and 1-adamantanecarboxylic acid (Aldrich) were used as received.

Synthesis of QD-Fc nanoparticles. The nanocrystals were stored in chloroform, or toluene, and purified before use by precipitation with methanol and subsequent ultracentrifugation. After centrifugation, the transparent solution was discarded and the remaining solid was dispersed again in toluene or chloroform. Nanocrystals coated with the initial TOPO ligands (4 mL, 4×10^{-6} M) were added to a toluene solution containing FcUT (650 μL, 3.3×10^{-3} M) in a three-necked flask equipped with a condenser. The flask was immersed into a heating bath and the reaction was allowed to proceed for six days at 40 ºC under nitrogen environment. After the reaction, the ferrocenyl-coated nanoparticles were purified by centrifugation in chloroform and methanol solution (1:5, 10000rpm, 10min.), and the centrifugation was repeated twice.

Complexation of Fc-QDs with β-cyclodextrin. Purified ferrocene-modified QDs were dispersed in 1mL of chloroform (5.4×10^{-7}M) and mixed with 1mL of phosphate buffer solution containing β-CD (1.1×10^{-4} M). The molar ratio between the QD-Fc and β-CD was therefore equal to 1:200. The solution was stirred for 10 hours at room temperature, until the water phase became luminescent under UV irradiation. For reversible phase transfer, 145 μL of phosphate buffer solutions containing sodium 2-naphthalene sulfonate (7.6×10^{-3} M), or 100 μL phosphate buffer solutions containing 1-adamantanecarboxylic acid ($1.3\text{x}10^{-2}$M) have been added to the QD-[Fc-β-CD] solution to replace ferrocene from the inclusion complex with β-CD. The mixture was intensively shaken overnight. Samples from the organic and aqueous phases were taken for further analysis.

Methods. A Varian Cary 300 UV-Vis spectrophotometer was used to record the absorption spectra of the QD solutions in chloroform. The photoluminescence spectra were measured on an Edinburgh XE-900 spectrofluorometer. NMR spectra were measured by a Bruker Avance II 600 MHz NMR spectrometer at room temperature, using an SEI 2.5 mm probe head equipped with a z-axis gradient system. Tubes with the size of 2.5 mm were used to limit the convection during the pulsed field gradient (PFG) experiments. 1D diffusion-filtered ^{1}H experiments were performed using the bipolar

stimulated echo sequence with typically a diffusion time (Δ) of 100 ms, and gradients between 5 and 95 % of maximum 35 Gauss.

5.5 REFERENCES

1. Beecroft, L. L.; Ober, C. K. *Chem. Mater.* **1997**, *9*, 1302-1317.
2. Huynh, W. U.; Dittmer, J. J.; Alivisatos, A. P. *Science* **2002**, *295*, 2425-2427.
3. Rajeshwar, K.; Tacconi, N. R.; Chenthamarakshan, C. R. *Chem. Mater.* **2001**, *13*, 2765-2782.
4. Niemeyer, C. M. *Angew. Chem. Int. Ed.* **2001**, *40*, 4128-4158.
5. Rosi, N. L.; Mirkin, C. A. *Chem. Rev.* **2005**, *105*, 1547-1562.
6. Colvin, V. L.; Schlamp, M. C.; Alivisatos, A. P. *Nature* **1994**, *370*, 354-357**.**
7. Klein, D. L.; Roth, R.; Lim, A. K. L.; Alivisatos, A. P.; McEuen, P. L. *Nature* **1997**, *389*,699-701.
8. Coe, S.; Woo, W.-K.; Bawendi, M.; Bulovic, V. *Nature* **2002**,*420*, 800-803.
9. McDonald, S. A.; Konstantatos, G.; Zhang S.; Cyr, P. W.; Klem, E. J. D.; Levina, L.; Sargent E. H. *Nat. Mater.* **2005,** *4*, 149-152.
10. Chan, W. C. W.; Nie S. *Science* **1998**, *281*, 2016-2018.
11. Bruchez, M. Jr.; Moronne, M.; Gin, P.; Weiss, S.; Alivisatos, A. P. *Science* **1998**, *281*, 2013-2016.
12. Dubertret B.; Skourides, P.; Norris, D. J.; Noireaux, V.; Brivanlou, A. H.; Libchaber, A. *Science* **2002**, *298*, 1759-1760.
13. Gao, X.; Cui, Y.; Levenson, R. M.; Chung, L. W. K.; Nie, S. *Nat. Biotechnol.* **2004**, *22*, 969-976.
14. Michalet, X.; Pinaud, F. F.; Bentolila, L. A.; Tsay, J. M.; Doose, S.; Li, J. J.; Sundaresan, G.; Wu, A. M.; Gambhir, S. S.; Weiss, S. *Sience* **2005**, *307*, 538-544.
15. Medintz, I. L.; Clapp, A. R.; Mattoussi, H.; Goldman, E. R.; Fisher, B.; Mauro, J. M. *Nat. Mater.* **2003**, *2*, 630-638.
16. Katz, E.; Willner, I.; Wang, J. *Electroanalysis* **2004**, *16*, 19-44.
17. Anikeeva, N.; Lebedeva, T.; Clapp, A. R.; Goldman, E. R.; Dustin, M. L.; Mattoussi, H.; Sykulev, Y. *Proc. Nat. Acad. Sci.* **2006**, *103*, 16846-16851.
18. Boldt, K.; Bruns, O. T.; Gaponik, N.; Eychmuller, A. *J. Phys. Chem. B* **2006**, *110*, 1959-1963.

19. Pathak, S.; Choi, S.; Arnheim, N.; Thompson, M. E. *J. Am. Chem. Soc.* **2001,** *123*, 4103-4104.
20. Jaiswal, J. K.; Mattoussi, H.; Mauro, J. M.; Simon, S. M. *Nat. Biotechnol.* **2003**, *21*, 47-51.
21. Jiang, H.; Jia, J. *J. Mater. Chem.* **2008**, *18*, 344-349.
22. Pellegrino, T.; Manna, L.; Kudera, S.; Liedl, T.; Koktysh, D.; Rogach, A. L.; Keller, S.; Radler, J.; Natile, G.; Parak, W. J. *Nano Lett.* **2004**, *4*, 703-707.
23. Yu, W. W.; Chang, E.; Falkner, J. C.; Zhang, J. Y.; Al-Somali, A. M.; Sayes, C. M.; Johns, J.; Drezek, R.; Colvin, V. L. *J. Am. Chem. Soc.* **2007**, *129*, 2871-2879.
24. Wang, Y.; Wong, J. F.; Teng, X.; Lin, X. Z.; Yang, H. *Nano Lett.* **2003**, *3*, 1555-1559.
25. Feng, J.; Ding, S.-Y.; Tucker, M. P.; Himmel, M. E.; Kim, Y. H.; Zhang, S. B.; Keyes, B. M.; Rumbles, G. *Appl. Phys. Lett.* **2005**, *86*, 033108.
26. Depalo, N.; Comparelli, R.; Striccoli, M.; Curri, M. L.; Fini, P. *J. Phys. Chem. B* **2006**, *110*, 17388-17399.
27. Wu, H.; Zhu, H.; Zhuang, J.; Yang, S.; Liu, C.; Cao, Y. C. *Angew. Chem. Int. Ed.* **2008**, *47*, 3730-3734.
28. Yu, W. W.; Qu, L.; Guo, W.; Peng, X. *Chem. Mater.* **2003**, *15*, 2854-2860.
29. Rekharsky, M. V.; Inoue, Y. *Chem. Rev.* **1998**, 98, 1875-1917.
30. Castro, R.; Cuadrado, I.; Alonso, B.; Casado, C. M.; Moran, M.; Kaifer, A. E. *J. Am. Chem. Soc.* **1997**, *119*, 5760-5761.
31. Janczewski, D.; Tomczak, N.; Khin, Y. W.; Han, M. Y.; Vancso G. J. *Eur. Pol. J.* **2009**, *45*, 3-9.

Chapter 6

Fabrication and Luminescence of Designer Surface Patterns with β-CD Functionalized Quantum Dots via Multivalent Supramolecular Coupling*

Supramolecular microcontact printing was used to obtain controlled patterns consisting of Quantum Dots (QDs) functionalized at their periphery with β-cyclodextrin (β-CD) in combination with adamantyl terminated dendrimeric "glues". Functionalization of core-shell CdSe/ZnS QDs was achieved by surface ligation. Immobilization of the QDs from solution onto glass substrates printed with (a) adamantyl-terminated poly(propylene imine) dendrimers and (b) via direct microcontact printing of QDs onto the dendrimer layer both yielded stable and robust multilayer structures. The stability of the patterns was primarily due to multivalent supramolecular host-guest interactions between β-CD located at the QD surface and adamantyl groups at the dendrimer periphery as the dendrimers acted as a "supramolecular glue". The surface-immobilized QDs were capable to form host-guest complexes with other molecules of interest at binding cavities not occupied by adamantyl groups. Complex formation with ferrocene-functionalized molecules at these sites led to partial quenching of the luminescence emission of QDs demonstrating the principle for sensing using the QD multilayer structures.

* Part of this Chapter has been published in: Dorokhin, D.; Hsu, S. H.;Tomczak, N.; Reinhoudt, D. N.; Huskens, J.; Velders, A. H.; Vancso G. J. *ACS Nano* **2010**, DOI: 10.1021/nn901109x.

6.1 INTRODUCTION

Host-guest molecular interactions, well known in the field of molecular biology, have been explored for supramolecular assembly of synthetic molecular and nanoscale components to obtain functional nanostructures.[1-3] The prerequisite for the assembly is that the constitutive building blocks have the structurally defined ability for molecular recognition. Directed host-guest assembly on surfaces allows one to build up hierarchical structures and integrate them into devices.[3-6] Preparation of well-defined surface assemblies was demonstrated for molecules,[7,8] dendrimers,[9-11] nanocolloids[12-14] and proteins.[6,15] Host-guest interactions are reversible, either upon addition of guests (hosts) having higher binding constant to hosts (guests),[16-17] or by chemical or electrochemical reactions in the host-guest couples.[10,18] Host guest chemistry also offers the possibility for error correction.

Assembly of Quantum Dots (QDs) on surfaces is primarily explored in the context of their applications in optoelectronics[19-21] and sensing.[22,23] For supramolecular assembly in water the QDs must be coated with ligands that endow the QDs with colloidal stability in aqueous buffers and simultaneously display molecular recognition ability.[22] To this end, cyclodextrin-coated QDs are attractive materials as cyclodextrin is a well-known host of a multitude of small molecule guests binding to the CD cavity.[22,24-31] Binding of QDs via single host-guest complexes results in less stable structures as the stability of the QD layer is defined by a single supramolecular bond. Multivalent binding is therefore desired to provide stable supramolecular structures.[13] Additionally, well-defined patterns of QDs on relevant surfaces are often needed to provide spatially defined luminescent regions e.g. for electrochromic displays or a background reference in sensing applications.[19]

This chapter describes the fabrication of luminescent structures by selective binding of functional dendrimers and β-CD modified QDs via supramolecular host-guest interactions. The stability of the assemblies is provided by multivalent interactions between the assembly components enabling the fabrication of multilayer structures. Microcontact printing of the assembly components is demonstrated to be an effective method in preparation of the assemblies. Additionally, the unused hosts on the surface of the QDs allow for consecutive molecular recognition of other guest molecules to form more complex architectures. Robust platforms for luminescence sensing can be obtained when guests modulating the QD

emission are used. In particular, this chapter demonstrates that ferrocene functionalized dendrimers bind to previously unoccupied cavities of the β–CD modified QDs and effectively quench the QD luminescence, modulating therefore the optical properties of the QD assemblies.

6.2 RESULTS AND DISCUSSION

6.2.1 Functionalization of QDs with β-CD Derivative

To create supramolecularly assembled patterns of QDs proper functionalization of the QD surface and substrate is required. This is necessary for providing relevant interactions between the respective pattern components. Accordingly, multivalent host-guest complexation chemistry in aqueous solution was chosen to provide for stable, well-ordered layers. The QDs used for the assembly, therefore, should display high colloidal stability in aqueous buffers. In this study commercially available carboxylate-functionalized CdSe/ZnS QDs with the first absorption peaks at 580 nm and 595 nm, respectively, were used. The corresponding maxima of the emission of the QDs are located at 597 nm and 608 nm, respectively (Figure 6.1a,b).

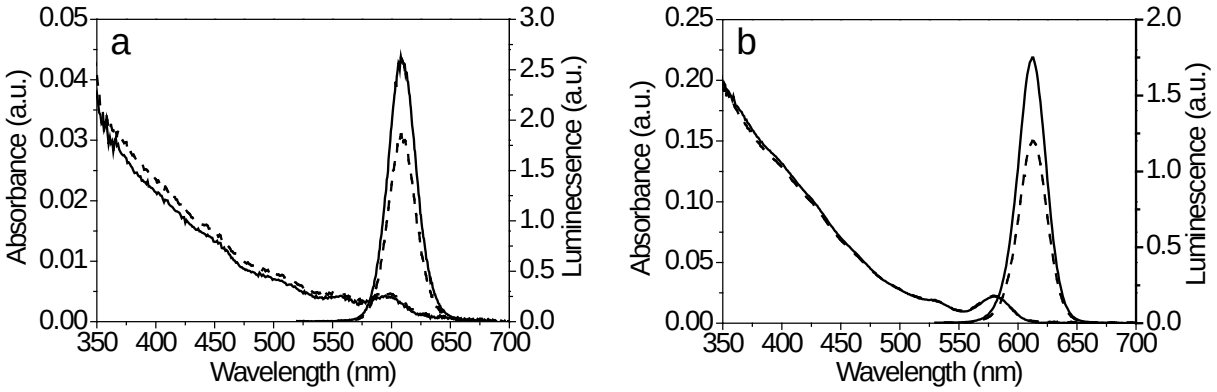

Figure 6.1 Absorption and emission spectra of (a) EviTag600, (b) eFluor605 carboxylate-functionalized CdSe/ZnS quantum dots (solid) and functionalized with β-CD$(NH_2)_7$ (dash) in PBS buffer. Excitation wavelength is 500 nm.

The carboxylic groups on the surface of the QDs stabilize the nanoparticles in aqueous media and provide functionality for binding of amine terminated β-CD molecules (Figure 6.2a). Surface functionalization with β-CD is performed *via* EDC-activated reaction between the

carboxylic groups and amines. The resulting β-CD-modified QDs (QD/β-CD) (Figure 6.2b) show no remarkable changes in their absorption spectra, however the luminescence decreases slightly.

6.2.2 Preparation of QD Supramolecular Assemblies

For immobilization of QD/β-CD on surfaces materials based on their ability to form multivalent host-guest interactions were chosen, since such interactions are important to form kinetically stable assemblies.[13] The immobilization steps are schematically shown in Figure 6.2e. The first step is to create a monolayer of β-CD (**2**) on the glass substrate (**1**) (see Figure 6.2e). This β-CD layer serves as the multivalent anchoring platform for all subsequent immobilization steps and allows for thermodynamically and kinetically stable positioning and patterning of molecules, for example dendrimers.[1,9]

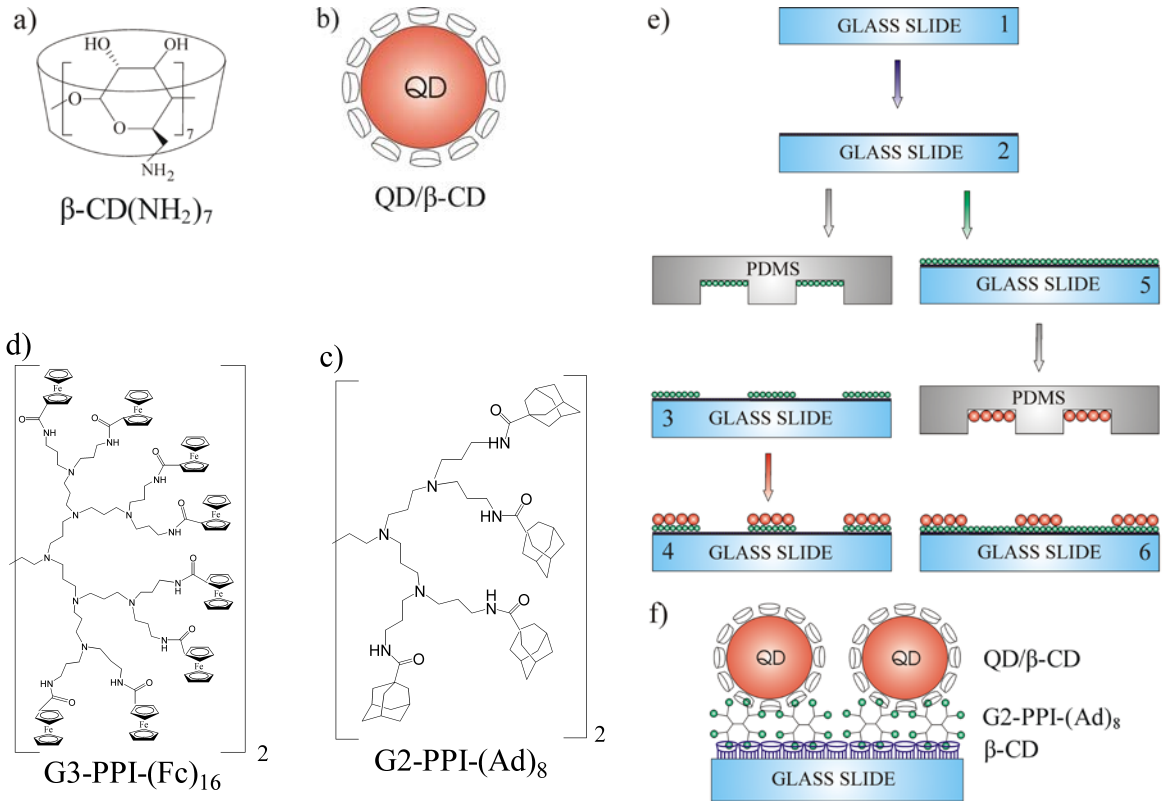

Figure 6.2 Chemical structures of a) heptamine β-cyclodextrin (β-CD$(NH_2)_7$), (b) QDs functionalized with β-CD$(NH_2)_7$, (c) adamantyl-terminated poly(propylene imine) dendrimer (2^{nd} generation, G2-PPI-$(Ad)_8$) and (d) ferrocenyl-terminated poly(propylene imine) dendrimer (3^{rd} generation, G3-PPI-$(Fc)_{16}$). e) Scheme of the immobilization methods and (f)

the structure of the resulting multilayer assembly. The numbers written on the glass slides represent the preparation steps and are explained in the main text.

6.2.2.1 Immobilization of QDs onto Planar Surfaces from Solution

Two complementary methods for the supramolecular pattern building with QDs were explored. In the first method a layer of adamantyl-terminated dendrimers (G2-PPI-$(Ad)_8$) (Figure 6.2c) on β-CD functionalized substrate is formed by microcontact printing (μCP) (**3**).[32] Owing to the high number of functional units on the periphery of the G2-PPI-$(Ad)_8$ the dendrimers bind multivalently to the β-CD layer.[12] Additionally, there are many functional groups left exposed to the solution, which are available for complexation with other hosts. QDs bearing surface-immobilized β-CD can therefore also bind by multivalent interactions to the adamantyl-functionalized G2-PPI-$(Ad)_8$ dendrimers. The QD attachment to the G2-PPI-$(Ad)_8$ layer is performed by simply casting a drop of a QD water solution onto the functionalized surface (**4**). Immobilization of QD/β-CD is highly selective to G2-PPI-$(Ad)_8$ leaving a background β-CD layer in the non-patterned region.

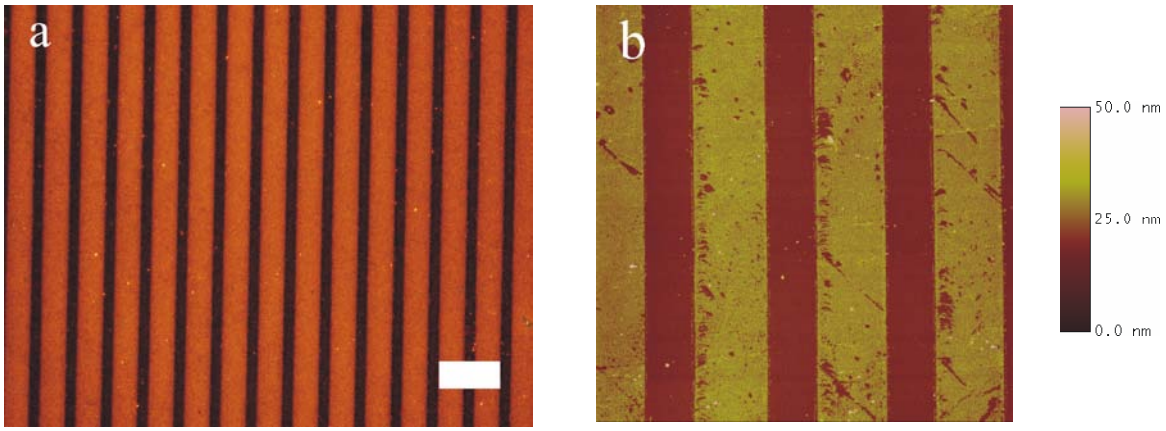

Figure 6.3 Fluorescence images (a) and AFM height images (b) of micropatterns of QDs/β-CD on glass substrate obtained by drop casting the QDs on microcontact printed G2-PPI-$(Ad)_8$ dendrimers. The scale bar is 25 μm. AFM image scan size is 50×50 μm.

The fluorescence emission from the QD/β-CD pattern is shown in Figure 6.3a. The 10 μm fluorescent lines and 5 μm spacing correspond to the spacing on the PDMS stamp used to print the G2-PPI-$(Ad)_8$ dendrimers. This result indicates that the QDs were attached to the

substrate selectively only to the areas where the G2-PPI-$(Ad)_8$ molecules were previously printed. The average pattern height measured by AFM (Figure 6.3b) is equal to ~10 nm, which approximately corresponds to the combined height of the G2-PPI-$(Ad)_8$ and QD/β-CD layers. Additionally, AFM imaging proved unequivocally that QDs did not attach directly to the β-CD layer. The defects in the QD pattern, as visualized by AFM, may be related to a lower coverage of adamantyl-terminated dendrimers on the β-CD layer due to incomplete coverage of the PDMS stamp by the dendrimers during the microcontact printing step.

6.2.2.2 Direct Printing of QDs onto Planar Surfaces

The second fabrication method was based on direct printing of QD/β-CD onto glass slides covered with G2-PPI-$(Ad)_8$ (**5**). The β-CD-modified glass substrate was first immersed in a 10 mM solution of G2-PPI-$(Ad)_8$. After drying, a PDMS stamp inked with QD/β-CD was brought into contact with the substrate (**6**). Following stamp removal the excess of QD/β-CD was rinsed off with a PBS buffer. The fluorescence image of the resulting pattern is shown in Figure 6.4.a (5 μm lines and 10 μm spacing on the PDMS stamp).

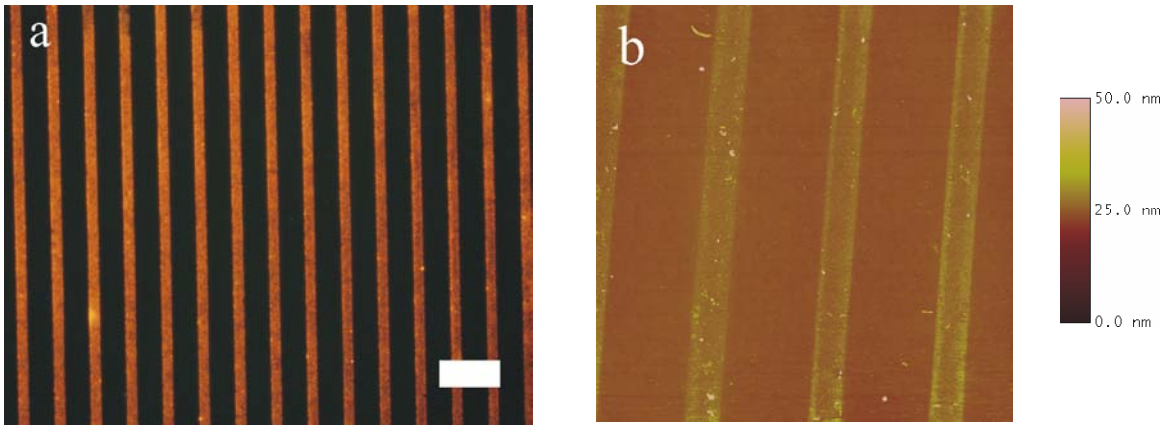

Figure 6.4 Fluorescence images (a) and AFM height images (b) of QDs/β-CD patterns on glass substrate obtained by microcontact printing of the QDs onto a full G2-PPI-$(Ad)_8$ layer. The scale bar is 25 μm. AFM image scan size is 50×50 μm.

The height of the QD patterns, as obtained from the AFM image (Figure 6.4b) is equal to ~6 nm, in good agreement with the estimated size of the QD/β-CD conjugate. Similar to the first method the fluorescence and AFM imaging revealed that there were no QDs present in the

space between the patterns. This means that there was no substantial diffusion of the QDs across the G2-PPI-$(Ad)_8$ functionalized surface after microcontact printing. This is primarily due to the high molar mass of the QDs and to the multivalent nature of the QD attachment to the substrate.

6.2.3 Molecular Recognition *via* Host-Guest Interactions

Immobilized QD/β-CD should be capable to form host-guest complexes with other molecules of interest. In particular the formation of specific host-guest complexes on the surface of QDs can modulate the emission of the QDs. In previous chapters it has been demonstrated that ferrocene moieties in close proximity to the QD surface efficiently quench the QD luminescence. To check whether a similar quenching takes place also in the system described here, dendrimers functionalized with ferrocene at the periphery (G3-PPI-$(Fc)_{16}$) (Figure 6.1d) were chosen.[10,11] These dendrimers can be solubilized in water under the conditions of low pH and presence of cyclodextrin.[33] Multiple number of functionalities at the dendrimer periphery should provide for a stable multivalent attachment to the QD/β-CD layers.

For subsequent experiments the patterns prepared *via* the first method using a homogeneous β-CD substrate with printed adamantyl "glue" were chosen. Here QD pattern were obtained by attachment from the solution and in between these patterns there was β-CD layer exposed. The G3-PPI-$(Fc)_{16}$ dendrimers were microcontact-printed perpendicularly across the QD/β-CD patterns. The resulting cross-patterns were characterized by fluorescence and AFM microscopy.

An AFM topography height image of the cross-printed sample is shown in Figure 6.5a. There are four planes with different heights corresponding to the primary β-CD layer (**I**), printed adamantane dendrimers with QD/β-CD on top (**II**), ferrocene dendrimers on top of the β-CD layer (**III**), ferrocene dendrimers printed on top of the QD/β-CD/G2-PPI-$(Ad)_8$ layer (**IV**). The mean values of the height for each region with respect to region **I** are equal to ~10 nm (**II**), ~3 nm (**III**) and ~13 nm (**IV**). The height difference between regions **I** and **III** corresponds approximately to the estimated height of the G3-PPI-$(Fc)_{16}$ dendrimers. Accordingly, the height difference between regions **IV** and **II** is the same as between regions **I** and **III**. These results indicate that the transfer of the dendrimers to the surface was successful, and that the QD layer was not compromised by the cross stamping of G3-PPI-

$(Fc)_{16}$. In particular, there was no lift-off of the QDs upon contact with the dendrimer-coated stamp. By providing stable multivalent binding between the respective components it was possible therefore to obtain multilayer structures.

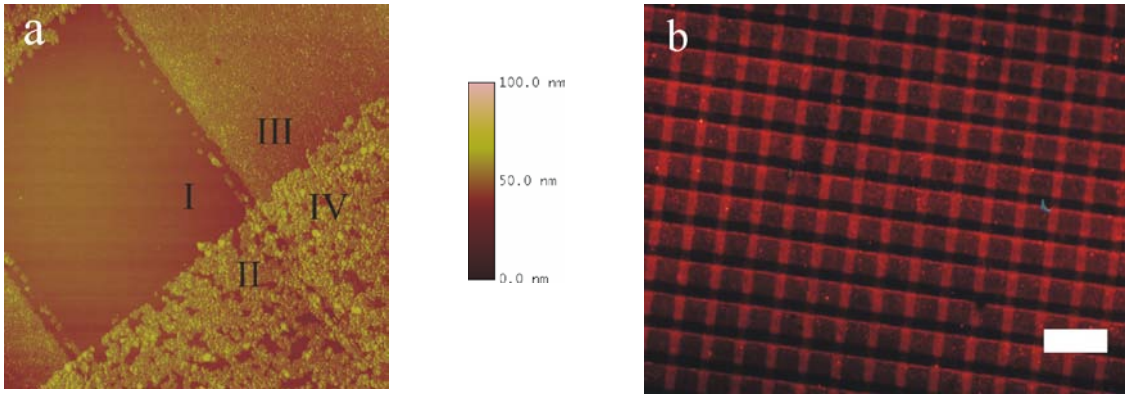

Figure 6.5 a) AFM height image of the crossed patterns. (I) Primary β-CD layer, (II) printed adamantane dendrimers with QD/β-CD on top, (III) ferrocene dendrimers on top of the β-CD layer, (IV) ferrocene dendrimers printed on top of the QD/β-CD / G2-PPI-$(Ad)_8$ layer. Scan size is 10×10 μm. b) Fluorescence image of a QDs/β-CD pattern cross-printed with G3-PPI-$(Fc)_{16}$ dendrimers. The luminescence of the QDs in the cross-printed regions visibly decreased. The scale bar is 30 μm.

Figure 6.5b shows a fluorescence image of QDs cross-patterned with G3-PPI-$(Fc)_{16}$ dendrimers. In the areas where these dendrimers are in contact with QD/β-CD the luminescence of the nanoparticles visibly decreased. The QDs in the areas with no G3-PPI-$(Fc)_{16}$ printed on top retained their original luminescence. The quenching effect clearly observed in fluorescence imaging is due to the formation of host-guest complexes between the ferrocenyl groups and the immobilized β-CD hosts at the QD surface. The quenching mechanism likely involves a charge transfer process between photoexcited QDs and the ferrocene groups (chapter 3). Modulation of the QD optical properties in the multilayer structures was therefore shown and it represents a proof-of-principle for molecular sensing of water-soluble species able to bind to the β-CD cavity.

6.3 CONCLUSIONS

This chapter describes two methods for the immobilization of water-soluble β-CD-functionalized QDs on planar surfaces based on multivalent supramolecular interactions. The β-CD molecules on the QD surface were available for subsequent host-guest complexation with molecules of interest. In particular, the luminescence of QDs was modulated by introducing ferrocene-functionalized dendrimers by cross printing on top of the QD layer. In regions where the ferrocenyl dendrimers formed host-guest complexes with β-CD-functionalized QDs the luminescence intensity decreased, likely due to a photoinduced charge transfer between the ferrocene and QDs.

6.4 EXPERIMENTAL

Materials. Carboxylate-functionalized core-shell CdSe/ZnS EviTag600 and eFluor605 quantum dots were obtained from Evident Technologies (New York, US) and eBioscience (San Diego, US), respectively. 3-aminopropyl triethoxysilane (APTES), *N*-[3-(trimethoxysilyl)propyl]ethylenediamine (TPEDA), 1,4-phenylene diisothiocyanate (DITC) and *N*-(3 dimethylaminopropyl)-*N'*-ethylcarbodiimide hydrochloride (EDC) were purchased from Aldrich. PBS buffer solution (pH=7.4) was obtained from B. Braun Melsungen AG (Melsungen, Germany). Heptamine β-cyclodextrin (β-CD$(NH_2)_7$), adamantyl-terminated poly(propylene imine) (2^{nd} generation, G2-PPI-$(Ad)_8$), ferrocenyl-terminated poly(propylene imine) (3^{rd} generation, G3-PPI-$(Fc)_{16}$) dendrimers were synthesized according to previously reported procedures.[10,33,34] For all the experiments Milli-Q water with resistivity higher than 18 MΩ·cm was used.

Synthesis of β-CD modified QDs. 50μL of a PBS buffer solution containing carboxilated QDs (EviTag600 or eFluor605, 10μM) was mixed with 200 μL of EDC×(10 $^{-4}$g) and the solution was stirred for 30 minutes. Subsequently, 250 μL of β-CD$(NH_2)_7$ (2×10^{-4}g) was added to the mixture and the mixture was shaken overnight. The resulting materials were purified by ultracentrifugation (40000 rpm, 30 minutes) or used as prepared.

Preparation of β-CD monolayer. β-CD monolayers on glass were obtained as described previously by Onclin *et al*.[35] Microscope cover slides (Deckglaser, 24x24mm, Menzel-Glaser) were activated with Piranha solution (concentrated H_2SO_4 mixed with 33% H_2O_2 in a volume ratio of 3:1; *Warning! Piranha solutions must be handled with caution*) for 20 minutes to form a hydroxyl layer on the surface. The substrates were intensively rinsed with MilliQ water and dried under N_2. The substrates

were then put into a high vacuum desiccator together with 0.1mL of TPEDA. After overnight incubation, the slides were rinsed with ethanol and dichloromethane to remove excess of silanes and subsequently dried with a nitrogen stream. The attachment of 1,4-phenylene diisothiocyanate was performed in a 20 mM solution of toluene at 60˚C during 2 hr. Samples were thoroughly rinsed with toluene and dried in a nitrogen flow. The β-CD attachment was performed during 2 hr in an aqueous solution of β-cyclodextrin heptamine (0.1mM, pH=7) at 60˚C. Samples were thoroughly rinsed with water and dried in a nitrogen flow.[35-37]

Microcontact printing of functionalized dendrimers. Stamps were prepared by casting a 10:1 (v/v) mixture of poly(dimethylsiloxane) (PDMS) and curing agent (Sylgard 184, Dow Corning) onto a silicon master with a 5 or 10 μm wide contact lines and period 15 μm. After overnight curing at 60 ºC, the stamps were oxidized by oxygen plasma for 1 min and subsequently inked by casting a drop of a 1mM aqueous solution of G2-PPI-$(Ad)_8$ or G3-PPI-$(Fc)_{16}$ dendrimers onto the stamp for 10 mins. Before printing, the stamps were blown dried in a stream of nitrogen. The stamps were brought into conformal contact with the substrate for 10 min. After stamp removal, the printed substrates were rinsed with water and dried with nitrogen.

Immobilization of QDs on functionalized glass slides. Immobilization of QD/β-CD on the glass surface was performed using two different procedures (Figure 6.2e). In the first procedure, 100 μL of a 10^{-6}M QD solution was deposited on the glass slide **3** patterned previously with G2-PPI-$(Ad)_8$ (**2**). After 10 minutes the substrate was rinsed with a PBS buffer and dried under N_2 resulting in pattern **4**. In the second procedure the QDs were microcontact printed directly onto the G2-PPI-$(Ad)_8$ functionalized glass slide **5**. The QDs (100μL, 10^{-6}M) were casted onto the PDMS stamp and after 10 minutes dried under N_2. The PDMS stamp was brought into contact with the substrate slide for 5min and carefully removed. Finally, the glass slides were washed with PBS buffer and dried under N_2 resulting in pattern **6**.

Methods. The absorption spectra of the QD solutions were measured with a Varian Cary 300 UV-Vis spectrophotometer. The photoluminescence spectra were measured with an Edinburgh XE-900 spectrofluorometer (λ_{ex}=500nm). Fluorescence imaging was performed using an inverted fluorescence microscope (Olympus IX71) equipped with a mercury lamp (U-RLF-T) and a digital camera (Olympus DP70). Olympus filter cube U-MWG was used to filter the excitation and emission light ($\lambda_{ex}\leq$350nm, $\lambda_{em}\geq$420nm). Topography imaging of the coated glass substrates was performed at ambient conditions in air with a NanoScope III atomic force microscope (Veeco/Digital Instruments, Santa Barbara, CA) equipped with a J-scanner. A single beam Si cantilever with a nominal spring constant of 42 nN/nm (Nanosensors, Germany) was used for imaging in the tapping mode.

6.5 REFERENCES

1. Descalzo, A. B.; Martinez-Manez, R.; Sancenon, F.; Hoffman, K.; Rurack, K. *Angew. Chem. Int. Ed.* **2006**, *45*, 5924-5948.
2. Nijhuis, C. A.; Ravoo, B. J.; Huskens, J.; Reinhoudt, D. N. *Coord. Chem. Rev.* **2007**, *251*, 1761-1780.
3. Kinge, S.; Crego-Calama, M.; Reinhoudt, D. N. *ChemPhysChem* **2008**, *9*, 20-42.
4. Rabe, J.; Buttgenbach, S.; Schroder, J.; Hauptmann, P. *IEEE Sens. J.* **2003**, *3*, 361-368.
5. Dickert, F. L.; Landgraf, S.; Sikorski, R. *J. Mol. Model.* **2000**, *6*, 491–497.
6. Villalonga, R.; Cao, R.; Fragoso A. *Chem. Rev.* **2007,** *107*, 3088-3116.
7. Mulder, A.; Onclin, S.; Peter, M.; Hoogenboom, J. P.; Beijleveld, H.; ter Maat, J.; Garcia-Parajo, M. F; Ravoo, B. J.; Huskens, J.; van Hulst, N. F.; Reinhoudt, D. N. *Small* **2005**, *1*, 242–253.
8. Mahalingam, V.; Onclin, S.; Peter, M.; Ravoo, B. J.; Huskens, J.; Reinhoudt, D. N. *Langmuir* **2004**, *20*, 11756-11762.
9. Huskens, J.; Deij, M. A.; Reinhoudt D. N. *Angew. Chem. Int. Ed.* **2002**, *41*, 4467-4471.
10. Nijhuis, C. A.; Huskens, J.; Reinhoudt D. N. *J. Am. Chem. Soc.* **2004**, *126*, 12266-12267.
11. Nijhuis, C. A.; Yu, F.; Knoll, W.; Huskens, J.; Reinhoudt D. N. *Langmuir* **2005**, *21*, 7866–7876.
12. Crespo-Biel, O.; Dordi, B.; Reinhoudt D. N.; Huskens, J. *J. Am. Chem. Soc.* **2005**, *127*, 7594-7600.
13. Ludden, M. J. W.; Reinhoudt, D. N.; Huskens J. *Chem. Soc. Rev.*, **2006**, *35*, 1122–1134.
14. Maury, P.; Peter, M.; Crespo-Biel, O.; Ling, X. Y.; Reinhoudt, D. N.; Huskens J. *Nanotechnology* **2007**, *18*, 044007.
15. Ludden, M. J. W.; Li, X.; Greve, J.; van Amerongen, A.; Escalante, M.; Subramaniam, V.; Reinhoudt, D. N.; Huskens J. *J. Am. Chem. Soc.* **2008**, *130*, 6964–6973.
16. Castro, R.; Cuadrado, I.; Alonso, B.; Casado, C. M.; Moran, M.; Kaifer, A. E. *J. Am. Chem. Soc.* **1997**, *119*, 5760–5761.

17. Rekharsky, M. V.; Inoue, Y. *Chem. Rev.* **1998**, *98*, 1875-1917.
18. Ling, X. Y.; Reinhoudt, D. N.; Huskens J. *Chem. Mater.* **2008,** *20*, 3574–3578.
19. Kim, L. A.; Anikeeva, P. O.; Coe-Sullivan, S. A.; Steckel, J. S.; Bawendi, M. G. Bulovic, V. *Nano Lett.* **2008**, *8*, 4513–4517.
20. Klar, T. A.; Franzl, T.; Rogach, A. L.; Feldmann J. *Adv. Mater.* **2005**, *17*, 769-773.
21. Wang, X.; Summers, C. J.; Wang, Z. L. *Nano Lett.* **2004**, *4*, 423-426.
22. Galian, E. R.; de la Guardia, M. *Trends Anal. Chem.* **2009**, *28*, 279-291.
23. Algar, W. R.; Massey, M.; Krull, U. J. *Trends Anal. Chem.* **2009**, *28*, 292-306.
24. Han, C.; Haibing, L. *Small* **2008**, *4*, 1344-1350.
25. Freeman, R.; Finder, T.; Bahshi, L. L.; Willner I. *Nano Lett.* **2009**, 9, 2073-2076.
26. Li, H. B.; Han, C. P. *Chem. Mater.* **2008**, *20*, 6053-6059.
27. Ralkshit, S.; Vasudevan, S. *ACS Nano* **2008**, *2*, 1473-1479.
28. Depalo, N.; Comparelli, R.; Striccoli, M.; Curri, M. L.; Fini, P.; Giotta, L.; Agostiano, A. *J. Phys. Chem. B* **2006**, *110*, 17388–17399.
29. Palaniappan, K.; Xue, C.; Arumugam, G.; Hackney, S. A.; Liu, J. *Chem. Mater.* **2006**, *18*, 1275–1280.
30. Palaniappan, K.; Hackney, S. A.; Liu, J. *Chem. Commun.* **2004**, 2704–2705.
31. Han, C. P.; Li, H. B. *Chin. Chem. Lett.* **2008**, *19*, 215-218.
32. Xia, Y. N.; Whitesides, G. M. *Annu. Rev. Mater. Sci.* **1998**, *28*, 153-184.
33. Michels, J. J.; Baars, M. W. P. L.; Meijer, E. W.; Huskens, J.; Reinhoudt, D. N. *J. Chem. Soc. Perkin Trans. 2* **2000,** 1914-1916.
34. Guillo, F.; Jullien, L.; Hamellin, B.; Lehn, J.-M.; De Robertis, L.; Driguez, H. *Bull. Soc. Chim. Fr.* **1995**, *132*, 859-861.
35. Onclin, S.; Mulder, A.; Huskens, J.; Ravoo, B. J.; Reinhoudt, D. N. *Langmuir* **2004**, *20*, 5460-5466.
36. Ling, X. Y.; Reinhoudt, D. N.; Huskens, J. *Langmuir* **2006**, *22*, 8777-8782.
37. Auletta, T.; Dordi, B.; Mulder, A.; Sartori, A.; Onclin, S.; Bruinink, C. M.; Peter, M.; Nijhuis, C. A.; Beijleveld, H.; Schonherr, H.; Vancso, G. J.; Casnati, A.; Ungaro, R.; Ravoo, B. J.; Huskens, J.; Reinhoudt, D. N. *Angew. Chem. Int. Ed.* **2004**, *43*, 369-373.

Chapter 7

Fluorescence Lifetime Imaging of Resonance Energy Transfer in Supramolecular Surface Patterns of β-CD Functionalized QD Hosts and Organic Dye Guests

Detection of an analyte via supramolecular host-guest binding and Quantum Dot-based Fluorescence Resonant Energy Transfer (FRET) signal transduction mechanism is demonstrated. Surface patterns consisting of CdSe/ZnS Quantum Dots (QDs) functionalized at their periphery with β-cyclodextrin (β–CD) were obtained by immobilization of the QDs from solution onto glass substrates printed with adamantyl-terminated poly(propylene imine) dendrimeric "glue". Subsequent formation of host-guest complexes between vacant β–CD on the QD surface and an adamantyl-functionalized lissamine rhodamine was confirmed by fluorescence microscopy, spectroscopy and Fluorescence Lifetime Imaging Microscopy (FLIM). Based on the Förster theory, the FRET efficiency of the donor-acceptor pair was calculated to be equal to 18 %.

7.1 INTRODUCTION

Semiconductor nanoparticles (Quantum Dots, QD) represent a novel class of bright, highly stable nanoscale emitters, which are extensively researched for applications in biolabelling and (bio)sensing.[1-8] The sensing schemes involving QDs rely most often on the QDs as signal transducers of the sensing events. Energy or electron transfer processes are usually used as the signal transduction mechanisms.[9-10] In fluorescence resonance energy transfer (FRET) a photoexcited molecule (donor) transfers the energy to an energy acceptor in close proximity to the donor, typically within 10 nm.[11] QDs are generally thought to be good FRET donors due to their very broad absorption spectrum and narrow emission lines. One can therefore benefit from a reduced signal crosstalk, by maximizing direct excitation of the QDs far away from the absorption band of the energy acceptors. Additionally, due to low photobleaching rates of the QDs, FRET can be observed on longer time-scales compared to standard organic chromophores. QD-based FRET[10,11-21] has been recently explored as the optical transduction mechanism in numerous sensing schemes for the detection of DNA,[22,23] RNA,[24,25] proteins,[26] for the monitoring of enzymatic activity,[27-31] metabolic pathways,[32] DNA-related processes,[33-35] and for the environmental sensing of e.g. solution pH,[36] ions,[37] TNT or saccharides,[38,39] down to the single QD level.[22,35,40,41] A particularly intriguing concept in QD-based sensing is that of supramolecular host-guest recognition on QD surfaces and optical transduction of the sensing events *via* the modulation of the optical properties of the QDs. Although the concept is not new,[42] functional QD materials exploring this idea were realized only recently. In particular, cyclic oligosaccharide receptors, like cyclodextrins, located on the surface of the QDs were shown to be capable of forming host-guest complexes with hydrophobic molecules, which were complimentary by size to the cavity of the oligosaccharide.[43-50] Moving one step forward, FRET-based signal transduction can be exploited in the design of surface bound sensing platforms for molecular recognition.[51-55] The advantages of a surface-based sensing platform include: absence of aggregation of the QDs during sensing, small reaction volumes needed, and reusability of the surfaces.

This chapter reports on FRET recognition of host-guest complex formation on surfaces. FRET occurs between CdSe/ZnS QD donors functionalized with β-cyclodextrin incorporated into supramolecular multilayer structures and functionalized lissamine rhodamine dyes adsorbed from solution or microcontact printed on top of the QD layer. FRET signals are

clearly observed using fluorescence microscopy, spectroscopy, and Fluorescence Lifetime Imaging Microscopy (FLIM). The FRET efficiency upon supramolecular binding is assessed.

7.2 RESULTS AND DISCUSSION

7.2.1 Preparation of QDs Patterns on Planar Surfaces

Commercially available carboxylate-functionalized CdSe/ZnS QDs with the first absorption peak located at 502 nm and the emission maximum located at 525 nm (Figure 7.1d) were surface-derivatized with β-CD(NH_2)$_7$ (Figure 7.1a) following the procedure described in the chapter 6. The β-CD functionalized QDs (QD/β-CD) are shown in figure 7.1b. No remarkable changes in absorption spectra of the QDs after anchoring the β-CD (Figure 7.1a) were observed; however the luminescence of QD/β-CD decreased slightly in comparison to the initial QDs (Figure 7.1d).

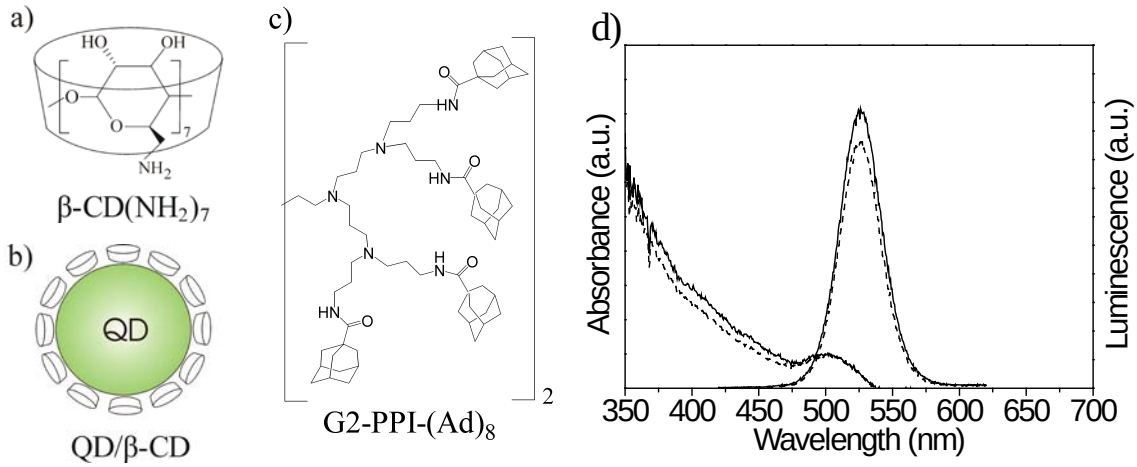

Figure 7.1 Chemical structures of (a) β-cyclodextrin heptamine (β-CD(NH_2)$_7$) (b) QDs coated with β-CD and (c) adamantyl-terminated poly(propylene imine) (2nd generation, G2-PPI-(Ad)$_8$). d) Absorption and luminescence emission of CdSe/ZnS quantum dots before (solid) and after (dash) surface derivatization with β-CD(NH_2)$_7$. Excitation wavelength is 450 nm.

The β-CD molecules bound to the surface of the QDs were shown to be capable of forming multiple host-guest complexes with other molecules in solution or at interfaces (chapter 5 and 6).[46]

The previous chapter describes the preparation of a multilayer structure consisting of QD/β-CD and a molecular dendrimeric "glue" printed onto planar, optically transparent surfaces. Briefly, the fabrication method is based on exploring the β-CD molecular printboard monolayer onto which additional layers of materials are built exclusively *via* supramolecular interactions (Figure 7.2).[56,57] Multivalent supramolecular chemistry used in the multilayer build-up ensures that the structures are kinetically stable and no pattern damage is introduced during subsequent building steps.[58] In the process, the adamantyl-functionalized dendrimeric "glue" (G2-PPI-$(Ad)_8$) (Figure 7.1c) was microcontact printed using a PDMS stamp onto the β-CD modified glass substrate. Subsequently, the QD/β-CD nanoparticles were casted onto the G2-PPI-$(Ad)_8$ preprinted glass slide. The β-CD located on the QDs surface formed multivalent host-guest complexes with the adamantyl groups of the "glue". The QDs bind therefore stably only to the regions coated with the glue (excess of nanoparticles adsorbed to regions without the "glue" can be effectively washed away) resulting in structure **1** shown in Figure 7.2.

The vacant β-CD molecules on the surface of the QD not participating in host-guest interactions with the dendrimeric "glue" are still able to form host-guest complexes with other guest molecules. The formation of the complexes can happen directly in a solution of the guest resulting in structure **2** (Figure 7.2) or by other means e.g. the guests can be transferred on top of the QD/β-CD layer by stamp-assisted microcontact printing, resulting in structure **3** (Figure 7.2).

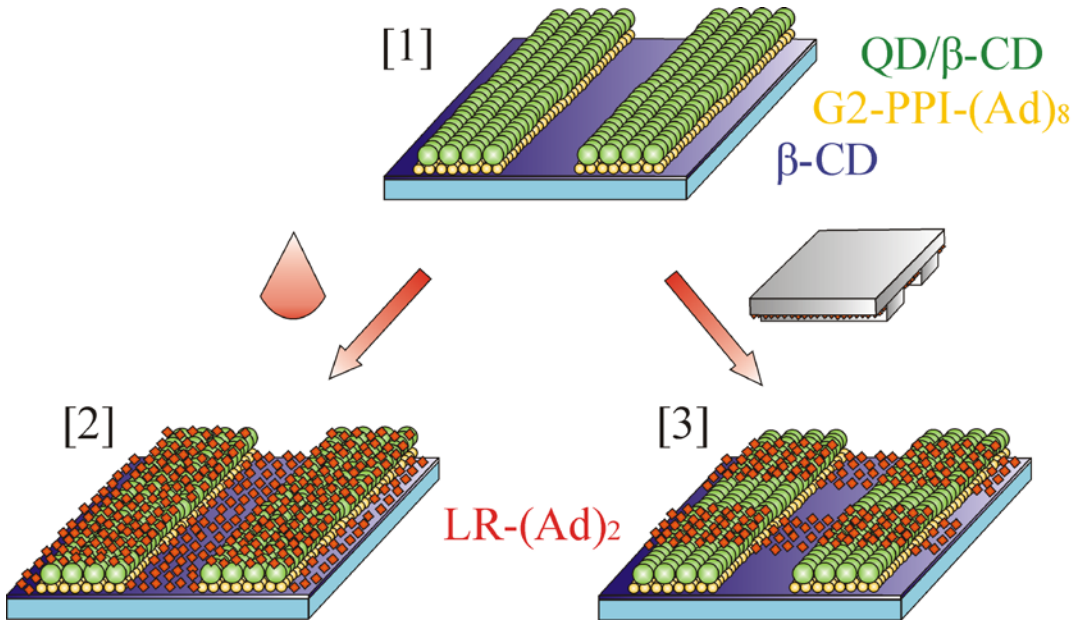

Figure 7.2 Scheme of the multilayer supramolecular QD sensing platform and two different surface binding protocols. Immersing the platform **1** into a solution of LR-$(Ad)_2$ results in structure **2**. Microcontact printing of LR-$(Ad)_2$ across the QD patterns results in structure **3**.

7.2.2 Deposition of Lissamine Rhodamine Chromophore

The guest molecule, a lissamine rhodamine chromophore functionalized with two adamantyl "tails" (LR-$(Ad)_2$) (Figure 7.3a), was chosen for the experiments. The emission of the QD and the absorption and emission of (LR-$(Ad)_2$) as shown in Figure 7.3b indicate that FRET between this donor/acceptor pair should be possible.

Figure 7.4 shows fluorescence images of the QD pattern after adding a LR-$(Ad)_2$ solution on top of **1** (Figure 7.4 a,b,c) resulting in structure **2**. The filter sets used defined the excitation and emission range during the experiments for the case when only the QDs were excited (Figure 7.4a), only the dyes were excited (Figure 7.4b) and for the case where only the QDs were excited but only the emission of the dyes could be observed (Figure 7.4c).The fluorescence signal observed in the latter case is a clear indication that FRET between the QDs and LR-$(Ad)_2$ occurred. The QD/β-CD pattern is absorbing below 350 nm and after FRET to LR-$(Ad)_2$ the emission signal is collected above 615 nm exclusively in the region of the QD pattern (compare Figure 7.4a and 7.4c).

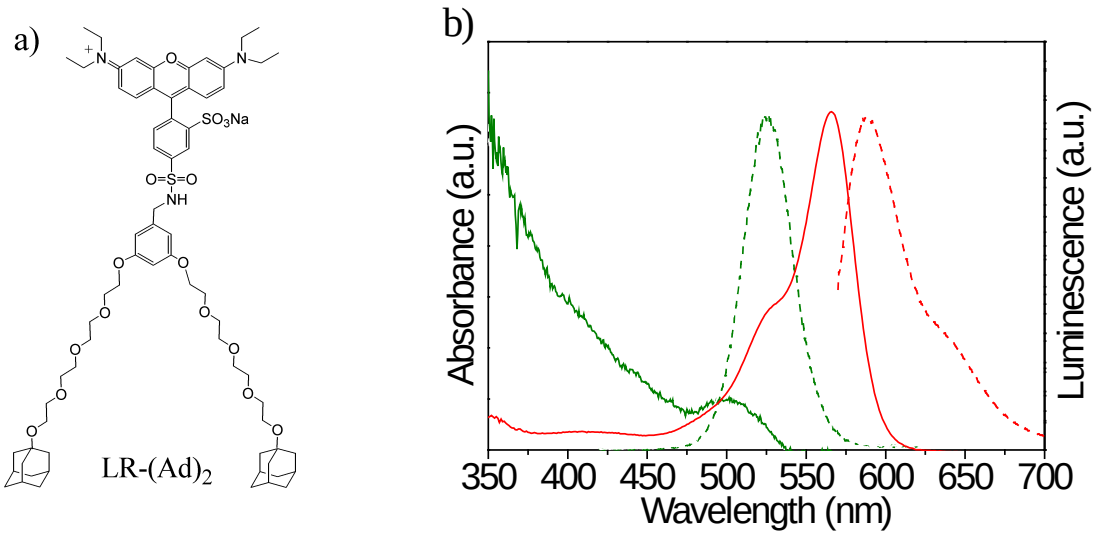

Figure 7.3 (a) Chemical structure of lissamine rhodamine divalent adamantyl (LR-$(Ad)_2$). (b) Absorption (red, solid) and emission (red, dashed) spectra of LR-$(Ad)_2$ in water. Excitation wavelength is 550nm. Absorption (green, solid) and luminescence emission (green, dashed) of CdSe/ZnS quantum dots. Excitation wavelength is 450nm.

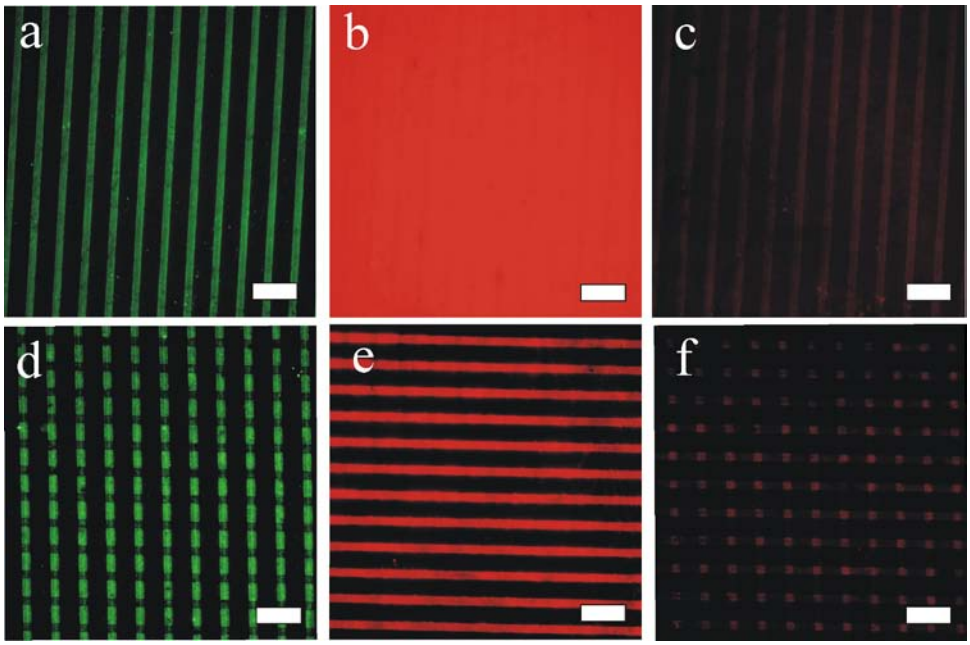

Figure 7.4 Fluorescence images of QDs/β-CD pattern **1** treated with LR-$(Ad)_2$ from solution resulting in structure **2** in Figure 7.2 (a,b,c), and cross-printed with LR-$(Ad)_2$ molecules resulting in structure **3** in Figure 7.2 (d,e,f). Images were recorded with the following filter sets: (a,d) $\lambda_{ex} \leq 350$nm, $\lambda_{em} \geq 420$nm; (b,e) $\lambda_{ex} = 510$-550nm, $\lambda_{em} \geq 590$nm and (c,f) $\lambda_{ex} \leq 350$nm, $\lambda_{em} \geq 615$nm. The scale bars are 25 μm.

Similar results were observed when printing the LR-$(Ad)_2$ chromophores perpendicularly across the QD/β-CD pattern resulting in structure **3** (Figure 7.2). The fluorescence image in Figure 7.4e shows clearly that LR-$(Ad)_2$ was printed perpendicularly to the QD/β-CD pattern. Evidence for FRET in the structure is clearly obtained by examining Figures 7.4d and 7.4f. FRET results in a decrease of the donor QD luminescence and simultaneous appearance of the emission of a fluorescence signal of the dye acceptor. A characteristic square pattern is visible in Figure 7.4f; an evidence that FRET happens only where both the donor and acceptor are present.

7.2.3 Fluorescence Lifetime Imaging Microscopy of QDs Patterns

In order to provide essential information about the fluorescence mechanism and the interaction between QD-donor and LR-$(Ad)_2$ chromophor derivatives as an acceptor the sample was examined using fluorescence lifetime imaging microscopy (FLIM).

Emission spectra obtained at different locations on the crossprinted patterns are shown in Figure 7.5. When exciting the QDs at 469 nm, the luminescence of the QDs and the fluorescence of the dye are both observed in the cross printed regions. As the direct dye excitation is minimal at this wavelength, the fluorescence signal detected above the emission of the QDs must be due to energy transfer from the excited QDs to the dye immobilized onto the QD layer. Additional evidence for FRET is obtained from FLIM. The FLIM shows the fluorescence intensity and fluorescence lifetime at each pixel of the confocally scanned image. Intensity and FLIM images for the same region of interest are shown in Figure 7.6.

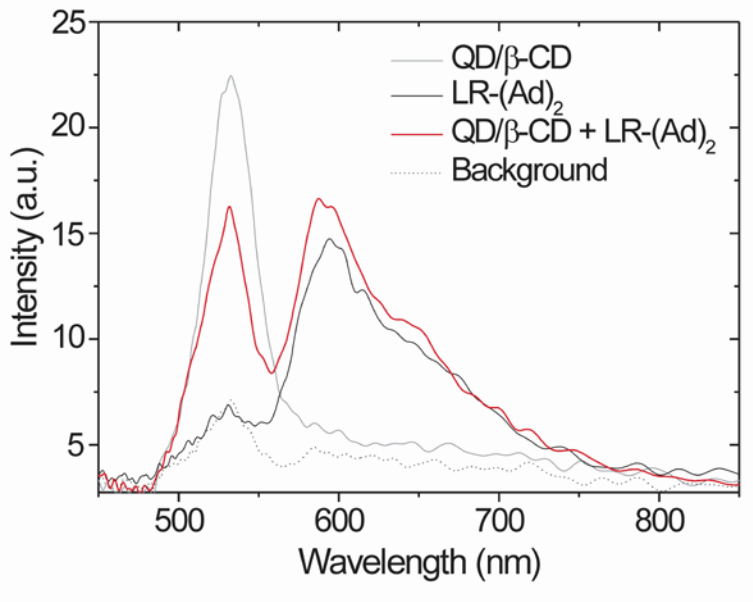

Figure 7.5 Luminescence and fluorescence spectra of QD/β-CD and LR-$(Ad)_2$, respectively, obtained from different positions on the cross-printed patterns. Excitation wavelength is equal to 469 nm.

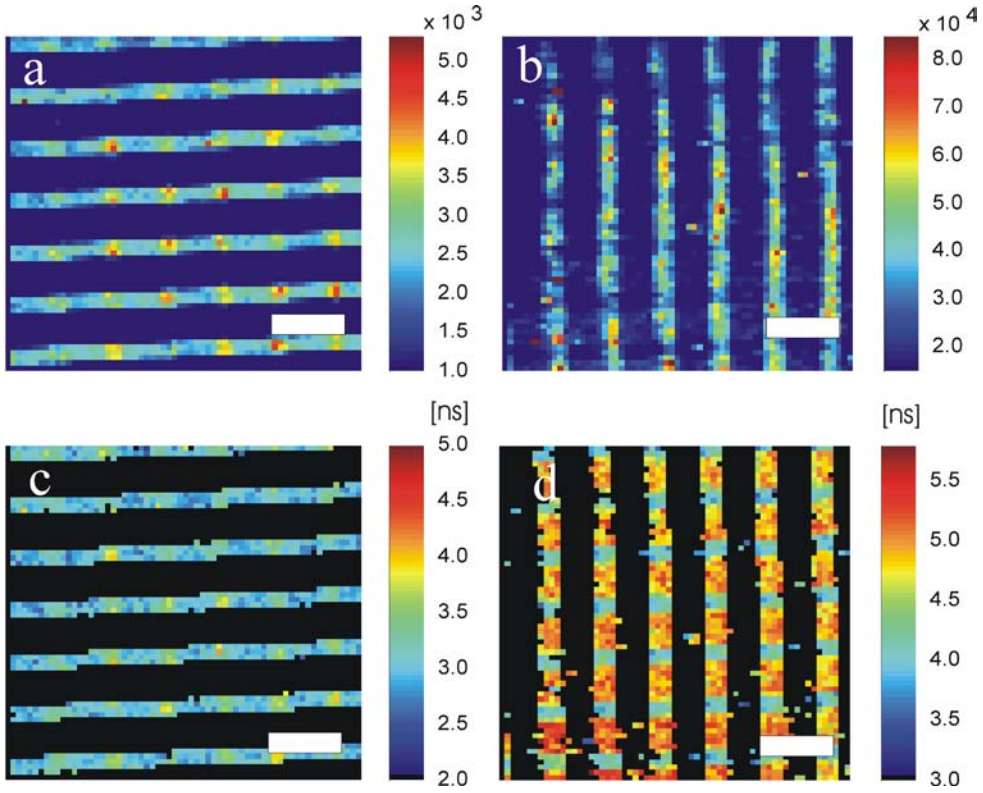

Figure 7.6 (a,b) Fluorescence intensity (c,d) and lifetime images of QD/β-CD patterns crossprinted with LR-$(Ad)_2$ molecules. (a,c) Emission from the dye; (b,d) emission from the QDs. The scale bars are 20 μm.

To eliminate cross-talk, separate filter sets for the emission of the QDs and for the dyes were used. The key result is the increase of the luminescence intensity of LR-$(Ad)_2$ (Figure 7.6a) together with a correlated decrease of the luminescence lifetimes of the QDs (Figure 7.6d). In areas where the QD/β-CD are in contact with LR-$(Ad)_2$ due to formation of host-guest complexes between the β-CD cavity and adamantane functionalized tails of the LR-$(Ad)_2$, and a decrease of lifetime is observed (Figure 7.6d). Furthermore, in Figure 7.6c an increase of the lifetime of LR-$(Ad)_2$ fluorophores in the crosspatterned areas is also observed. All these results are a signature of FRET in the crossprinted regions of the sample. Additionally, one can look at the intensity profiles along the QD/β-CD and LR-$(Ad)_2$ patterns (Figure 7.7). The decrease of the nanocrystals' luminescence is remarkably correlated with the emission of the dye. For an excitation wavelength at which direct excitation of the dye is minimal such result clearly indicates a FRET process.

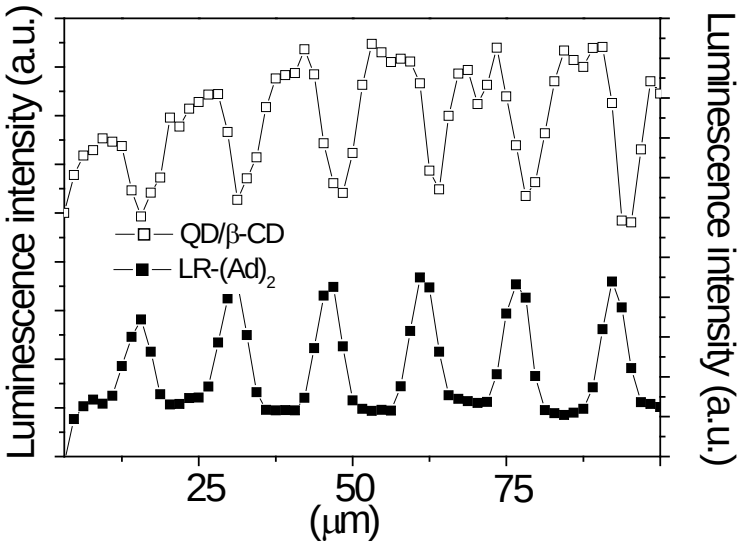

Figure 7.7 Luminescence intensity profiles obtained along the QDs/β-CD (□) and LR-$(Ad)_2$ (■) patterns.

From the FLIM image shown in Figure 7.6d a histogram of the luminescence lifetimes can be obtained (Figure 7.8a) (examples of luminescence decays and their fits are shown in Figure 7.8b). A clear double-peak distribution is visible with the peak at longer lifetimes corresponding to the QDs without the dye acceptor, and the lower lifetime peak corresponding to the regions crossprinted with the dye.

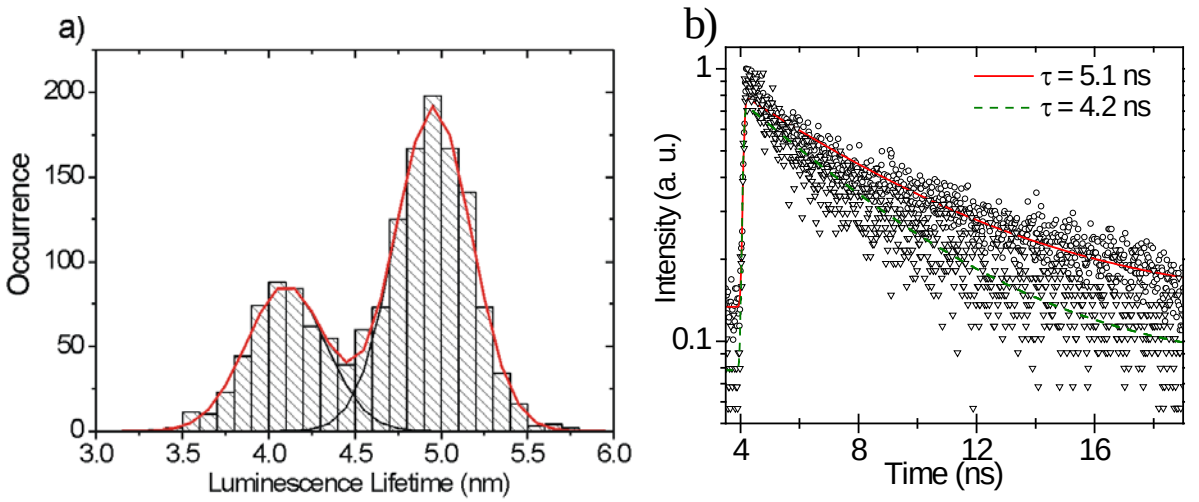

Figure 7.8 Histogram of luminescence lifetime (a) acquired during FLIM imaging. The histogram was fitted to a Gaussian multipeak distribution function. Typical lifetime decays of QDs.

The peak values of the histograms were obtained by fitting a Gaussian multipeak distribution function and the obtained values were used to calculate the effective FRET efficiency (E_f) in the system using the following equation:

$$E_f = 1 - \frac{\tau_{DA}}{\tau_D} \tag{7.1}$$

where τ_D is the donor's lifetime without the acceptor and τ_{DA} is the lifetime of the donor in the presence of the acceptor.[11] For the system an experimental value of E_f equal to 18 % was obtained. This relatively low FRET efficiency value is primarily the result of the long linker in the LR-$(Ad)_2$ dye and the thick organic shell on the QDs (polymeric coating and the β-CD ligand).

7.3 CONCLUSIONS

A supramolecular multilayer structure comprising of β-CD functionalized QDs and dendrimers micropatterned substrate was obtained. Vacant β-CD formed host-guest supramolecular complexes with dye molecules functionalized with adamantyl groups. Fluorescence microscopy, spectroscopy and FLIM proved that a FRET process occurred in the regions where the dye was bound to the β-CD functionalized QD. A FRET efficiency of 18% was obtained for the supramolecular patterns. This value could be further improved by decreasing the distance between the chromophores and the QD. The QDs patterns are efficient molecular recognition platforms based on the FRET signal transduction mechanism.

7.4 EXPERIMENTAL

Materials. Water-soluble core-shell CdSe/ZnS QDs (eFluor525) functionalized with carboxylic groups on their surface were purchased from eBioscience (San Diego, US). 3-aminopropyl triethoxysilane (APTES), *N*-[3-(trimethoxysilyl)propyl]ethylenediamine (TPEDA), 1,4-phenylene diisothiocyanate (DITC) and *N*-(3 dimethylaminopropyl)-*N'*-ethylcarbodiimide hydrochloride (EDC) were purchased from Aldrich. PBS buffer solution (pH=7.4) was obtained from B. Braun Melsungen AG (Melsungen, Germany). β-Cyclodextrin heptamine (β-CD$(NH_2)_7$), lissamine rhodamine divalent adamantyl (LR-$(Ad)_2$) and adamantyl-terminated poly(propylene imine) (2^{nd} generation, G2-PPI-$(Ad)_8$) dendrimers were synthesized according to previously reported procedures.[59,60] For all experiments Milli-Q water with a resistivity higher than 18 MΩ·cm was used.

Synthesis of β-CD modified QDs. 50μL of a PBS buffer solution containing carboxylate-functionalized QDs (eFluor525, 10μM) was mixed with 200 μL of EDC ($\approx 10^{-4}$g) and the solution was stirred for 30 minutes. Subsequently, 250 μL of β-CD$(NH_2)_7$ (2×10^{-4}g) was added to the mixture and the mixture was shaken overnight. The resulting solution of β-CD coated QD was used as prepared.

Preparation of β-CD monolayer. β-CD monolayers on glass were obtained as described previously.[61] Microscope glass cover slides (Deckglaser, 24x24mm, Menzel-Glaser) were activated with Piranha solution (concentrated H_2SO_4 mixed with 33% H_2O_2 in a volume ratio of 3:1; *Warning! Piranha solutions must be handled with caution*) for 20 minutes to form a hydroxyl layer on the surface. The substrates were intensively rinsed with MilliQ water and dried under N_2. The substrates were then put into a high vacuum desiccator together with 0.1 mL of TPEDA. After overnight incubation, the slides were rinsed with ethanol and dichloromethane to remove excess of silanes and

subsequently dried with a nitrogen stream. The attachment of 1,4-phenylene diisothiocyanate was performed in a 20 mM solution of toluene at 60ºC during 2 hr. Samples were thoroughly rinsed with toluene and dried in a nitrogen flow. The β-CD attachment was performed during 2 hr in an aqueous solution of β-cyclodextrin-heptamine (0.1 mM, pH = 7) at 60ºC. The samples were rinsed with water and dried in a nitrogen flow.[62,63]

Microcontact printing of G2-PPI-$(Ad)_8$ and LR-$(Ad)_2$. Stamps were prepared by casting a 10:1 (v/v) mixture of poly(dimethylsiloxane) (PDMS) and curing agent (Sylgard 184, Dow Corning) onto a silicon master with a 5×10 μm pattern spacing. After overnight curing at 60 ºC the stamps were oxidized by oxygen plasma for 1 min and subsequently inked by casting a drop of a 1 mM aqueous solution of G2-PPI-$(Ad)_8$ dendrimer, or LR-$(Ad)_2$, onto the stamp for 10 min. Before printing, the stamps were blown dried in a stream of nitrogen. The stamps were brought into conformal contact with the substrate for 10 min. After stamp removal, the printed substrates were rinsed with water and dried with nitrogen.

Immobilization of QD/β-CD onto functionalized glass slides. Immobilization of QD/β-CD on the glass surface was performed using the procedure described in the previous chapter. Briefly, 100 μL of a 10^{-6} M QD/β-CD solution was casted on the glass slide previously modified with β-CD and subsequently patterned with G2-PPI-$(Ad)_8$. After 10 minutes the substrate was rinsed with a PBS buffer and dried under N_2.

Immobilization of LR-$(Ad)_2$ onto QD-functionalized glass slides. Immobilization of LR-$(Ad)_2$ on the glass surface was performed by casting 100 μL of a 10^{-6} M LR-$(Ad)_2$ solution onto the glass slide previously modified with QD/β-CD. After 10 minutes the substrate was rinsed with a PBS buffer and dried under N_2.

Methods. A UV-Vis spectrophotometer Varian Cary 300 was used to measure the absorption spectrum of the QD and dye solutions. The photoluminescence spectra were recorded with an Edinburgh XE-900 spectrofluorometer (λ_{ex}=500nm). Fluorescence imaging was performed using a Olympus IX71 inverted microscope equipped with a mercury lamp (U-RLF-T) and a digital camera (Olympus DP70). Suitable filter sets and dichroic mirrors were used to filter the excitation and emission light.

A custom-built scanning confocal microscope was used to acquire luminescence and fluorescent spectra and to perform fluorescence lifetime imaging (FLIM).[64,65] The microscope was equipped with an water immersion objective (100×, NA=1.4, Olympus). A picosecond pulsed laser emitting at 469

nm and modulated at 20 MHz (BDL475, Becker & Hickl, Germany) was used as the excitation light source.

A time-correlated single photon counting (TCSPC) module (SPC-830, Becker & Hickl, Germany) combined with a single photon avalanche diode detector (SPAD, PDM series, 50 ps timing resolution, MPD, Italy) was used for fluorescence lifetime imaging (FLIM). The intensity of the excitation light was kept low enough to ensure that only one photon per laser pulse was arriving to the detectors between the pulses. FLIM images were obtained by raster scanning the sample and acquiring the fluorescence decay curves at each pixel position. To avoid crosstalk during the lifetime measurements, BP525-15 (Semrock) and BP582-15 (Semrock) bandpass emission filters were inserted in the detection path for the emission of the QDs and the dyes, respectively. The software package SPCImage (Becker & Hickl) was used for the processing of the lifetime data. The fluorescence lifetime values were obtained by fitting the fluorescence decay curves with a single exponential decay function (Figure 7.8b). Fluorescence spectra were obtained using a prism spectrometer by dispersing the emitted light onto a cooled CCD camera (Newton EMCCD, DU970N-BV, Andor, Northern Ireland). A calibrated light source (Cal-2000 Mercury Argon Calibration source, Ocean Optics) was applied to calibrate the wavelength.

7.5 REFERENCES

1. Alivisatos, A. P. *Science* **1996**, *271*, 933–937.
2. Bruchez, M., Jr.; Moronne, M.; Gin, P.; Weiss, S.; Alivisatos, A. P. *Science* **1998**, *281*, 2013–2016.
3. Chan, W. C. W.; Nie, S. *Science* **1998**, *281*, 2016-2018.
4. Dubertret, B.; Skourides, P.; Norris, D. J.; Noireaux, V.; Brivanlou, A. H.; Libchaber, A. *Science* **2002**, *298*, 1759-1762.
5. Larson, D. R.; Zipfel, W. R.; Williams, R. M.; Clark, S. W.; Bruchez, M. P.; Wise, F. W.; Webb, W. W. *Science* **2003**, *300*, 1434-1436.
6. Wu, X.; Liu, H.; Liu, J.; Haley, K. N.; Treadway, J. A.; Larson, J. P.; Ge, N.; Peale, F.; Bruchez, M. P. *Nat. Biotechnol.* **2003**, *21*, 41-46.
7. Alivisatos, A. P. *Nat. Biotechnol.* **2004**, *22*, 47-52.
8. Medintz, I. L.; Uyeda, H. T.; Goldman, E. R.; Mattoussi, H. *Nat. Mater.* **2005**, *4*, 435-446.
9. Somers, R. C.; Bawendi, M. G.; Nocera, D. G. *Chem. Soc. Rev.* **2007**, *36*, 579-591.
10. Gill, R.; Zayats, M.; Willner, I. *Angew. Chem. Int. Ed.* **2008**, *47*, 7602-7625.

11. Lakowicz, J. R. *Principles of Fluorescent Spectroscopy*, 3nd Ed., Springer, **2006,** ISBN: 978-0-387-31278-1.
12. Kagan, C. R.; Murray, C. B.; Nirmal, M.; Bawendi, M. G. *Phys. Rev. Lett.* **1996**, *76*, 1517-1520.
13. Willard, D. M.; Carillo, L. L.; Jung, J.; Van Orden, A. *Nano Lett.* **2001**, *1*, 469-474.
14. Crooker, S. A.; Hollingsworth, J. A.; Tretiak, S.; Klimov, V. I. *Phys. Rev. Lett.* **2002**, *89*, 186802.
15. Medintz I. L.; Trammel, S. A.; Mattoussi, H.; Mauro, J. M. *J. Am. Chem. Soc.* **2004**, *126*, 30-31.
16. Clapp A. R.; Medintz, I. L.; Mauro, J. M.; Fisher, B. R.; Bawendi, M. G.; Mattoussi, H. *J. Am. Chem. Soc.* **2003**, *126*, 301-310.
17. Medintz, I. L.; Clapp, A. R.; Mattoussi, H.; Goldman, E. R.; Mauro, J. M. *Nat. Mater.* **2003**, *2*, 630-638.
18. Medintz, I. L.; Konnert, J. H.; Clapp, A. R.; Stanish, I.; Twigg, M. E.; Mattoussi, H.; Mauro, J. M.; Deschamps J. R. *Proc. Nat. Acad. Sci.* **2004**, *101*, 9612-9617.
19. Clapp, A. R.; Medintz, I. L.; Mattoussi, H. *ChemPhysChem* **2006**, *7*, 47-57.
20. Raymo F. M.; Yildiz, I. *PCCP* **2007**, *9*, 2036-2043.
21. Dennis, A. M.; Bao, G. *Nano Lett.* **2008**, *8*, 1439-1445.
22. Zhang, C. Y.; Yeh, H. C.; Kuroki, M. T.; Wang, T. H. *Nat. Mater.* **2005**, *4*, 826-831.
23. Dubertret, B. *Nat Mater.* **2005**, *4*, 797-798.
24. Zhang, C. Y.; Johnson, L. W. *J. Am. Chem. Soc.* **2006**, *128*, 5324–5325.
25. Bakalova, R.; Zhelev, Z.; Ohba, H.; Baba, Y. *J. Am. Chem. Soc.* **2005**, *127*, 11328-11335.
26. Levy, M.; Cater, S. F.; Ellington, A. D. *ChemBioChem* **2005**, *6*, 2163-2166.
27. Medintz, I. L.; Clapp, A. R.; Brunel, F. M.; Tiefenbrunn, T.; Uyeda, H. T.; Chang, E. L.; De- schamps, J. R.; Dawson, P. E.; Mattoussi, H. *Nat. Mater.* **2006**, *5*, 581-586.
28. Kim, Y. P.; Oh, Y. H.; Oh, E.; Ko, S.; Han, M. K.; Kim, H. S. *Anal. Chem.* **2008**, *80*, 4634-4641.
29. Xu, C.; Xing, B.; Rao, J. *Biochem. Biophys. Res. Commun.* **2006**, *344*, 931-935.
30. Yao, H.; Zhang, Y.; Xiao, F.; Xia, Z.; Rao, J. *Angew. Chem. Int. Ed.* **2007**, *46*, 4346-4349.
31. Shi, L.; DePaoli, V.; Rosenzweig, N.; Rosenzweig, Z. *J. Am. Chem. Soc.* **2006**, *128*, 10378-10379.

32. Freeman, R.; Gill, R.; Shweky, I.; Kotler, M.; Banin, U.; Willner, I. *Angew. Chem. Int. Ed.* **2009**, *48*, 309-313.
33. Patolsky, F.; Patolsky, F.; Gill, R.; Weizmann, Y.; Mokari, T.; Banin, U.; Winner, I. *J. Am. Chem. Soc.* **2003**, *125*, 13918-13919.
34. Gill, R.; Willner, I.; Shweky, I.; Banin, U. *J. Phys. Chem. B* **2005**, *109*, 23715-23719.
35. Hohng, S.; Ha, T. *ChemPhysChem* **2005**, *6*, 956-960.
36. Snee, P. T.; Somers, R. C.; Nair, G.; Zimmer, J. P.; Bawendi, M. G.; Nocera, D. G. *J. Am. Chem. Soc.* **2006**, *128*, 13320–13321.
37. Chen, C. Y.; Cheng, C. T.; Lai, C. W.; Wu, P. W.; Wu, K. C.; Chou, P. T.; Choub, Y. H.; Chiub, H. T. *Chem. Commun.* **2006**, 263–265.
38. Goldman, E. R.; Medintz, I. L.; Whitley, J. L.; Hayhurst, A.; Clapp, A. R .; Uyeda, H. T.; Deschamps, J. R.; Lassman, M. E.; Mattoussi H. *J. Am. Chem. Soc.* **2005**, *127*, 6744-6751.
39. Freeman, R.; Bahshi, L.; Finder, T.; Gill, R.; Willner, I. *Chem. Commun*. **2009**, 764-766.
40. Zhou, D. J.; Piper, J. D.; Abell, C.; Klenerman, D.; Kang, D. J.; Ying, L. M. *Chem. Commun.* **2005**, 4807-4809.
41. Grecco, H. E.; Lidke, K. A.; Heintzmann, R.; Lidke, D. S.; Spagnuolo, C.; Martinez, O. E ; Jares-Erijman, E. A.; Jovin. T. M. *Microsc. Res. Technol*. **2004**, *65*, 169-179.
42. Willner, I.; Eichen, Y. *J. Am. Chem. Soc.* **1987**, *109*, 6862-6863.
43. Dorokhin, D.; Tomczak, N. ; Han, M. Y.; Reinhoudt, D. N.; Velders, A. H.; Vancso G. J. *ACS Nano* **2009**, *3*, 661-667.
44. Palaniappan, K.; Xue, C.; Arumugam, G.; Hackney, S. A.; Liu, J. *Chem. Mater*. **2006**, *18*, 1275–1280.
45. Palaniappan, K.; Hackney, S. A.; Liu, J. *Chem. Commun.* **2004**, 2704 – 2705.
46. Rekharsky, M. V.; Inoue, Y. *Chem. Rev.* **1998**, *98*, 1875-1917.
47. Freeman, R.; Finder, T.; Bahshi, L. L.; Willner I. *Nano Lett.* **2009**, 9, 2073-2076.
48. Han, C. P.; Li, H. B. *Chin. Chem. Lett.* **2008**, *19*, 215-218.
49. Li, H. B.; Han, C. P. *Chem. Mater*. **2008**, *20*, 6053-6059.
50. Ralkshit, S.; Vasudevan, S. *ACS Nano* **2008**, *2*, 1473-1479.
51. Medintz, I. L.; Sapsford, K. E.; Clapp, A. R.; Pons, T.; Higashiya, S.; Welch, J. T.; Mattoussi, H. J. *Phys. Chem. B* **2006**, *110*, 10683-10690.
52. Sapsford, K. E.; Medintz, I. L.; Golden, J. P.; Deschamps, J. R.; Uyeda, H. T.; Mattoussi, H. *Langmuir* **2004**, *20*, 7720-7728.

53. Kloepfer, J. A.; Cohen, N.; Nadeau, J. L. *J. Phys. Chem. B* **2004**, *108*, 17042-17049.

54. Algar, W. R.; Krull, U. J. *Langmuir* **2009**, *25*, 633-638.

55. Geissbuehler, I.; Hovius, R.; Martinez, K. L.; Adrian, M.; Thampi, K. R.; Vogel H. *Angew. Chem. Int. Ed.* **2005**, *44*, 1388-1392.

56. Crespo-Biel, O.; Dordi, B.; Reinhoudt D. N.; Huskens, J. *J. Am. Chem. Soc.* **2005**, *127*, 7594-7600.

57. Ludden, M. J. W.; Reinhoudt, D. N.; Huskens J. *Chem. Soc. Rev.* **2006**, *35*, 1122–1134.

58. Huskens, J. *Curr. Op. Chem. Biol.* **2006**, *10*, 537-543.

59. Mulder, A.; Onclin, S.; Peter, M.; Hoogenboom, J. P.; Beijleveld, H.; ter Maat, J.; Garcia-Parajo, M. F.; Ravoo, B. J.; Huskens, J.; van Hulst, N. F.; Reinhoudt, D. N. *Small* **2005**, *1*, 242-246.

60. Beulen, M. W. J.; Bugler, J.; Lammerink, B.; Guerts, F. A. J.; Biemond, E.; van Leerdam, K. G. C.; van Veggel, F. C. J. M.; Engbersen, J. F. J.; Reinhoudt, D. N. *Langmuir* **1998**, *14*, 6424-6429.

61. Onclin, S.; Mulder, A.; Huskens, J.; Ravoo, B. J.; Reinhoudt, D. N. *Langmuir* **2004**, *20*, 5460-5466.

62. Ling, X. Y.; Reinhoudt, D. N.; Huskens, J. *Langmuir* **2006**, *22*, 8777-8782.

63. Auletta, T.; Dordi, B.; Mulder, A.; Sartori, A.; Onclin, S.; Bruinink, C. M.; Peter, M.; Nijhuis, C. A.; Beijleveld, H.; Schonherr, H.; Vancso, G. J.; Casnati, A.; Ungaro, R.; Ravoo, B. J.; Huskens, J.; Reinhoudt, D. N. *Angew. Chem. Int. Ed.* **2004**, *43*, 369-373.

64. Blum, C.; Cesa, Y.; Escalante, M.; Subramaniam, V. *J. R. Soc. Interface* **2009**, *6*, S35-S43.

65. Escalante, M.; Blum, C.; Cesa, Y.; Otto, C.; Subramaniam, V. *Langmuir* **2009**, *25*, 7019-7024.

Chapter 8

Grafting of Redox Active Organometallic Polymers to Quantum Dots: Synthesis, Characterization and Luminescence

Synthesis of CdSe/ZnS quantum dots (QDs) coated with poly(ferrocenylsilanes) (PFS) is described. The QD-PFS hybrid materials were obtained by grafting thiol-functionalized PFS polymers with different molar masses, 7750 g/mol (PFS32) and 12500 g/mol (PFS50), directly to the surface of QDs via a ligand exchange reaction. The grafting of the polymer chains has been observed by pulsed field gradient (PFG) ^{1}H NMR spectroscopies. Due to grafting of the PFS, the luminescence of the QDs decreased and the absorption and emission spectra shifted to longer wavelengths.

8.1 INTRODUCTION

Interfacing functional polymers directly with Quantum Dots (QD) is essential in applications where charge or energy transfer reactions are operational. These applications include optoelectronics,[1-6] photovoltaics,[7-11] and sensing.[12-15] Polymer chains can be attached to the QD surface *via* functionalized chain ends or *via* multiple side- or main-chain chemical functionalities able to bind to the nanocrystals' surface. For optoelectronic applications the QD surface has been functionalized with electroactive polymers, such as poly(paraphenylene vinylene),[16-18] poly(thiophenes),[19,20] or polyfluorenes.[21] Close contact between the polymers and the QDs resulted in improved charge transfer efficiency and improved device performance. Poly(ferrocenylsilanes) (PFS) are a class of electroactive polymers with a backbone consisting of alternating ferrocene and (alkyl)silane units.[22] Such a unique chemical structure results in remarkable catalytic,[23] optoelectronic (redox),[24] and etch-resistant properties.[25,26] The catalytic properties were explored in the synthesis of carbon nanotubes,[27] while the etch resistivity was applied in lithography for the fabrication of magnetic materials for high-density data storage,[28] and ceramics composed of Fe and Si oxides.[29] The redox activity of PFS is primarily due to the presence of the ferrocene unit, but the nearby silicon atom plays a significant role in charge delocalization. The PFS response to an externally applied potential was explored in, e.g., the fabrication of stimulus responsive materials, such as capsules for drug delivery.[30]

Cyr et al. reported on the optical properties of QDs in the presence of PFS in solution and in thin films.[31] However, grafting of PFS via chain ends directly to the QD surface has not been reported. This chapter describes the preparation of CdSe/ZnS QDs with grafted poly(ferrocenylsilanes) (PFS). Two PFS polymers with different molar masses, 7750 g/mol (PFS32) and 12500 g/mol (PFS50), and with chain ends functionalized with thiols were directly attached to the QD surface using the 'grafting to' approach.[32] The grafting of the polymer chains has been confirmed by diffusion ordered NMR spectroscopy. Noticeable differences in the diffusion coefficient for QD-PFS32 and QD-PFS50 were observed during the NMR experiments. Grafting of the polymers resulted in changes in the optical properties of QDs. A red shift in the absorption and emission spectra as well as quenching of the luminescence is reported.

8.2 RESULTS AND DISCUSSION

8.2.1 Coating of QDs with Polymers

The initial core-shell CdSe/ZnS QDs are coated with trioctylphosphine oxide ligands. This ligand originates from the synthetic protocol and stabilizes the nanoparticles in nonpolar solvents.[33] The optical properties of the QDs are characterized by spectroscopic methods. The UV-Vis and emission spectra of purified CdSe/ZnS QDs are shown in Figure 8.1. The first adsorption peak is located at 553 nm. From this value the size of the QD core is estimated to be 3.3 nm.[34] The luminescence spectrum shows a narrow and symmetric emission peak with a maximum located at 567nm. The quantum yield (QY) of the QDs is calculated to be equal to 27.3 by comparing the integrated luminescence intensity to that of the $[Ru\ (bpy)_3]^{2+}$ complex standard.[35,36]

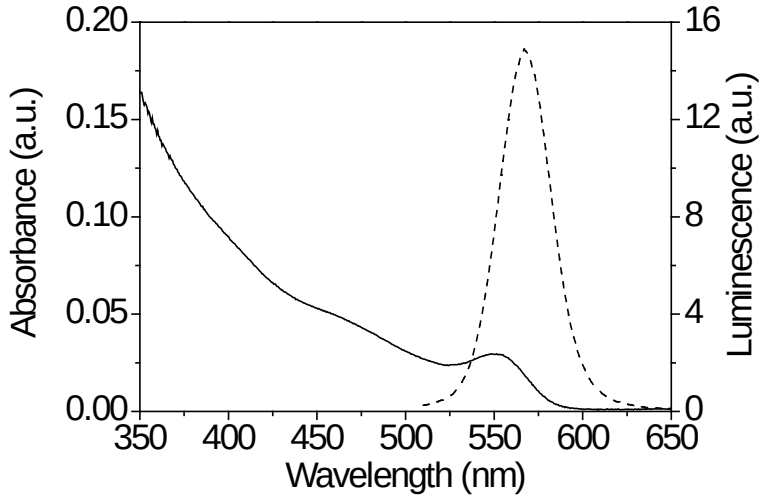

Figure 8.1 Absorption (solid) and emission (dashed) spectra of TOPO-coated CdSe/ZnS QDs in toluene. Excitation wavelength is 500 nm.

Thiols are known to bind strongly to the ZnS surface of QDs.[37] To coat the QDs with PFS, polymer chains end-functionalized with thiols were used. Two PFS polymers having different molar mass were employed for the coatings.[38] The number of monomer units in the polymer was equal to 32 and 50, for PFS32 and PFS50, respectively. Since both the QDs and the PFS are soluble in nonpolar solvents, grafting of the polymers to TOPO-coated QDs can occur via simple ligand exchange reaction (Figure 8.2). During the reaction, the QDs were mixed with a 120 times excess of the PFS polymer ligand. Since the polymer chains are bulky molecules, the reaction time was extended up to 6 days and the reaction temperature was set to 40 ºC. To

remove the unreacted polymer chains and unbound TOPO molecules the reaction mixture was cooled down and subsequently ultracentrifuged. The PFS coated QDs were then easily dispersed in a nonpolar solvent, like toluene or chloroform.

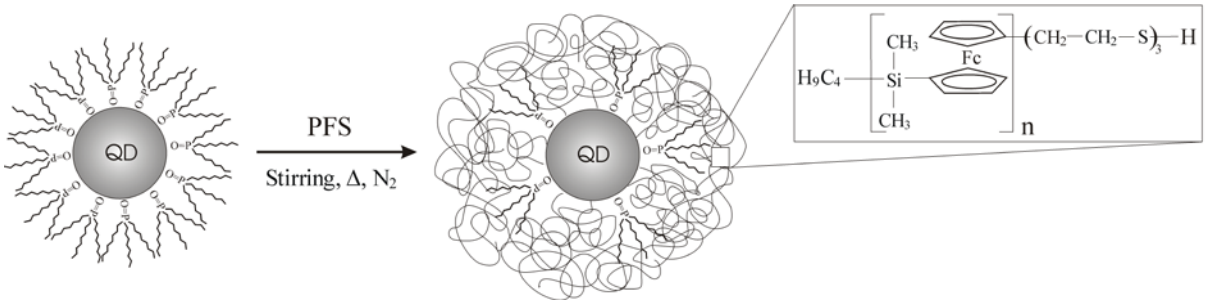

Figure 8.2 Scheme of the ligand exchange between TOPO-coated CdSe/ZnS QDs thiol-functionalized poly(ferrocenylsilane) (PFS) (n=32 for PFS32, n=50 for PFS50). The polymer on the QD surface is not drawn to scale.

8.2.2 Diffusion Ordered ^{1}H NMR Spectroscopy of QDs

The surface of the QDs was characterized by pulsed field gradient ^{1}H NMR (PFG NMR) spectroscopy. This technique proves to be useful in characterization of large systems like nanoparticles or polymers.[39-44] Using the PFG method, the self diffusion coefficient can be estimated, which is directly related to the hydrodynamic radius of the nanoparticles through the Stokes-Einstein equation. For a mixture of compounds one can therefore discriminate the resonance from different components via their diffusion coefficients.[45,46] The PFG NMR data for polymer coated QDs as well as for free PFS and TOPO-coated QDs have been obtained.

In Figure 8.3a a DOSY ^{1}H NMR spectrum of TOPO-functionalized CdSe/ZnS QDs is shown. The broad peak at 1.4 ppm and a smaller peak at 1.3 ppm correspond to the alkyl chain protons of TOPO. PFG ^{1}H NMR spectra of QDs coated with PFS32 and PFS50 are shown in Figure 8.3b and 8.3c, respectively. In both spectra peaks between 4 and 4.5 ppm are clearly observed and are assigned to the protons of the cyclopentadienyl rings of the ferrocene. The signal at 0.6 ppm is attributed to protons of the methyl groups on Si in the PFS chain. The ^{1}H resonance from the alkyl chains of the remaining TOPO is also observed at 1.4 and 1.3 ppm. The peaks at 4-4.5 ppm for PFS50 are broader than those of PFS32. This is due to a lower

mobility of the polymeric chains attached to the nanocrystal's surface. The sharper peaks of PFS32 might in turn indicate an uncomplete ligand exchange.

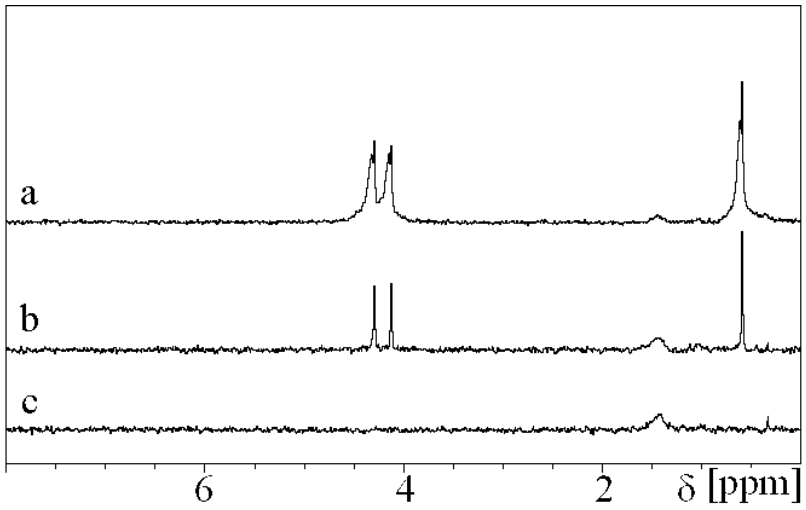

Figure 8.3 DOSY ^{1}H NMR spectra of CdSe/ZnS QDs coated with (a) PFS50, (b) PFS32 (c) TOPO.

A comparative study using 2D diffusion ordered ^{1}H NMR spectroscopy (DOSY) at the same experimental conditions allows one to discriminate between free polymer ligands in the solution and those attached to the nanoparticle's surface. In addition, the influence of the polymer molar mass on the structure of the resulting hybrid materials can be assessed. Assemblies with larger hydrodynamic radius should have lower diffusion coefficient values. The spread in the diffusion coefficient values may also indicate heterogeneity in the assemblies' structure or indicate aggregation of the QDs. Aggregation of the QDs in solution increases their hydrodynamic radius, hence the aggregates should diffuse slower compared to single QDs.

In Figure 8.4 2D DOSY ^{1}H NMR spectra of QD-TOPO, PFS32, PFS50, QD-PFS32, and QDPFS50 are shown. On the 2D DOSY graphs the chemical shifts are plotted against the diffusion coefficients. The signals from protons of small, and therefore rapidly diffusing molecules like toluene (2.1 ppm and 7.1 ppm), water (1.6 ppm) and acetone (0.5 ppm) can be clearly observed in the lower part of the graphs (higher diffusion coefficients) and serve as calibration standards. The distinct signals corresponding to these small molecules overlap for all experiments indicating similar experimental conditions for all sets of measurements.

The signals at 1.2 ppm and the corresponding diffusion coefficients of ~ 9.7-9.8 m^2/s are related to the protons of the alkyl chains of TOPO on the QD surface. Chemical shifts between 4-4.5 ppm and 0.5 ppm of species diffusing at ~9.7 m^2/s correspond to freely diffusing polymer chains. Upon binding of the PFS chains to the QD surface (proton signals at 4-4.5, ~1.4, and ~0.6 ppm) the diffusion of the assemblies remarkably decreases to <10m^2/s. This allows us to distinguish between the assemblies and any unbound material.

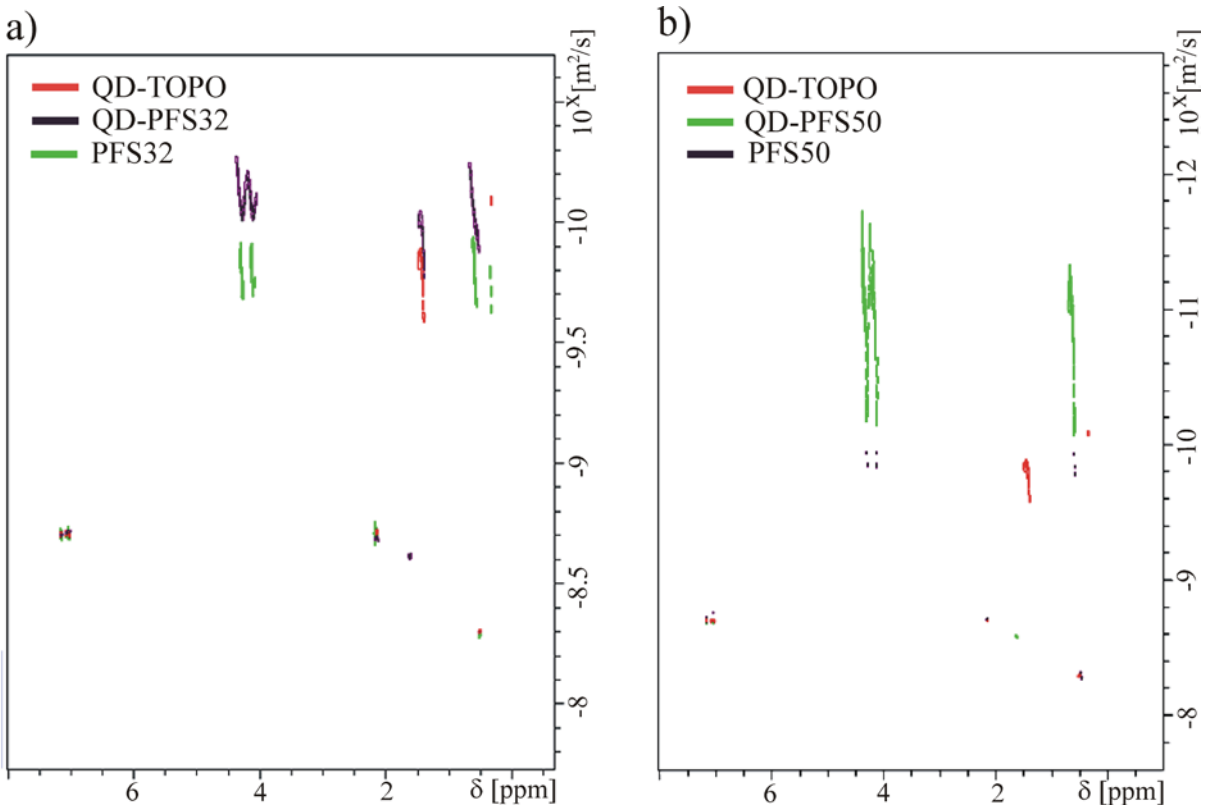

Figure 8.4 2D DOSY experiments performed for (a) PFS32 and (b) PFS50 in toluene-*d*.

There are differences between the spectra obtained for QD-PFS32 and QD-PFS50. In the case of PFS32, there is still some TOPO on the surface present. The NMR signals related to the remaining TOPO are clearly shifted along the diffusion coefficient axis indicating that the TOPO is bound to the QDs. For QD-PFS50 it seems that there is no remaining TOPO present on the surface. This is surprising since PFS50 is a rather more bulky ligand than PFS32. Another striking difference is that the signals of the QD-PFS50 sample are spread considerably along the diffusion coefficient axis over almost two orders of magnitude. The reason for the observed behavior may be the formation of larger aggregates of QD-PFS50 in solution or from different conformation of the PFS chain on the QD surface.

8.2.3 Optical Properties of QDs Coated with PFS Polymer

The absorption and emission spectra of QD-PFS hybrids are shown in Figure 8.5. The first absorption peak of the QDs is located at 563 nm for both compounds and it is red-shifted by ~10 nm compared to TOPO-functionalized QDs (553 nm). Additionally, for QD-PFS50 a broad band at 450 nm, typical for PFS polymers, is detected. The band does not disappear after additional purification steps and the NMR experiments did not show free PFS50 present in solution. This indicates that the new band is from PFS coated on the QD surface. The additional absorption band is also observed for QD-PFS32, although it is much less pronounced.

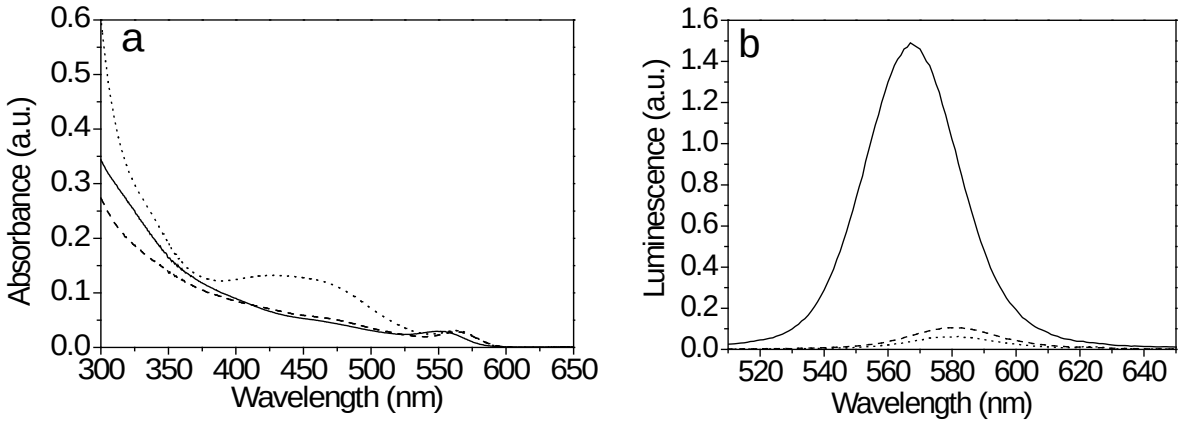

Figure 8.5 (a) Absorption and (b) emission spectra of TOPO-QDs (solid), QD-PFS32 (dash), and QD-PFS50 (dot) in toluene. The absorption is red shifted and an absorption band of PFS is clearly visible. The emission of PFS-QDs is strongly quenched and red shifted by 12 nm.

The luminescence intensity of the PFS-coated QDs significantly decreased. The QY values of PFS32 and PFS50 are equal to 2.0 and 1.4 %, respectively. The emission peak is also shifted towards longer wavelengths. The PFS used here lacks phosphine or NH_2 side groups, which could attach to the QD surface and passivate surface defects.[31] Enhancement of the QD luminescence is therefore not expected.[31,47] The thiol functionality should be in principle able to passivate the surface defects, but the bulkiness of the polymers may prevent to passivate all defect sites. It is expected that the passivation by a thiol end-functionalized polymer will be less effective than when using small organic ligand or side-group functionalized polymers. However, lower surface passivation alone cannot account for the observed decrease in the luminescence. The ligands are attached to the ZnS shell and not directly to the CdSe core,

therefore their influence on the band-edge recombination process is smaller. Additionally, there is no increase in the luminescence at longer wavelengths associated with recombination from surface traps. The quenching is induced likely by the polymer itself.[31] In particular, ferrocene was shown to be a good quencher of QD luminescence (chapters 3-6).[31,47-49] The quenching mechanism is based on a charge transfer between the photoexcited QDs and the ferrocene in close proximity to the QD (chapter 3).[31] The abundance of ferrocene in PFS should make these polymers effective quenchers as well. Quenching based on a short distance electron transfer mechanism explains the weak molar mass effect of the polymers on the luminescence, since only the ferrocenes that are close to the QD surface can effectively donate electrons. It would be of great interest to investigate whether a charge generated at the free end of the polymer may be conducted to the QD by, e.g., a hopping mechanism. In view of charge dissipation in electrolytic solutions, lower molar mass PFS polymers would have to be used for these experiments.

8.3 CONCLUSIONS

CdSe/ZnS QDs were coated with poly(ferrocenylsilanes) with different molar masses, 7750 g/mol (PFS32) and 12500 g/mol (PFS50). The QD/polymer hybrid materials were obtained by grafting thiol end-functionalized PFS polymers to the surface of QDs by a ligand exchange reaction. The grafting of the polymer chains was monitored by pulsed field gradient (PFG) and diffusion filtered (DOSY) ^{1}H NMR spectroscopies. Upon grafting of the PFS, the luminescence of the QDs decreased and the absorption and emission spectra shifted to longer wavelengths. The quenching was due to an electron transfer process between the ferrocene in the polymer and the QD surface.

8.4 EXPERIMENTAL

Materials. The synthesis of core-shell CdSe/ZnS QDs is described by Janczewski *et al.*[33] Thiol-functionalized poly(ferrocenyldimethylsilanes) with controlled molar masses 7750 g/mol (PFS32) and 12500 g/mol (PFS50), and narrow polydispersity were prepared by anionic ring-opening polymerization according to the procedure reported by Peter *et al.*[38] The solvents toluene and *d*-toluene (100% atom) were purchased from Aldrich.

Grafting of PFS to CdSe/ZnS. The trioctylphosphine oxide (TOPO)-stabilized QDs were purified by precipitation with methanol and centrifugation at 10000 rpm for 10 minutes. The solid residue containing the QDs was redisolved in toluene. Purified nanocrystals (1 mL, 5×10^{-5} M) and PFS (PFS32, 4 mL, 1.5×10^{-3} M; PFS50: 4 mL, 1.5×10^{-3} M) toluene solutions were mixed in a flask and closed with a N_2 balloon to prevent solvent evaporation. The reaction was carried out for 6 days at 40°C. After the reaction the solutions were distributed into Teflon tubes and ultracentrifuge at 50000 g for 3 hours. The procedure was repeated 3 times. Purified QD-PFS conjugates were further analyzed by spectroscopic techniques.

Methods. The absorption spectra were measured using a Varian Cary 300 UV-Vis spectrophotometer. To record the photoluminescence spectra an Edinburgh XE-900 spectrofluorometer was used. Nuclear magnetic resonance (NMR) experiments were performed on a Bruker Avance II 600 MHz NMR spectrometer at ambient temperature, equipped with an SEI 2.5 mm probe head and a z-axis gradient system. To limit the convection during the pulsed field gradient (PFG) experiments, tubes with the size of 2.5 mm were used. 1D diffusion-filtered ^{1}H experiments were performed using the bipolar stimulated echo sequence with typically a diffusion time (Δ) of 100 ms, and gradients between 5 and 95 % of maximum 35 G. For the PFG NMR experiments *d*-toluene was chosen due to its low flow.

8.5 REFERENCES

1. Colvin, V. L.; Schlamp, M. C.; Alivisatos, A. P. *Nature* **1994**, *370*, 354–357.
2. Dabbousi, B. O.; Bawendi, M. G.; Onitsuka, O.; Rubner, M. F. *Appl. Phys. Lett.* **1995**, *66*, 1316–1318.
3. Schlamp, M. C.; Peng, X.; Alivisatos, A. P. *J. Appl. Phys.* **1997**, *82*, 5837-5842.
4. Gao, M. Y.; Richter, B.; Kirstein, S. *Adv. Mater.* **1997,** *9*, 802-805.
5. Gaponik, N. P.; Talapin, D. V.; Rogach A. L. *PCCP* **1999**, *1*, 1787-1789.

6. Gaponik, N. P.; Talapin, D. V.; Rogach, A. L.; Eychmüller, A. *J. Mater. Chem.* **2000**, *10*, 2163-2166.
7. McDonald, S. A.; Konstantatos, G.; Zhang S.; Cyr, P. W.; Klem, E. J. D.; Levina, L.; Sargent E. H. *Nat. Mater*. **2005,** *4*, 149-152.
8. Shim, M.; Guyot-Sionnest, P. *Nature* **2000**, *407*, 981-983.
9. O'Regan, B.; Grätzel, M. *Nature* **1991**, *353*, 737–740.
10. Godovsky, D. Y.; Varfolomeev, A. E.; Zaretsky, D. F.; Chandrakanthi, R. L. N.; Kundig, A.; Weder, C.; Caseri, W. *J. Mater. Chem.* **2001**, *11*, 2465-2469.
11. Huynh, W. U.; Peng, X.; Alivisatos, A. P. *Adv. Mater*. **1999**, *11*, 923-927.
12. Constantine, C. A.; Gattás-Asfura, K. M.; Mello, S. V.; Crespo, G.; Rastogi, V.; Cheng, T. C.; DeFrank, J. J.; Leblanc, R. M. *Langmuir* **2003**, 19, 9863-9867.
13. Constantine, C. A.; Gattás-Asfura, K. M.; Mello, S. V.; Crespo, G.; Rastogi, V.; Cheng, T. C.; DeFrank, J. J.; Leblanc, R. M. *J. Phys. Chem. B* **2003**, *107*, 13762-13764.
14. Ionov, L.; Sapra, S.; Synytska, A.; Rogach, A. L.; Stamm, M.; Diez, S. *Adv. Mater.* **2006**, *18*, 1453-1457.
15. Pardo-Yissar, V.; Bourenko, T.; Wasserman, J.; Willner, I. *Adv. Mat*. **2002**, *14*, 670-673.
16. Skaff, H.; Sill, K.; Emrick, T. *J. Am. Chem. Soc.* **2004**, *126*, 11322–11325.
17. Odoi, M. Y.; Hammer, N. I.; Sill, K.; Emrick, T.; Barnes, M. D. *J. Am. Chem. Soc.* **2006**, *128*, 3506-3507.
18. Hammer, N. I.; Early, K. T.; Sill, K.; Odoi, M. Y.; Emrick, T.; Barnes, M. D. *J. Phys. Chem. B* **2006**, *110*, 14167-14171.
19. Liu, J. S.; Tanaka, T.; Sivula, K.; Alivisatos, A. P.; Fréchet, J. M. J. *J. Am. Chem. Soc.* **2004**, *126*, 6550-6551.
20. Milliron, D. J.; Alivisatos, A. P. ; Pitois, C. ; Edder, C.; Fréchet, J. M. J. *Adv. Mater.* **2003**, *15*, 58-61.
21. Yang, C. H.; Bhongale, C. J.; Chou, C. H.; Yang, S. H.; Lo, C. N.; Chen, T.; M.; Hsu, C. S. *Polymer* **2007**, *48*, 116-128.
22. Manners, I. *Synthetic Metal-Containing Polymers* **2004**, Wiley-VCH.
23. Kulbaba, K.; Manners, I. *Macromol. Rapid Commun.* **2001**, *22*, 711-724.
24. Arsenault, A. C.; Míguez, H.; Kitaev, V.; Ozin, G. A.; Manners, I. *Adv. Mater.* **2003**, *15*, 503-507.

25. Korczagin, I.; Lammertink, R. G. H.; Hempenius, M. A.; Golze, S.; Vancso, G. J. *Adv. Polym. Sci.* **2006**, *200*, 91-117.
26. Korczagin, I.; Golze, S.; Hempenius, M. A.; Vancso, G. J. *Chem. Mater.* **2003**, *15*, 3663-3668.
27. Hinderling, C.; Keles, Y.; Stöckli, T.; Knapp, H. F.; De Los Arcos, T.; Oelhafen, P.; Korczagin, I.; Hempenius, M. A.; Vancso, G. J.; Pugin, R.; Heinzelmann, H. *Adv. Mater.* **2004**, *16*, 876-879.
28. Cheng, J. Y.; Ross, C. A.; Chan, V. Z. H.; Thomas, E. L.; Lammertink, R. G. H.; Vancso, G. J. *Adv. Mater.* **2001,** *13*, 1174-1178.
29. Petersen, R.; Foucher, D. A.; Tang, B. Z.; Lough, A.; Raju, N. P.; Greedan, J. E.; Manners, I. *Chem. Mater.* **1995**, *7*, 2045–2053.
30. Ma, Y.; Dong, W. F.; Hempenius, M. A.; Mohwald, H.; Vancso, G. J. *Nat. Mater.* **2006**, *5*, 724-729.
31. Cyr, P. W.; Tzolov, M.; Hines, M. A.; Manners, I.; Sargent, E. H.; Scholes, D. *J. Mater. Chem.* **2003**, *13*, 2213-2219.
32. Tomczak, N.; Janczewski, D.; Han, M. Y.; Vancso, G. J. *Prog, Polym. Sci.* **2009**, *34*, 393-430.
33. Janczewski, D.; Tomczak, N.; Khin, Y. W.; Han, M. Y.; Vancso G. J. *Eur. Pol. J.* **2009**, *45*, 3-9.
34. Yu, W. W.; Qu, L.; Guo, W.; Peng, X. *Chem. Mater.* **2003**, *15*, 2854-2860.
35. Montalti, M.; Credi, A.; Prodi, L.; Gandolfi, M. T. *Handbook of Photochemistry*, 3rd. Ed., CRC Press, **2006**, pp. 572-576.
36. Lakowicz, J. R. *Principles of Fluorescent Spectroscopy*, 2nd Ed., Kluwek Academic/ Plenum Press, **1999**, pp. 10-12.
37. Querner, C.; Reiss, P.; Bleuse, J.; Pron, A. *J. Am. Chem. Soc.* **2004**, *126*, 11574-11582.
38. Peter, M.; Lammertink, R. G. H.; Hempenius, M. A.; van Os, M.; Beulen, M. W. J.; Reinhoudt, D. N.; Knoll, W.; Vancso, G. J. *Chem. Commun.* **1999**, 359-360.
39. Price, W. S. *Concepts Magn. Reson.* **1997**, *9*, 299-336.
40. Price, W. S. *Concepts Magn. Reson.* **1998**, *10*, 197-237.
41. Johnson, C. S. *Prog. NMR Spectrosc.* **1999**, *34*, 203-256.
42. Stilbs, P. *Prog. NMR Spectrosc.* **1987**, *19*, 1-45.
43. Karger, J.; Pfeifer, H.; Heink, W. *Adv. Magn. Opt. Reson.* **1988**, *12*, 1-89.

44. Nicolay, K.; Braun, K. P. J.; de Graaf, R. A.; Dijkhuizen, R. M.; Kruiskamp, M. J. *NMR Biomed.* **2001**, *14*, 94-111.
45. Hens, Z.; Moreels, I.; Martins, J. C. *ChemPhysChem* **2005**, *6*, 2578-2584.
46. Moreels, I.; Martins, J. C.; Hens, Z. *ChemPhysChem* **2006**, *7*, 1028-1031.
47. Chandler, R. R.; Coffer, L. J.; Atherton, S. J.; Snowden, P. T. *J. Phys. Chem.* **1992**, *96*, 2713-2717.
48. Palaniappan, K.; Hackney, S. A.; Liu, J. *Chem. Commun.* **2004**, 2704-2705.
49. Mulrooney, R. C.; Singh, N.; Kaur, N.; Callan, J. F. *Chem. Commun.* **2009**, 686-688.

Summary

This thesis demonstrates the power of chemical surface engineering in the design and fabrication of functional hybrid materials made of Quantum Dots. The small size of the QDs, in the range of 1 to 10 nm, and related stability in solution, require a careful consideration of a proper surface chemistry for the ligand shell. By a judicious choice of the coating one can remarkably influence the physicochemical and photophysical properties of the semiconductor nanocrystals as well as design and engineer new generations of advanced nanoscale materials. This work describes in detail the synthetic approaches to chemical surface functionalization of QDs with electroactive ligands, including ferrocenyl thiols and poly(ferrocenylsilanes), and with β-cyclodextrin (β-CD) ligands suitable for supramolecular host-guest assembly. These functional ligands are shown to be important components in the engineering of new types of QD hybrid materials. The influence of the electroactive ligands on the optical properties of QDs was investigated by spectroscopic and electrochemical methods. These investigations gave an important insight into the quenching mechanisms of QDs by ferrocene and to the fundamental electron transfer processes in hybrid materials composed of QDs and electro-active ligands. Additionally, ferrocene groups located on the QD surface were shown to be able to take part in host-guest complexation reactions with β-cyclodextrin in solution. This ability was useful in the phase transfer of hydrophobic nanoparticles between solvents of markedly different polarities. The complexation ability of β-CD-functionalized QDs and adamantyl dendrimers was exploited for the preparation of supramolecular multilayer structures on surfaces. Surface bound QDs were shown to be able to transduce optically the binding events to the β-CD cavity, a proof-of-principle for a sensor design. This thesis demonstrates that both FRET and ET can be used as the transduction mechanisms. Thus, proper surface design and engineering of QDs gives unique opportunities to obtain the new class of hybrid materials using numerous functionalization approaches and surface chemistries. The following paragraphs summarize the results obtained.

Chapter 2 introduces the most important terms and definitions related to QDs, and describes the QD structure, synthesis and photophysical properties. Chemical engineering of the QD surface ligand shell via ligand exchange and methods for the immobilization of QDs on surfaces were discussed. The analytical tools for the characterization of QDs were introduced, and finally some applications of QDs in optoelectronics, sensing and life sciences were described.

Chapter 3 describes the investigation of the photoluminescence quenching of QDs by ferrocene. Ferrocenyl thiols with variable length of the alkyl thiol were coated on the surface of CdSe/ZnS QDs. The ferrocene was shown to be a good quencher of QD luminescence and the quenching efficiency depended on the distance between ferrocene and the QD. By decreasing the spacer length the quenching efficiency was shown to increase. A quenching mechanism involving a hole transfer between the photoexcited QD and the ferrocene was proposed.

Electrochemical characterization of TOPO-coated and ferrocenyl-coated QDs in non-aqueous solution is presented in Chapter 4. Cathodic reduction and anodic oxidation processes involving the QD HOMO and LUMO levels as well as defect states were identified by cyclic voltammetry. The electrochemical bandgap was estimated from the anodic and cathodic redox peaks and found to match well the optical bandgap estimated from the absorption spectrum. Cyclic voltammetry showed that the redox potentials of the QDs are modified due to the presence of ferrocene on the surface of the QD. A new electrochemical peak associated with oxidation of ferrocene appeared on the cyclic voltammograms and the anodic and cathodic redox peaks of the QDs were shifted to more negative potentials due to the presence of the Fc ligand. Concurrent shift of the ferrocene redox peaks indicates that our system displayed features of a “molecular hybrid”, where both the QD and the ligand influence each other.

In Chapter 5 ferrocene-coated QDs were shown to undergo reversible phase transfer to and from the aqueous phase upon formation/release of inclusion complexes of β-cyclodextrin with the ferrocene units on the surface of the QDs. The release has been achieved by decomplexation *via* competitive reaction of β-cyclodextrin with naphthalene and adamantane derivatives. The emission of QDs in the water phase was quenched due to the presence of the cyclodextrin. The use of adamantane as the decomplexating agent resulted in clear and

transparent solutions of QDs in the chloroform phase unlike for the case of naphthalene where aggregation of the QDs was observed. The choice of the decomplexating agent was therefore crucial to establish a reversible phase transfer of QDs.

Chapter 6 describes two routes to obtain QD patterns on surfaces using multivalent supramolecular host-guest interactions. To this end, β-CD-functionalized QDs were obtained by covalent coupling of amine-terminated β-CD to carboxy-functionalized QDs. The QD/β-CD materials were employed in the formation of a multilayer structure using dendrimeric supramolecular "glue". The stability of the resulting patterns was demonstrated by further formation of host-guest complexes with the unused β-CD cavities on the QD surface. In particular, the luminescence of QDs was modulated by complexation reactions with ferrocene-functionalized dendrimers printed across the QD patterns. Due to the presence of ferrocene the luminescence of the QDs visibly decreased.

Chapter 7 describes how the supramolecular multilayer assemblies described in Chapter 6 could be used as sensing platforms using FRET as the signal transduction mechanism. The vacant β-CD cavities located on the surface of the QDs formed host-guest complexes with adamantyl-functionalized dyes. Fluorescence microscopy, spectroscopy and FLIM experiments clearly demonstrated that a FRET process was occurring only in the areas where the analyte formed host-guest complexes with the β-CD functionalized QDs.

Finally, the modification of QDs with poly(ferrocenylsilanes) (PFS) using a "grafting to" approach is described Chapter 8. Two thiol end-functionalized PFS polymers of molar masses of 7750 g/mol and 12500 g/mol were attached to the nanocrystal's surface via ligand exchange reaction. The resulting QD/polymer hybrid material displayed spectral shifts in the absorbance and luminescence, which were accompanied by a decrease in the luminescence. The obtained QD/polymer conjugates were investigated using diffusion ordered ^{1}H NMR spectroscopy. This characterization technique gives evidence for the presence of the polymer chains on the QD surface.

Samenvatting

Dit proefschrift demonstreert de kracht van chemische oppervlakte engineering in het ontwerp en de fabricage van functionele hybride materialen op basis van Quantum Dots. De geringe afmetingen van QDs, in het gebied van 1 tot 10 nm, en de hieraan gerelateerde stabiliteit in oplossing, vereisen een zorgvuldige keuze van de oppervlaktechemie voor de ligandschil. Met een juiste keuze van de coating kan men de fysicochemische en fotofysische eigenschappen van de semiconductor nanokristallen sterk beïnvloeden en ook nieuwe generaties van geavanceerde nanoschaal materialen ontwikkelen. Dit werk beschrijft in detail de synthetische strategie voor de chemische oppervlaktefunctionalisering van QDs met electroactieve liganden, inclusief ferrocenyl thiols en poly(ferrocenylsilanes), en met β-cyclodextrine (β-CD) liganden die geschikt zijn voor supramoleculaire host-guest assembly. Deze functionele liganden blijken belangrijke componenten te zijn voor de ontwikkeling van nieuwe typen QD hybride materialen. De invloed van de electroactieve liganden op de optische eigenschappen van QDs werd onderzocht door spectroscopische en electrochemische methoden. Deze onderzoeken gaven een belangrijk inzicht in de quenching mechanismen van QDs door ferroceen en in de fundamentele electron overdrachtsprocessen in hybride materialen bestaand uit QDs en electroactieve liganden. Bovendien bleek dat ferroceen groepen gelocaliseerd op het QD oppervlak deel konden nemen aan host-guest complexeringsreacties met β-cyclodextrine in oplossing. Deze eigenschap was zeer nuttig voor het transport van hydrofobe nanodeeltjes tussen oplosmiddelen van sterk verschillende polariteit. Het complexerende vermogen van β-CD-gefunctionaliseerde QDs met adamantyl dendrimeren werd gebruikt voor de bereiding van supramoleculaire multilaagstructuren op oppervlakken. Aangetoond werd dat oppervlakte-gebonden QDs in staat zijn om optisch de binding events met de β-CD holte door te geven, een proof of principle voor een sensor. Dit proefschrift demonstreert dat zowel FRET als ET kunnen worden gebruikt als overdrachtsmechanismen. Het juiste oppervlakteontwerp van QDs geeft unieke kansen om een nieuwe klasse van hybride materialen te verkrijgen, gebruikmakend van talrijke

functionaliseringsmethoden en oppervlaktereacties. De volgende paragrafen vatten de behaalde resultaten samen.

Hoofdstuk 2 introduceert de belangrijkste termen en definities gerelateerd aan QDs en beschrijft de QD structuur, synthese en fotofysische eigenschappen. Chemische modificatie van de QD oppervlakte ligandschil door liganduitwisseling en methoden voor de immobilisatie van QDs op oppervlakken worden bediscussieerd. De analytische gereedschappen voor de karakterisering van QDs worden geïntroduceerd, en tenslotte worden enkele toepassingen van QDs in optoelectronica, sensing en life sciences beschreven.

Hoofdstuk 3 beschrijft het onderzoek naar de fotoluminescentie quenching van QDs door ferroceen. Ferrocenyl thiols met variabele lengten van de alkyl thiol werden gehecht aan het oppervlak van CdSe/ZnS QDs. Ferroceen bleek een goede quencher te zijn van QD luminescentie en de quenchingefficientie was afhankelijk van de afstand tussen ferroceen en de QD. Het verkleinen van de spacerlengte bleek de quenchingefficientie te verhogen. Een quenchingmechanisme gebaseerd op hole transfer tussen de foto-geëxciteerde QD en ferroceen werd voorgesteld.

Electrochemische karakterisering van TOPO-gecoate en ferrocenyl-gecoate QDs in niet-waterige oplossing werd gepresenteerd in Hoofstuk 4. Kathodische reductie- en anodische oxidatieprocessen die QD HOMO en LUMO niveaus omvatten maar ook defect states werden geïdentificeerd door cyclische voltammetrie. De electrochemische bandgap werd geschat op basis van de anodische en kathodische pieken en bleek goed overeen te komen met de optische bandgap geschat uit het absorptiespectrum. Cyclische voltammetrie liet zien dat de redoxpotentialen van de QDs veranderen door de aanwezigheid van ferroceen aan het oppervlak van de QDs. Een nieuwe electrochemische piek geassocieerd met de oxidatie van ferroceen verscheen in het cyclisch voltammogram en de anodische en kathodische redoxpieken van de QDs verschoven naar meer negatieve potentialen door de aanwezigheid van het Fc ligand. De verschuiving van de ferroceen redoxpieken geeft aan dat ons systeem eigenschappen vertoont van een “moleculair hybrid” waar zowel de QD als de ligand elkaar beïnvloeden.

In Hoofdstuk 5 werd aangetoond dat ferroceen-gecoate QDs reversibel kunnen worden overgebracht naar en uit een waterige fase door vorming/splitsing van complexen tussen β-

cyclodextrine met de ferroceen eenheden aan het oppervlak van de QDs. De decomplexering werd bereikt door competitieve reactie van β-cyclodextrine met naphthaleen en adamantaan derivaten. De emissie van QDs in de waterfase werd gequenched door de aanwezigheid van β-cyclodextrine. Het gebruik van adamantaan als decomplexerend agens resulteerde in heldere en transparante oplossingen van QDs in chloroform in tegenstelling tot het geval van naphthaleen waar aggregatie van de QDs werd waargenomen. De juiste keuze van het decomplexerings agens was daarom essentieel om een reversibele overdracht tussen de organische en waterige fase te bewerkstelligen.

Hoofdstuk 6 beschrijft twee routes om QD patronen te creëeren op oppervlakken, gebruikmakend van multivalente supramoleculaire host-guest interacties. Om dit doel te bereiken werden β-CD-gefunctionaliseerde QDs gemaakt door covalente koppeling van amine-getermineerde β-CD aan carboxy-gefunctionaliseerde QDs. De QD/β-CD materialen werden gebruikt voor de vorming van een multilaagstructuur met behulp van een dendrimeer-gebaseerde supramoleculaire “lijm”. De stabiliteit van de resulterende patronen werd aangetoond door verdere vorming van host-guest complexen door de onbezette β-CD holten op het QD oppervlak. Het was opmerkelijk dat de luminescentie van de QDs beïnvloed werd door complexeringsreacties met de ferroceen-gefunctionaliseerde dendrimeren geprint over de QD patronen. Door de aanwezigheid van ferroceen nam de luminescentie van de QDs zichtbaar af.

Hoofdstuk 7 beschrijft hoe de supramoleculaire multilaag structuren behandeld in Hoofdstuk 6 konden worden gebruikt als sensing platforms, gebruikmakend van FRET als signaaloverdrachtsmechanisme. De onbezette β-CD holten aanwezig op het oppervlak van de QDs vormden host-guest complexen met adamantyl-gefunctionaliseerde kleurstoffen. Fluorescentiemicroscopie, spectroscopie en FLIM experimenten toonden duidelijk aan dat een FRET proces alleen plaatsvond in de gebieden waar de kleurstof host-guest complexen vormde met de β-CD-gefunctionaliseerde QDs.

Tenslotte wordt de modificatie van QDs met poly(ferrocenylsilanes) (PFS), door middel van een “grafting to” route, beschreven in Hoofdstuk 8. Twee thiol-eindgefunctionaliseerde PFS polymeren met molaire massa’s van 7750 g/mol en 12500 g/mol werden bevestigd aan het oppervlak van de nanokristallen door middel van een ligand uitwisselingsreactie. De resulterende QD/polymeer hybride materialen vertoonden spectrale verschuivingen in de

absorptie en luminescentie, gepaard gaand met een afname in de luminescentie. De verkregen QD/polymeer assemblies werden bestudeerd met behulp van diffusion ordered ^{1}H NMR spectroscopie. Met deze techniek werd de aanwezigheid van de polymeerketens aan het QD oppervlak aangetoond.

Acknowledgments

And now I will write probably the most read part of every thesis called acknowledgments. Usually here the author reflects his/her professional and personal relations with all people which he/she has met during the last four years or may be longer in some cases…

First of all I'd like to thank my promoters who gave me the opportunity to perform this work and made me a really independent researcher. I'd like to acknowledge my first promoter Prof. Julius Vancso for his strategic view on the project and for a large amount of freedom he gave me. You have always been critical and encouraging. I truly appreciate it. I want to express my gratitude to my other promoter Prof. David Reinhoudt, whose group I joined in the second year of my PhD. Your professional attitude helped me to become an independent researcher.

It would be difficult to complete this thesis without the help of Nikodem, my coach from Singapore who translated Master Yoda English into correct form. I really appreciate our discussions in the field of nanotechnology which was sometimes converted into real life chats. In this view, the invention of Skype communication seems as a great progress for all scientific society. I still have to visit you on your territory in Singapore. Now my dedication goes to Dr. Aldrik Velders who is my co-supervisor in Twente. He is an expert of "Apollo 600MHz". His support and endless control experiments are unforgettable. Dr. Mark Hempenius, the most respectful person and scientist I have met.

Coming to the part where most of my friends and colleagues are mentioned. I will mention them in chronological order as I met them over these years. Firstly I'd like to mention here the bravest world traveler who visited the country of the greatest writers of the 19th century. Of course these lines are devoted to Thomas Pushkin. There is another person I'm thinking about who "flatmating" with me for three years and was good drinking company at the same time. Our indescribable road trip to Italy can be a good plot for a movie. Now I move to our

slimmest communist Oya. I know you always have a sandwich from yesterday for poor researchers. The first Dutch lunch I had with you Eugenia, it is a pity that you stayed with us just for a short time. What would be MTP without hot pot and cocktail maker In Yee and his "strict" wife Xing Yi. We had a good time at your place. Szczepan, I hope one day our idea to open a couple of journals such as "Huge vs Small" and "Soft Matter Doesn't Matter" will be realized. The best sexy dancer Monique probably has reached professional level. We will support you during the next championship. I do not forget the pain in the … my dear squash coaches Marina and Michel.

And now I will mention a person who was always near by to cheer us up and providing meal supplies, which is important for an exhausted researcher's mind. It is a very good friend Janet who spent with us (me and Eddy) a long time and could stand all jokes and humor. Thanks to Valeria for standing our constant presence at Janet/your place and for being a good party girl. Melba, the best wisher, remembers also you and especially your sonorous laugh… Once I will come to visit you in Barcelona. The most relaxing time was provided by Carlo (Nonno). He is the driving force of hakuna matata. Mirko thanks for introducing me to the world of bodypump in the local fitness center. For sure, I remember my nice Sicilian holidays in hot Palermo and lovely San Vito la Cappo. Davide, you still have to visit me in Moscow. I won't promise to you the hot weather but definitely to see something over there. Jelemita qué pasa dear? Muy bien is the answer. It is nice to have you around to support each other with hard jokes and rough humor…definitely we see each other my alternative Dutch teacher. I wish to have a lot of snow and a good ride with you guys Henk and Kim. I hope we will go surfing on the snow once again together. From our trip to Berlin I will always remember questioning myself: Albert, how much do we need to eat to die? The calmest climber Riccardo was the strictest coach in the climbing center forcing me to try suicidal routes. Also I haven't forgotten you Bilge, our friendship and comical understanding keeps getting better and better. I had a good party time and funny tennis lessons with Francesca. Joost, you're the best representative from the local Twente community with an international sense of humor.

My new flat mate and a good friend Jordi please look after for our penthouse apartment, which I will visit many more times. I wish you will "enjoy the forest view" together with Raluca. I have never visited so many museums in such a short period of time like in NY. I had this "cultural shock" together with Arancha. The little Nuria, it cannot be "a lot of mouth", but there can be many thanks for summer time together with us here in Twente.

Newly discovered team for having a good time Raffealla, Cem, Mauritzo, Nick, Giulia are also acknowledged. The night life in Enschede was supported by Bas, Christaan, Can, Laura, Stefano, and many others…

This acknowledgement cannot be completed without my Russian supporters; Mityay, Ivan and Sasha & Sasha. You are always welcome to visit me in everyplace where life will bring me.

I especially would like to thank my colleagues with whom I had fruitful collaborations Prof. Jurriaan Huskens and Shu Han Hsu. Part of this research could not be accomplished without the assistance of Prof. Vinod Subramaniam and Dr. Christian Blum.

And of course, there is no research without technical support. Clemens, you have fantastic skills that keep the entire research institute running. I assume that you are able to fix a nuclear submarine with tape and a screw driver. Thank to Genevieve for constantly giving me an advice concerning all possible life scenarios in the Netherlands. In the end, I appreciate all members of MTP, SMCT and MnF groups for daily life at the UT and for the professional support whenever need.

Particular thank goes to all sport clubs which I was visiting, Sailing, Tennis, Gliding, Climbing and so on. They really helped me to kill most of the boring evenings and weekends. I really had a lot of fun and enjoyed the time spent doing these sports

My dear parents nobody and nothing could support me as much as you did during all of these years. Thank you very much for your understanding and encouragment…

About the author

Denis Dorokhin was born in Moscow, Russia. He received his Bachelor's Degree in Chemical Technology and Biotechnology at the Academy of Fine Chemical Technology named after L. M. Lomonosov in June 2001. In July 2003 he graduated from Peoples' Friendship University of Russia receiving the Master degree of Science. In the same year he also received Bachelor's Degree in Management of Chemical Industry Enterprises, M.V. Lomonosov Moscow State Academy of Fine Chemical Technology. After graduation he had various internship positions of the IAESTE (International Association for the Exchange of Students Technical Experience) program at the Town Hall Analytical Laboratory of Torremolinos (Spain) and the Otto-Von-Guericke-University of Magdeburg (Germany). Since November 2005, he is PhD student at University of Twente in the group of Prof. G. J. Vancso and in November 2006 he also joined the group of Prof D. N. Reinhould. The results of his research are described in this Thesis. Since February 1st 2010, he will start a new research project devoted to the development of BioToxChip at Wageningen University.